Stretto di Messina

Concessionaria per la progettazione, realizzazione e gestione del collegamento stabile tra la Sicilia
e il Continente Organismo di Diritto Pubblico
(Legge n° 1158 del 17 dicembre 1971, modificata dal D.Lgs. n°114 del 24 aprile 2003)

EurolinK

PONTE SULLO STRETTO DI MESSINA

PROGETTO DEFINITIVO

EUROLINK S.C.p.A.

IMPREGILO S.p.A. (MANDATARIA)
SOCIETÀ ITALIANA PER CONDOTTE D'ACQUA S.p.A. (MANDANTE)
COOPERATIVA MURATORI E CEMENTISTI - C.M.C. DI RAVENNA SOC. COOP. A.R.L. (MANDANTE)
SACYR S.A.U. (MANDANTE)
ISHIKAWAJIMA - HARIMA HEAVY INDUSTRIES CO. LTD (MANDANTE)
A.C.I. S.C.P.A. - CONSORZIO STABILE (MANDANTE)

IL PROGETTISTA	IL CONTRAENTE GENERALE	STRETTO DI MESSINA	STRETTODI MESSINA
Ing E.M.Veje COWI EurolinK Dott. Ing. E. Pagani Ordine Ingegneri Milano n° 15408	PROJECT MANAGER (Ing. P.P. Marcheselli)	Direttore Generale e RUP Validazione (Ing. G. Fiammenghi)	Amministratore Delegato (Dott. P. Cucci)

Unità Funzionale	OPERA D'ATTRAVERSAMENTO	PS0014_F0
Tipo di sistema	SOVRASTRUTTURE	
Raggruppamento di opere/attività	TORRI	
Opera - tratto d'opera - parte d'opera	General	
Titolo del documento	General Design Principles, Annex	

CODICE C G 1 0 0 0 P R G D P S V T 4 0 0 0 0 0 0 0 0 0 1 F0

REV	DATA	DESCRIZIONE	REDATTO	VERIFICATO	APPROVATO
F0	20-06-2011	EMISSIONE FINALE	CHSX	MJK	CHSX/LSJ

NOME DEL FILE: PS0014_F0

INDICE

1 Introduction

This report describes the principles used to design the following tower structural elements:

- Legs
- Cross Beams
- Base Anchorage

The design is based on that shown in the Tender Design.

In this project phase it was found advantageous to introduce the following changes to the tender design:

- The tower height was increased from 382.6 m to 399 m to compensate for the increase in deck weight;
- Flat plate longitudinal stiffeners replace T-shaped longitudinal stiffeners in the tower legs and cross beams;
- The tower leg transverse stiffener arrangement was revised to simplify fabrication and assembly of the tower leg segments;
- The tower leg transverse diaphragm arrangement was revised to eliminate unnecessary material;
- Braced frames replace the moment resisting frame transverse stiffening in the cross beams;
- Multi-strand post-tensioning tendons replace the anchor bolts in the tower base anchorage to simplify and reduce the reinforcing in the tower foundation; and
- Specifications of tuned mass dampers were modified based on the results of wind tunnel testing.

Calculations are typically based on the global IBDAS model version 3.3f.

A bridge elevation and plan are shown in Figure 1-1 and longitudinal and transverse tower elevations are shown in Figure 1-2.

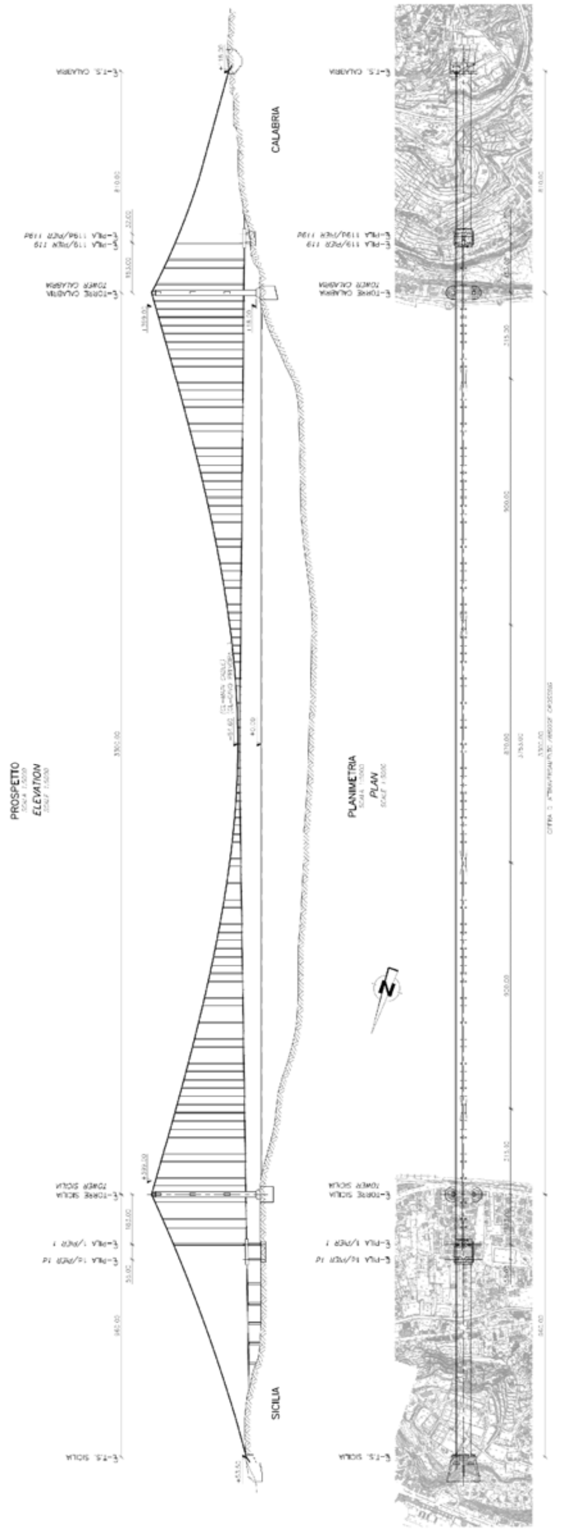

Figure 1-1: Bridge elevation and plan.

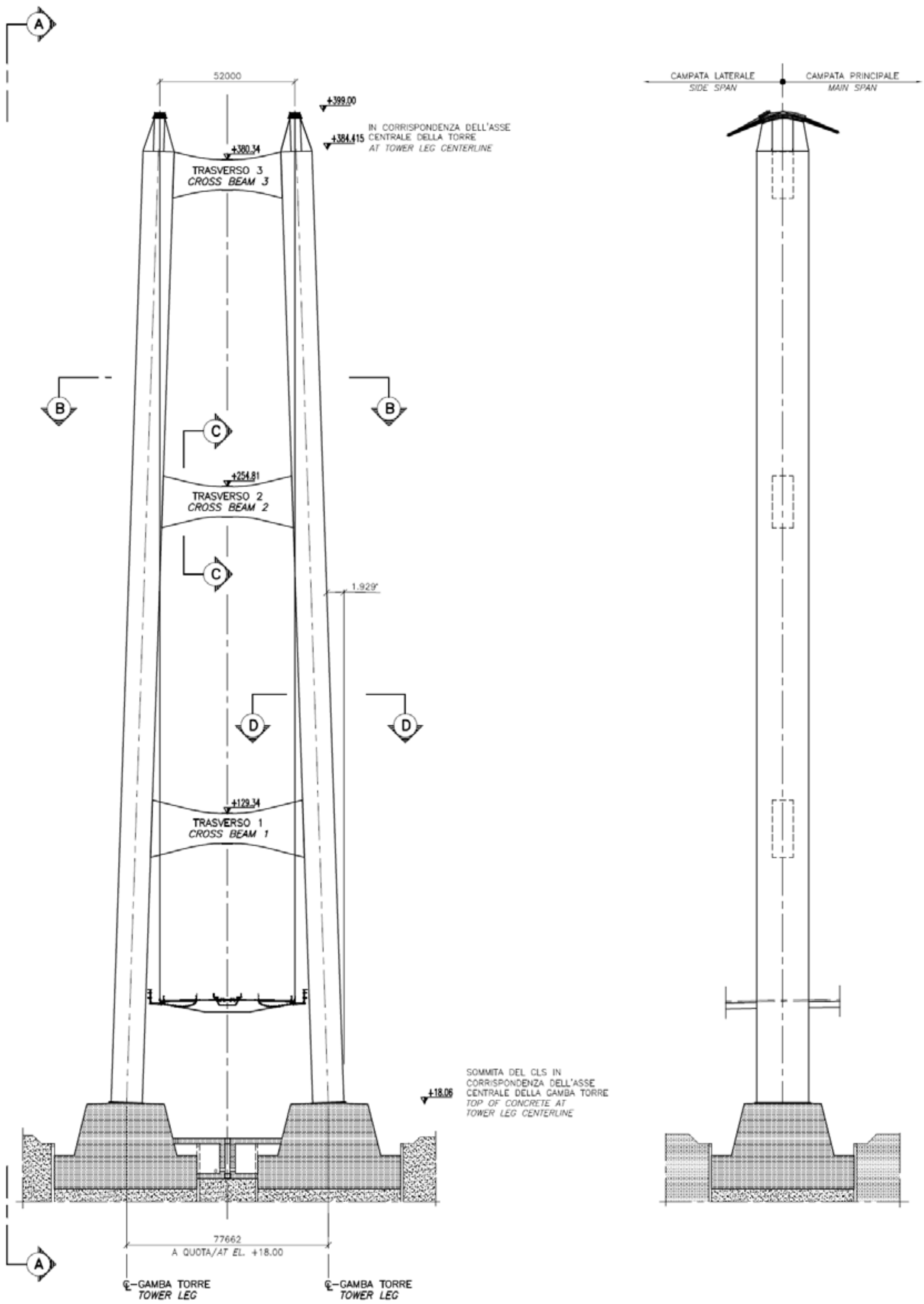

Figure 1-2: Tower elevations.

1.1 Scope

This report describes the design principles for the structural elements of the two main towers, between the top of the concrete foundations (El. +18.06) and the underside of the main cable saddles (El. +384.415).

Design verifications are summarized in CG1000-P-RX-D-P-SV-T4-00-00-00-00-01 “Specialist Technical Design Report – Towers” with more detailed calculations being presented in the design reports for each structural component (tower legs, cross beams and base anchorage).

1.2 Report Outline

This report is organized into the following sections:

- Section 1 includes this introduction, provides a list of reference materials, including design specifications, design codes, material specifications, reference drawings and complementary reports;
- Section 2 provides definitions for terms that are commonly used in referencing particular tower components;
- Section 3 describes the four limit states that are considered in the tower design, serviceability, ultimate, fatigue and structural integrity;
- Section 4 provides descriptions of the materials that are used for each tower component;
- Section 5 provides descriptions of particular aspects of the structural analysis and tower modelling; and
- Section 6 describes the design principles, including philosophy and code references, by which the tower components are verified for the limit states;

1.3 References

1.3.1 Design Specifications

GCG.F.04.01 “Engineering – Definitive and Detailed Design: Basis of Design and Expected Performance Levels,” Stretto di Messina, 2004 October 27.

GCG.F.05.03 "Design Development – Requirements and Guidelines," Stretto di Messina, 2004 October 22.

GCG.G.03.02 "Structural Steel Works and Protective Coatings," Stretto di Messina, 2004 July 30.

CG.10.00-P-RG-D-P-GE-00-00-00-00-00-02 "Design Basis, Structural, Annex," COWI (Current Revision).

1.3.2 Design Codes

"Norme tecniche per le costruzioni," 2008 (NTC08).

EN 1991 Eurocode 1: Actions on Structures – Part 2: Traffic loads on bridges

EN 1993 Eurocode 3: Design of Steel Structures – Part 1-1: General rules and rules for buildings

EN 1993 Eurocode 3: Design of Steel Structures – Part 1-2: General rules – Structural fire design

EN 1993 Eurocode 3: Design of Steel Structures – Part 1-5: Plated structural elements

EN 1993 Eurocode 3: Design of Steel Structures – Part 1-8: Design of joints

EN 1993 Eurocode 3: Design of Steel Structures – Part 1-9: Fatigue

EN 1993 Eurocode 3: Design of Steel Structures – Part 1-10: Selection of steel for fracture toughness and through thickness properties

EN 1993 Eurocode 3: Design of Steel Structures – Part 2: Steel Bridges

EN 1998 Eurocode 8: Design of structures for earthquake resistance – Part 1: General rules, seismic actions and rules for buildings

EN 1998 Eurocode 8: Design of structures for earthquake resistance – Part 2: Bridges

Rete Ferroviaria Italia - Istruzione No. 44F "Verifiche a fatica dei ponti ferroviari"

1.3.3 Material Specifications

EN 10025-1:2004 Hot-rolled products of structural steels – Part 1: General delivery conditions.

EN 10025-2:2004 Hot-rolled products of structural steels – Part 2: Technical delivery conditions for non-alloy structural steels.

EN 10025-3:2004 Hot-rolled products of structural steels – Part 3: Technical delivery conditions for normalized / normalized weldable fine grain structural steels.

EN 10025-4:2004 Hot-rolled products of structural steels – Part 4: Technical delivery conditions for thermomechanical rolled weldable fine grain structural steels.

EN 10164:2004 Steel products with improved deformation properties perpendicular to the surface of the product – Technical delivery conditions.

EN ISO 898-1:2009 Mechanical properties of fasteners made of carbon steel and alloy steel – Part 1: Bolts, screws and studs.

EN 20898-2:1994 Mechanical properties of fasteners – Part 2: Nuts with special proof load values – coarse thread (ISO 898-2:1992).

UNI EN 14399:2005-3 High-strength structural bolting assemblies for preloading - Part 3: System HR - Hexagon bolt and nut assemblies

EN 10138-3:2006 Prestressing steels. Strand

EN ISO 14555:1998 Welding-Arc stud welding of metallic materials. May 1995.

EN ISO 13918:1998 Welding-Studs for arc stud welding-January 1997.

1.3.4 Drawings

The reference tower design drawings for this report are listed in Table 1-1.

Drawing Title	Drawing Number
Tower Sicilia - General Arrangement	CG.10.00-P-AX-D-P-SV-T4-TS-00-00-00-01_0
Typical - Leg - Cross Section & Vertical Joints	CG.10.00-P-WX-D-P-SV-T4-TO-00-00-00-01_0
Tower Sicilia - Leg - Sections & Plate Thicknesses	CG.10.00-P-WX-D-P-SV-T4-TS-00-00-00-01_0
Typical - Leg - Cross Diaphragms	CG.10.00-P-AX-D-P-SV-T4-TO-00-D0-00-01_0
Typical - Leg - Cross Diaphragms, Details	CG.10.00-P-BX-D-P-SV-T4-TO-00-D0-00-01_0
Typical - Leg - Horizontal Joints	CG.10.00-P-AX-D-P-SV-T4-TO-00-00-00-01_0

Typical - Leg - Horizontal Joints, Details	CG.10.00-P-BX-D-P-SV-T4-TO-00-00-00-01_0
Typical - Cross Beam no. 1	CG.10.00-P-AX-D-P-SV-T4-TO-T0-00-00-01_0
Typical - Cross Beam no. 2	CG.10.00-P-AX-D-P-SV-T4-TO-T0-00-00-02_0
Typical - Cross Beam no. 3	CG.10.00-P-AX-D-P-SV-T4-TO-T0-00-00-03_0
Typical - Cross Beams - Details	CG.10.00-P-BX-D-P-SV-T4-TO-T0-00-00-01_0
Typical - Cross Beam Connection to Tower leg	CG.10.00-P-WX-D-P-SV-T4-TO-T0-00-00-02_0
Typical - Connection from Girder	CG.10.00-P-AX-D-P-SV-T4-TO-00-00-00-03_0
Typical - Base Section 1	CG.10.00-P-AX-D-P-SV-T4-TO-00-00-00-04_0
Typical - Base Section 2	CG.10.00-P-AX-D-P-SV-T4-TO-00-00-00-05_0
Typical - Base Section, Details	CG.10.00-P-BX-D-P-SV-T4-TO-00-00-00-02_0
Typical - Top Section	CG.10.00-P-AX-D-P-SV-T4-TO-00-00-00-06_0
Typical - Tuned Mass Dampers - Support Structure	CG.10.00-P-AX-D-P-SV-T4-TO-00-00-00-07_0
Typical - Tuned Mass Dampers	CG.10.00-P-AX-D-P-SV-T4-TO-00-00-00-08_0
Typical - Leg - Steelwork Modifications 1	CG.10.00-P-BX-D-P-SV-T4-TO-00-00-00-04_0
Typical - Leg - Steelwork Modifications 2	CG.10.00-P-BX-D-P-SV-T4-TO-00-00-00-05_0
Typical - Cross Beams - Steelwork Modifications	CG.10.00-P-BX-D-P-SV-T4-TO-T0-00-00-06_0
Tower Calabria - General Arrangement	CG.10.00-P-AX-D-P-SV-T4-TC-00-00-00-01_0
Tower Calabria - Leg - Sections & Plate Thicknesses	CG.10.00-P-WX-D-P-SV-T4-TC-00-00-00-01_0

Table 1-1: Reference tower drawings.

1.3.5 Complementary Reports

The tower design reports listed in Table 1-2 provide supplementary information about the tower design principles and verifications.

Report Title	Report Number
Specialist Technical Design Report, Towers	CG.10.00-P-RX-D-P-SV-T4-00-00-00-00-01
Design Report - Tower Legs incl. Joints and Splices	CG.10.00-P-CL-D-P-SV-T4-00-00-00-00-01
Design Report - Cross Beams	CG.10.00-P-CL-D-P-SV-T4-00-00-00-00-02
Design Report - Tower Base	CG.10.00-P-CL-D-P-SV-T4-00-00-00-00-03

Table 1-2: Reference tower design reports.

2 Nomenclature

The section provides descriptions of terms commonly used throughout the report to refer to various tower components:

Legs – the vertical elements of the towers, extending from the tops of the concrete pedestals at elevation +18.06 to the undersides of the main cable saddles at elevation +384.415.

Cross Beams – the transverse beams connecting the tower legs at elevations +129.34 (Cross Beam 1), +254.81 (Cross Beam 2) and +380.34 (Cross Beam 3). The elevations provided are at the top of the cross beam at the bridge centreline.

Skin Plates – The plates around the perimeter of the tower legs or cross beams (Plates A, B, C and D of the tower legs and the webs and flanges of the cross beams).

Transverse Webs – the vertical transverse plates connecting the two sides of each tower leg; plates G and H. Also referred to more generically as internal plates.

Longitudinal Webs – the vertical longitudinal plates connecting the tower leg skin plates and transverse webs parallel to the bridge axis; plates F and E. Also referred to more generically as a internal plates.

Longitudinal Stiffeners – the longitudinal plate elements used to stiffen the vertical tower leg plates and the flanges and webs of the cross beams.

Transverse Diaphragms – the transverse stiffening elements, typically located in each tower segment 1 m from the construction joint (Type 1), at the cross beam top and bottom flange connections to the tower legs (Type 2 or Type 3) and at the tuned mass damper elevations (Type 4)..

Transverse Stiffeners – the intermediate transverse stiffening elements connected to all tower leg vertical plate elements and longitudinal cross beam plate elements, regularly spaced between the transverse diaphragms.

Construction Joints – the field connected joints between tower leg segments.

Base Anchorage – all components of the connection between the tower leg and the tower foundation, including stiffening plates, anchorage pipes, base plates and multi-strand post-tensioning tendons.

Cable Saddle – the steel weldment over which the main cables pass and which distributes the cable load to the top of the tower leg.

Tie-back – the longitudinal displacement of the towers towards the side spans in the reference dead load condition.

3 Limit States

This section describes the limit states and corresponding performance requirements governing the proportioning of the tower components, in accordance with the project design basis GCG.F.04.01 and NTC08. The tower component performances are verified at Serviceability Limit States, Ultimate Limit States, Fatigue Limit States and Structural Integrity Limit States.

3.1 Serviceability Limit States

NTC08 Section 2.2.2 defines the following Serviceability Limit States (SLS) that are to be evaluated in a structural design:

- Local damage that can reduce the durability of the structure.
- Displacement or deformations that could limit the use of the structure, its efficiency and its appearance.
- Displacement or deformations that could compromise the efficiency and appearance of non-structural elements, plants and machinery.
- Vibrations that could compromise the use of the structure.
- Damage caused by fatigue that could compromise durability.
- Corrosion and/or excessive deterioration in materials due to atmospheric exposure.
- The project design basis GCG.F.04.01 Section 3.1 specifies the performance requirements for the structure under two levels of serviceability, or normal usage loads. The SLS performance requirements are listed in Table 3-1.

Limit State	Performance Requirement
SLS1	Road and rail runability is guaranteed. No structural damage. Structure remains elastic and all deformations are reversible.
SLS2	As for SLS1 except that only rail runability is guaranteed.

Table 3-1: SLS performance requirements.

Limit state SLS2 is used to verify tower components for temporary construction conditions and for the verification of particular components in the completed bridge.

The specific SLS that are verified for the tower components are:

- Stresses on effective cross-sections are all less than the material yield strength.
- Wind induced vortex shedding vibrations on the freestanding tower cause accelerations less than 0.5 m/s^2 under the SLS1 wind speed of 44 m/s, in accordance with GCG.F.05.03 Section 6.1.4.
- Pre-compression of the tower base anchorage is maintained.
- Fatigue related SLS are addressed in Section 3.3.

3.2 Ultimate Limit States

NTC08 Section 2.2.1 defines the following Ultimate Limit States (ULS) that are to be evaluated in a structural design:

- Loss of equilibrium of the structure or part of it.
- Excessive displacement or deformation.
- Arrival at the maximum resistance capacity of parts of the structure, joints or foundations.
- Arrival at the maximum resistance capacity of the structure as a whole.
- Arrival at ground collapse mechanisms.
- Failure of frames and joints due to fatigue.

- Failure of frames and joints due to other time-related effects.
- Instability of parts of the structure or structure as a whole.
- The project design basis GCG.F.04.01 Section 3.1 specifies the performance requirements for the structure under ultimate or rare loads. The performance requirements are listed in Table 3-2.

Limit State	Performance Requirement
ULS	Temporary loss of serviceability is allowed. The main structural system maintains its full integrity. Structural damage to secondary components is repairable by means of extraordinary maintenance works.

Table 3-2: ULS performance requirements.

The specific ULS that are evaluated for the tower components are:

- Stresses on effective cross-sections are not greater than the design material yield strength.
- Pre-compression of the tower base anchorage is maintained.
- Bolted connections that are slip-resistant at ULS do not slip.
- Bolt shear and plate bearing capacities are not less than demands for bolted connections that are slip resistant at SLS.
- Welded connections provide sufficient capacity.

Fatigue related ULS are addressed in Section 3.3.

3.3 Fatigue Limit States

NTC08 Sections 2.2.1 and 2.2.2 due not distinguish fatigue limit states (FLS) from serviceability and ultimate limits states with similar consequences and performance requirements. However, in NTC08 Section 4.2.2.1 and in this report, FLS are distinguished because the loads and load combinations used for verification are different, as are the means by which the elements are verified. NTC08 Sections 2.2.1 and 2.2.2 define the following fatigue related SLS and ULS that are to be evaluated in a structural design:

- Damage caused by fatigue that could compromise durability (SLS).
- Failure of frames and joints due to fatigue (ULS).

The specific FLS that are evaluated for the tower components are:

- Slip-critical bolted connections do not slip under SLS loads.
- Pre-compression of the tower base anchorage is maintained under SLS loads.
- Steel stresses under fatigue loading are not greater than the stress limit for the design details used and the expected number of cycles.

3.4 Structural Integrity Limit States

Consideration of Structural Integrity Limit States (SILS) is unique to this project and is a result of the structure's exceptional size and importance. These limit states are not considered in NTC08 and are described only in the project design basis. In general, the limit states considered are similar to those considered at the ULS, particularly for the tower, however, the return periods for the applied loads are longer (i.e., higher wind speeds and peak ground accelerations) and the performance criteria are relaxed from those applicable at the ULS. The performance requirements are listed in Table 3-3.

Limit State	Performance Requirement
SILS	Complete loss of serviceability, even protracted in time, is permitted. The survival of the following elements of the main structural system must be guaranteed: restraint and support system, main cables, saddles.

Table 3-3: SILS performance requirements.

The only difference in the ULS and SILS verification methods is that all material partial factors are assumed equal to 1.0 for the SILS verifications reflecting the fact that the design basis (GCG.F.04.01) Table 6 permits increased damage levels under the SILS. For the majority of the tower structural components damage is undesirable at any limit state; however, it is appropriate to allow the materials to achieve their nominal capacities under the rare and extreme loads considered at the SILS. This approach is consistent with that often used in designing major bridges for rare and extreme loads.

The specific SILS that are evaluated for the tower components are:

- Stresses on effective cross-sections are not greater than the nominal material yield strength.
- Pre-compression of the tower base anchorage is maintained.
- Bolted connections that are slip-resistant at ULS do not slip.
- Bolt shear and plate bearing capacities are not less than demands for bolted connections that are slip resistant at SLS.
- Welded connections provide sufficient capacity.

4 Materials

The mechanical properties of the tower construction materials are described in this section.

4.1 Structural Steel

Tower structural components are generally fabricated from Grade S460 ML structural steel with the exception of: the hot-rolled circular hollow sections comprising the cross beam internal bracing members, the tower base plate and the base anchorage stiffening plates, which are fabricated from Grade S355 ML structural steel. All structural steels shall be produced in accordance with EN 10025-4. The steels are assumed to have the mechanical properties listed in Table 4-1, in accordance with NTC08 Section 11.3.4.1. As an exception to the standard requirements of NTC08 and EN 10025-4 the mechanical properties of the steel shall not vary with material thickness for thicknesses up to 110 mm for S460ML steel and up to 150 mm for S355ML steel. The feasibility of the production of steel with the required properties has been confirmed.

Grade	Yield Strength, f_{yk} (MPa)	Tensile Strength, f_{tk} (MPa)
S 355 ML	355	470
S 460 ML	460	540

Table 4-1: Structural steel mechanical properties for thicknesses up to 110 mm for S460ML steel and up to 150 mm for S355ML steel.

All structural steel is also assumed to have the following properties, in accordance with NTC08 Section 11.3.4.1:

- Elastic modulus: $E = 210{,}000$ MPa

- Poisson's ratio: $\nu = 0.3$
- Shear modulus: $G = 80{,}770$ MPa
- Coefficient of thermal expansion: $\alpha = 12 \times 10^{-6} / °C$
- Density: $\rho = 7{,}850$ kg/m^3

The material partial factors (safety coefficients) used to verify structural steel elements are in accordance with NTC08 Sections 4.2.4.1.1, 4.2.4.1.4 and are listed in Table 4-2.

Verification	Partial Factor
Resistance of Class 1, 2, 3 and 4 sections	$\gamma_{M0} = 1.05$
Resistance to instability of members in road and rail bridges	$\gamma_{M1} = 1.10$
Resistance to fracture of sections under tension (weakened by holes)	$\gamma_{M2} = 1.25$
Fatigue resistance (useful fatigue life criterion with significant failure consequences)	$\gamma_{mf} = 1.35$

Table 4-2: Material partial factors for structural steel.

4.2 High Strength Bolts

High strength structural bolts of Grade 8.8 or Grade 10.9, produced in accordance with EN ISO 898, are used for all bolted connections and splices. Grade 8.8 bolts are used for connections of all non-structural components to the towers and Grade 10.9 bolts are used for the tower leg construction joint splices (except for the skin plates splices, which are welded). High strength bolts are assumed to have the mechanical properties listed in Table 4-3, in accordance with NTC08 Section 11.3.4.6.1 (except for the Grade 8.8 yield strength, which is incorrectly stated in NTC08).

Grade	Yield Strength, f_{yb} (MPa)	Tensile Strength, f_{tb} (MPa)
8.8	640	800
10.9	900	1000

Table 4-3: Structural bolt mechanical properties.

The material partial factors (safety coefficients) used to verify bolted connections and splices are in accordance with NTC08 Section 4.2.8.1.1 and are listed in Table 4-4.

Verification	Partial Factor
Resistance to bolt shear	$\gamma_{M2} = 1.25$
Resistance to bolt tension	
Resistance to bearing on plates	
ULS slip resistance	$\gamma_{M3} = 1.25$
SLS slip resistance	$\gamma_{M3} = 1.15$
Bolt preload force	$\gamma_{M7} = 1.10$

Table 4-4: Material partial factors for bolted connections and splices.

4.3 Post-tensioning Strand

All post-tensioning strands shall conform to the requirements of EN 10138-3. Post-tensioning strands are assumed to have the following mechanical properties:

- Nominal Yield Strength, $f_{py} = 1636$ MPa
- Ultimate Strength, $f_{pk} = 1860$ MPa
- Elastic modulus: $E = 195000$ MPa

Post-tensioning strands are proportioned considering a partial safety factor on their effective tension at the ULS/SILS of 1.1.

4.4 Welding Consumables

Welding consumables shall comply with the requirements of EN 1993-1-8 Section 4.2.

Welding procedures shall be selected so as to not reduce the properties of the thermo-mechanically processed plates.

The material partial factor, $\gamma_{M2} = 1.25$, used to verify welded connections and splices is in accordance with NTC08 Section 4.2.8.1.1.

5 Structural Analysis

The Messina Strait Bridge was modelled and analysed in the COWI proprietary analysis program IBDAS (Integrated Bridge Design and Analysis System). This section describes the approach to selected aspects of the structural analysis that affect the tower design. The bridge model and structural analysis, in general, are described in the report "CG.10.00-P-RG-D-P-SV-00-00-00-00-00-01 Global IBDAS Model, Description."

5.1 Load Combinations

The tower structural components are verified for the load combinations listed in the design basis (GCG.F.04.01) Section 6.8. The load components considered in the load combination tables are defined in Table 5-1. The combinations and associated partial factors for each load component are presented in Table 5-2, Table 5-3 and Table 5-4, respectively for SLS, ULS and SILS. The partial factor μ can take the value of 0.95 or 1.15 for steel components or 0.95 or 1.25 for concrete components, depending on whether the dead load causes a relieving or adverse effect. A hyphen in a cell under a load component column indicates that the load component is not included in the combination represented by the row. The SLS1 load combinations defined in the design basis are not used for the verification of any tower components and therefore are not provided below.

Component	Definition
PP	Self weight
PN	Self weight of non-structural elements
QL	Actions for the local sizing of the structural system (strength and deformation at the micro- and meso-level). Not relevant for tower design.
QA	Dense variable load. Actions for the global sizing of the structural system and for serviceability checks (Strength and deformation at the macro-level)
QR	Rarefied variable load. Actions for the global sizing of the structural system and for serviceability checks (Strength and deformation at the macro-level)
VV	Wind action
VS	Seismic action
VT	Thermal action
A	Accidental Actions

Table 5-1: Load components.

Combo	PP	PN	QR	QA	VV	VS	VT	A
1	1	0 / 1	-	-	-	-	0 / 1	-
2	1	0 / 1	-	-	1	-	0 / 1	-
3	1	0 / 1	-	-	-	1	0 / 1	-
4	1	1	-	1	-	-	0 / 1	-
5	1	1	-	1	1	-	0 / 1	-
6	1	1	-	1	-	1	0 / 1	-

Table 5-2: SLS2 load combinations.

Combo	PP	PN	QR	QA	VV	VS	VT	A
1	μ	0 / 1.5	-	-	-	-	0 / 1	-
2	μ	0 / 1.5	-	-	1	-	0 / 1	-
3	μ	0 / 1.5	-	-	-	1	0 / 1	-
4	μ	0 / 1.5	-	-	-	-	0 / 1	1
5	μ	0.9 / 1.5	-	1.5	-	-	0 / 1	-
6	μ	0.9 / 1.5	-	1.1	1	-	0 / 1	-
7	μ	0.9 / 1.5	-	1.1	-	1	0 / 1	-
8	μ	0.9 / 1.5	1	-	-	-	0 / 1	1

Table 5-3: ULS load combinations.

Combo	PP	PN	QR	QA	VV	VS	VT	A
1	μ	1	1	-	1	-	0 / 1	-
2	μ	1	1	-	-	1	0 / 1	-
3	μ	1	1	-	-	-	0 / 1	1

Table 5-4: SILS load combinations.

5.2 Global Behaviour

The design of most tower components is based on the results of the global bridge model analysed with IBDAS. This section describes the modelling of the following key global behavioural aspects of the towers:

- Second Order Effects and Imperfections

- Aerodynamics
- Consideration of the Permanent Tie-Back
- Seismic Analysis

5.2.1 Second Order Effects and Imperfections

This section presents an analytical procedure for combining the effects of flexural buckling with the axial loads and bending moments determined from a second order analysis completed with the global IBDAS model, based on the theoretical tower geometry. Consideration of geometric and structural imperfections is described in NTC08 Section 4.2.3.5; however, the provided provisions are not appropriate for assessing such effects for the towers. The presented procedure is consistent with Eurocode provisions for designing a column. However, the standard column-curve based Eurocode provisions were developed for pin ended columns of constant cross-section, and are not appropriate for the towers. The presented procedure calculates equivalent imperfections explicitly and considers the actual boundary conditions and variation of the cross-section properties with elevation.

EN 1993-2 Section 5.3.1(1) requires that appropriate allowances be incorporated in the structural analysis to consider the effects of imperfections, including residual stresses and geometrical imperfections. Section 5.3.1(2) specifies that “equivalent geometric imperfections” should be used and Section 5.3.2(11) states that the structure’s elastic critical buckling mode shape may be applied as a unique global and local imperfection. This approach is used to properly capture the effects of imperfections because it best represents the structural behaviour, applying the axial load induced second order moments in the same form as the buckling mode curvatures.

Provided the material remains elastic and the correct total axial load is considered, the effects of independent imperfections may be added together, as is apparent from the elastic amplification equation:

$$\left(\frac{e_a + e_b}{1 + N/N_{cr}}\right) = \left(\frac{e_a}{1 + N/N_{cr}}\right) + \left(\frac{e_b}{1 + N/N_{cr}}\right)$$

where e_a and e_b are independent elastic imperfections, N is the applied axial load and N_{cr} is the critical elastic buckling load.

Moments and stresses from the IBDAS output can be combined with corresponding bending moments and stresses due to the equivalent imperfection, which are calculated using the following additional IBDAS model outputs:

- Eigenvectors of deflections, bending moments and axial loads for the critical buckling mode;
- Critical elastic buckling load determined from the eigen-buckling analysis; and
- Total factored axial load for the each load combination.

The imperfections are called “equivalent imperfections” to distinguish them from the actual geometrical imperfections achieved during construction.

The proposed method uses the IBDAS non-linear analysis output and adds bending moments and axial loads to account for the flexural buckling effects. These moments are calculated from the total axial load in each load combination multiplied by the amplified equivalent initial imperfections. This procedure allows the IBDAS global model to be run without tower imperfections.

The equivalent initial imperfection is calculated so that the tower buckling resistance, in the absence of other bending moments, is equal to the buckling resistance that would be calculated using EN 1993-1-1 Section 6.3.1 with $\gamma_{M1} = 1.10$ and N_{cr} calculated for the tower, with the top restrained longitudinally, and the effective section properties calculated at the elevation of the maximum buckling induced compressive stresses, referred to as the “key” cross-section. For longitudinal buckling, this is at approximately the middle of the upper 70% of the tower height or at the tower base, depending on the foundation stiffness. For transverse buckling, this is just above or just below a cross beam or at the tower base.

EN 1993-1-1 Section 5.3.2(11) indicates that the imperfection “may” be calculated according to Equations 5.9, 5.10 and 5.11. These equations give the same failure load as the buckling curves in Section 6.3.1 when the check is made using the partial safety factor for buckling, γ_{M1}. The design of stiffened plate elements is governed by EN 1993-1-5, which is referenced in EN 1993-2 Section 6.5 for the plate buckling verification of members at the ultimate limit state. Cross section verifications using EN 1993-1-5 Section 4.6 are based on the partial safety factor for cross-sectional resistance, γ_{M0}, which equals 1.05 for bridges, in accordance with NTC08 Section 4.2.4.1.1. Therefore, the imperfection that is calculated from the buckling resistance, $N_{b,Rd}$, calculated in accordance with in EN 1993-1-1 Section 6.3.1 using $\gamma_{M1} = 1.10$, is larger than that which would apply to a column if cross-section verifications were based on γ_{M1}. The effect on the equivalent imperfection of using γ_{M1} to calculate the buckling capacity and γ_{M0} to verify cross-section capacities is illustrated by a sample calculation of imperfections in Appendix A.

5.2.1.1 Effect of Varying Axial Load in the Tower Legs

The tower leg axial force varies with elevation for two reasons:

1 The self weight increases continuously towards the tower base; and

2 Lateral loads cause shears in the cross beams that cause step-wise increases in tower leg axial forces.

The elastic critical buckling load is affected by the axial force distribution. However, the axial force variation between load combinations is sufficiently small that the effect on the elastic critical buckling loads (for the dominant modes) is very small and the effect on the stresses is insignificant.

5.2.1.2 Calculation Procedure

Ideally, the relative slenderness parameter, $\bar{\lambda}$, could be calculated in accordance with EN 1993-1-1 Section 6.3.1.2. However, the application of the provisions to a longitudinally stiffened column is not described. The buckling resistance of a longitudinally stiffened column with closely spaced transverse stiffeners/diaphragms is greater than the same column with widely spaced transverse stiffener/diaphragm. However, for loads less than that causing buckling of the longitudinal stiffeners, the behaviour is unrelated to transverse stiffener spacing. Therefore, the column area considered in the calculation of the equivalent imperfection is the effective cross-section area reduced only for plate buckling, $A_{eff} = A_{rp}$. This is equivalent to the area calculated using EN 1993-1-5 Eq. 4.5 with $\rho_c = 1.0$.

CALCULATE THE ELASTIC CRITICAL BUCKLING LOAD, N_{cr}, FOR THE TOWER

The elastic critical buckling load is calculated using an eigen-buckling analysis performed with the global IBDAS model considering the following boundary conditions:

- Translational restraint at the tower top in the bridge longitudinal direction (restraint provided by the main cables, which allow negligible translation in the buckling modes considered);
- Laterally unrestrained tower top; and

- Restrained tower base, as in the global model, to represent the correct foundation stiffness.

The section properties used should be based on the gross cross-section to comply with EN1993-1-1 Section 6.3.1.2(1).

The output required from the buckling analysis is the elastic critical buckling load, N_{cr}, and the eigen-vectors of deflection, bending moment and axial load for :

- The first buckling mode in the plane of the bridge centreline; and
- The lowest two buckling modes perpendicular to the plane of the bridge centreline. The lowest two modes are used because, although the elastic critical buckling load varies little between the modes, the resulting tower leg bending moment diagrams vary considerably.

The higher buckling modes are excluded from the analysis as the associated elastic critical loads are significantly higher.

CALCULATE THE EFFECTIVE AREA AT THE ELEVATION OF MAXIMUM COMPRESSIVE STRESS

Longitudinal Buckling

The height at which the maximum buckling induced compressive stress occurs in the buckled tower is determined from the eigen-vector of bending moments and the design axial load. The effective area, A_{rp}, at this "key" cross-section is determined in accordance with EN 1993-1-5 Section 4.

Lateral Buckling

The height at which the maximum bending moment occurs in the buckled tower is determined from the eigen-vectors of bending moments. The effective area, A_{rp}, at this "key" cross-section is determined in accordance with EN 1993-1-5 Section 4. The effective area at this cross-section is used to calculate the governing relative slenderness. Because the tower is of constant cross-section dimensions, the highest stress demands typically occur at the sections with maximum buckling moments, which occur just above or below the cross-beams or at the tower base.

CALCULATE THE RELATIVE TOWER SLENDERNESS FROM THE TOP TO THE BASE

The relative slenderness is calculated from $\bar{\lambda} = \sqrt{\dfrac{A_{rp} \cdot f_y}{N_{cr}}}$

CALCULATE THE FLEXURAL BUCKLING RESISTANCE

The flexural buckling resistance, $N_{b,Rd}$, is calculated in accordance with EN 1993-1-1 Section 6.3.1.1 (Eq. 6.48):

$$N_{b,Rd} = \frac{\chi A_{eff} f_y}{\gamma_{M1}} = \frac{\chi A_{rp} f_y}{\gamma_{M1}}$$

where χ is the buckling reduction factor based on the relative slenderness parameter and calculated for longitudinal and lateral buckling using Eq. 6.49, and all other variables are as previously defined. The buckling reduction factor is a function of the imperfection factor, α, which is selected based on the type of steel section being considered. The tower leg sections do not comprise any more longitudinal welding relative to their cross-section area than do typical welded steel box sections, and so the corresponding column buckling curve "b" is assumed to apply equally to the tower legs. The imperfection factor from Table 6.1 for column buckling curve "b" is 0.34.

CALCULATE THE MAXIMUM VALUE OF THE EQUIVALENT IMPERFECTION

The equivalent imperfection, e_0, is calculated so that the sum of the axial compressive stress, N_{Ed}/A_{rp}, and bending compressive stress, M_{Ed}/W_{rp}, at the "key" cross-section is equal to the design yield stress, f_y/γ_{M0}, when the axial load at the "key" cross-section is $N_{b,Rd}$ and no other loads are applied; considering the tower cross-section with the area, A_{rp}, and section modulus, W_{rp}, reduced for plate buckling only. This can be written for a symmetrical cross-section as:

$$\frac{N_{Ed}}{A_{rp}} + \frac{M_{Ed}}{W_{rp}} = \left(\frac{f_y}{\gamma_{M0}}\right)$$

This equation is identical to EN 1993-1-5 Eq. 4.14 for doubly symmetric cross-sections, for which the shift in the centroidal axis, e_n, is zero:

$$\frac{N_{Ed}}{\left(\frac{f_y A_{rp}}{\gamma_{M0}}\right)} + \frac{M_{Ed} + N_{Ed} e_N}{\left(\frac{f_y W_{rp}}{\gamma_{M0}}\right)} = 1$$

For the symmetric tower leg sections, the gross and effective section centroidal axes are the same and therefore $e_N = 0$ and:

$$\frac{N_{Ed}}{\left(\frac{f_y A_{rp}}{\gamma_{M0}}\right)} + \frac{M_{Ed}}{\left(\frac{f_y W_{rp}}{\gamma_{M0}}\right)} = 1$$

replacing the denominators in the above equation with $N_{rp,Rd} = \left(f_y A_{rp} / \gamma_{M0}\right)$ and $M_{rp,Rd} = \left(f_y W_{rp} / \gamma_{M0}\right)$ gives:

$$\frac{N_{Ed}}{N_{rp,Rd}} + \frac{M_{Ed}}{M_{rp,Rd}} = 1$$

Replacing the design compressive force, N_{Ed} with the buckling load, $N_{b,Rd}$, and the design moment, M_{Ed}, with the buckling moment, $N_{b,Rd} e_0 \left(1 - N_{b,Rd} / N_{cr}\right)^{-1}$ gives:

$$1 = \frac{N_{b,Rd}}{N_{rp,Rd}} + \frac{N_{b,Rd} \cdot e_0}{M_{rp,Rd}} \cdot \left(\frac{1}{1 - N_{b,Rd} / N_{cr}}\right)$$

which can be solved for the equivalent imperfection:

$$e_0 = \left(1 - \frac{N_{b,Rd}}{N_{rp,Rd}}\right) \cdot \left(1 - \frac{N_{b,Rd}}{N_{cr}}\right) \cdot \left(\frac{M_{rp,Rd}}{N_{b,Rd}}\right)$$

Prior to the submission of the final design documents, Stretto di Messina requested that the partial safety factor for cross-section verifications in accordance with EN 1993-1-5 Section 4.6 be increased to from 1.05 to 1.10. This change does not affect the equation presented for determining the equivalent imperfection, e_0; however, the cross-section axial load and moment capacities used in the equation must be based on γ_{M1} as shown below:

$$N_{rp,Rd} = \left(f_y A_{rp} / \gamma_{M1}\right)$$

$$M_{rp,Rd} = \left(f_y W_{rp} / \gamma_{M1}\right)$$

Although this change results in a decrease in the design stress capacity for the tower leg components, this increased conservatism is partially offset by the decrease in global buckling induced moments that are considered in the cross-section verifications.

CALCULATE THE BENDING MOMENTS DUE TO THE EQUIVALENT IMPERFECTION

The maximum buckling moment is calculated from the equivalent initial imperfection and the distribution of buckling moments is derived from the eigenvector of bending moments of the relevant buckling modes.

The maximum moment, M_{hk}, is calculated at the “key” section from the initial imperfection:

$$M_{hk} = \frac{N_{Ed,hk} \cdot e_0}{1 - N_{Ed,hk} / N_{cr}}$$

where the subscript “hk” indicates that the parameter is to be calculated at the “key” section and $N_{Ed,hk}$ is the key section axial force for each load combination

At a cross-section at elevation “h”, the buckling moment effect is: $M_h = M_{hk} \dfrac{\eta_{Mh}}{\eta_{Mhk}}$

where η_{Mhk} is the value of the eigen-vector for bending moment at the “key” section and η_{Mh} is the value of the eigen-vector for bending moment at height “h”.

The maximum tower buckling moment occurs at mid-height of the top 70% of the tower or at the tower base. The bending moments, axial load and section properties are different at these two locations and so the buckling stresses are checked at both locations to ensure that the critical “key” section is correctly identified.

The buckling moment eigenvector gives zero bending stresses at the inflection point, located at approximately 0.3H from the tower base. The analysis method presented would suggest that there are zero buckling effects at this location. However, considering realistic construction tolerances, it would be unsafe to ignore the presence of some imperfection related stresses at the inflection point. Therefore, the bending stress caused by the geometric construction tolerance is considered as the minimum value. For simplicity, the geometric construction tolerance is taken as H/2000 for longitudinal buckling and 1/2000 of the distance between cross beams for transverse buckling.

5.2.2 Aerodynamics

The tower behaviour, during and after construction, was investigated through 1:100 scale section model tests on the tower leg cross-section and 1:100 and 1:200 scale aeroelastic model tests of the free-standing towers. The tower model tests were completed by BMT Fluid Mechanics Ltd, in Teddington, UK (section model tests and 1:200 scale aeroelastic tests), the National Research Council in Ottawa, Canada (1:100 scale aeroelastic tests) and the Boundary Layer Wind Tunnel Laboratory in London, Canada (1:200 scale aeroelastic tests). The section model tests were used to confirm wind load coefficients. The current verification work is based on these updated wind load coefficients. These coefficients are summarized for the tower legs in Table 5-5. Coefficients are provided for drag, representing the along wind force, and lift, representing the across wind force. Both the drag and lift forces are normalized by the 20 m tower leg dimension to give the wind load coefficients. The upwind leg coefficients were determined from a section model test that included only one leg. The total wind load coefficients were determined from a section model test that included both tower legs. The downwind leg coefficients were determined by subtracting the upwind leg coefficient from the total coefficient for each wind angle. Additional details can be found in CG.10.00-P-CL-D-P-SB-S3-00-00-00-00-01 “Aerodynamic calculations.”

The aeroelastic model tests were performed to evaluate the susceptibility of the freestanding and completed bridge tower to vortex shedding induced vibrations and to determine the amount of additional damping that must be provided to limit these vibrations to an acceptable level. The aeroelastic tests indicate that additional damping must be provided during tower construction to reduce accelerations to below the 0.5 m/s^2 limit specified in GCG.F.05.03 Section 6.1.4. The aeroelastic tests also indicate vortex shedding induced vibrations in the completed bridge at full scale wind speeds of approximately 40 m/s and 65 m/s. The vibrations expected to occur at a wind speed of 40 m/s will be fully mitigated by the provision of eight tuned mass dampers in each tower leg. Each damper will have a mass of approximately 35 tonnes, a frequency of 0.466 Hz and will have 11% modal damping. Although the tuned mass dampers will reduce vibrations amplitudes at a wind speed of 65 m/s, accelerations are still expected to exceed 0.5 m/s^2. Therefore, the resulting additional stresses caused by the vibration deformations are considered as part of the global wind response considered in the tower leg and cross beam designs. Because the vortex shedding response is evaluated based on smooth flow conditions, the total wind load response considers the following two mutually exclusive conditions:

1 Static wind response combined with dynamic wind response; and

2 Static wind response combined with additional forces due to vortex shedding induced vibrations.

Angle (deg)	Total		Upwind Leg		Downwind Leg	
	C_D	C_L	C_D	C_L	C_D	C_L
0.0	1.8	0.0	1.8	0.0	0.0	0.0
5.0	1.7	0.0	1.7	0.2	0.0	-0.2
10.0	1.6	0.1	1.6	0.3	0.0	-0.3
15.0	1.8	0.3	1.4	0.5	0.4	-0.2
20.0	1.9	0.3	1.4	0.5	0.5	-0.2
25.0	2.0	0.3	1.4	0.4	0.6	-0.1
30.0	2.0	0.4	1.3	0.4	0.7	-0.1
35.0	1.9	0.3	1.2	0.4	0.7	-0.1
40.0	1.9	0.3	1.1	0.3	0.8	0.0
45.0	1.7	0.2	1.0	0.3	0.7	-0.1
50.0	1.5	0.1	0.8	0.2	0.7	-0.1
55.0	1.1	0.0	0.6	0.1	0.5	-0.1
60.0	0.8	0.2	0.4	0.3	0.4	-0.1
65.0	0.7	0.0	0.4	0.1	0.3	-0.1
70.0	0.7	0.5	0.3	0.0	0.4	0.5
75.0	0.4	0.5	0.3	0.3	0.3	0.1
80.0	0.5	0.9	0.2	0.5	0.3	0.4
85.0	0.6	0.6	0.3	0.3	0.3	0.3
90.0	0.6	0.0	0.3	0.0	0.3	0.0

Table 5-5: Tower leg wind load coefficients.

The effects of vortex shedding were determined by scaling the appropriate vibration modes by the expected maximum deformation amplitudes. The results of the wind tunnel test show that the vortex shedding vibrations expected to occur at a wind speed of 65 m/s will result in the maximum displacement amplitudes shown in Table 5-6.

Mode	Frequency	Maximum Displacement Amplitude
Mode # 164 (Transverse)	0.604 Hz	140 mm
Mode # 126 (Longitudinal)	0.477 Hz	30 mm

Table 5-6: Maximum displacement amplitudes due vortex shedding

The tower components are proportioned for the governing effects of the dynamic and vortex shedding wind load combinations.

5.2.3 Tower Top Tie-Back during Construction

The considerable difference in main and side span lengths results in considerable imbalances in the design stresses on the main span and side span sides of the tower leg cross-section. The maximum inward (bending towards the main span) and outward (bending towards the side span) leaning moments in the tower legs are of similar magnitude, but the maximum inward leaning moments result from maximum dead load in the main span and the maximum outward leaning moments result from minimum dead load in the main span. Thus, the maximum and minimum moments coexist with very different axial stresses, resulting in the imbalanced governing stresses. To approximately equilibrate the maximum design stresses on the main and side span sides of the cross-section, and thus reduce the maximum design stress, the tower tops are tied back prior to the main cable installation so that under dead load conditions in the completed bridge they remain leaning slightly towards the side spans.

The tower legs are fabricated without camber and are constructed vertically. The tie-back is introduced after completion of the tower leg construction via cables connecting the tower tops to the ground at or near the main cable anchor blocks. The tie-back cables remain in place until after the main cable installation, after which they are removed, transferring their load to the side span main cables.

At installation, the tie-back cables are stressed to achieve a tower top displacement in the completed bridge that results in the desired tower leg longitudinal moment distribution in the reference dead load condition. This process results in the towers leaning slightly towards the side spans in the completed bridge. The displacement initially imposed by the tie-back cables is larger than the final tower top displacement because of the elongation of the side span main cables that occurs during deck erection. In the reference dead load condition of the completed bridge, the tower leg longitudinal moments that compensate for the otherwise unbalanced governing compressive stresses are produced by a combination of a locked-in shear force applied by the main cables and the first and second-order moments caused by the axial loads acting on the out-of-plumb tower.

5.2.4 Seismic Analysis

The general concept submission tower design was based on the response spectrum analysis with the design spectra specified in the Design Basis. The analysis was performed assuming 5% viscous damping for all vibration modes. Subsequent to the general concept submission the tower design has been updated based on the non-linear time-history seismic analysis. The time-history analysis allows the behaviour of the deck buffers and foundation stiffness and damping to be more appropriately considered. The analysis model includes the effects of the tuned mass dampers provided to mitigate vortex shedding vibrations.

The time-history analysis uses time histories compatible with the design spectra specified in the Design Basis and attached to the document DT.ISP.S.I.R2.001 "Storie temporali dell'azione sismica". The 1992 Tender Documents provide four sets of input time histories for the Calabria shore and four sets for the Sicily shore. These eight inputs are all compatible with the same design spectrum specified for both shores and therefore they are treated as eight independent inputs, allowing the average results of the eight analyses to be used for design in accordance with EN 1998-2 Section 4.2.4.3. On account of the exceptional importance of the bridge, the towers will also be assessed for the envelope of the time-history analysis results considering all material partial factors equal to 1.00. The objective of this additional assessment is to identify the extent of damage that might be caused by a larger than anticipated seismic event.

The suspended deck is very flexible, and seismic responses of the two towers are essentially decoupled. Therefore, the effects of multi-support excitations (due to different soil conditions, time shift or incoherence) during an actual seismic event would be insignificant for seismic responses of the towers and each set of input time histories is applied to all supports for each analysis.

The 5% damped response spectrum for each horizontal time-history input is compared to the target ULS design spectra in Figure 5-1 to Figure 5-8 for periods up to 10 s. The provided horizontal time-history components are labelled as component 1 and component 2 (directions 1 and 2 in the figures), with no indication of whether they are longitudinal or transverse to the bridge axis; however, given that all inputs are compatible with the same design spectrum the particular directionality of the horizontal components will have negligible effect on the average time-history results. For the analyses completed it has been assumed that direction 1 is parallel to the bridge axis and direction 2 is transverse to the bridge axis. The spectrum of each time-history input deviates slightly from the target design spectrum throughout the full period range with no bias towards being more or less severe than the target. Dispersions of the time-history inputs contribute to variability in the time-history responses of the structure. This contribution must be considered when evaluating the overall statistical characteristics of the tower responses to the eight inputs.

The average 5% damped spectrum of the eight time-history inputs is compared to the target design spectrum in Figure 5-9. Also included in Figure 5-9 on the secondary vertical axis are the standard deviation and coefficient of variation (COV) of the time-history inputs as a function of period. The average time-history input spectrum is very consistent with the target design spectrum, suggesting that the average time history force effects should provide an appropriate representation of the target design level. As expected the standard deviation of the time-history spectra decrease with increasing period. The COV of the time-history spectra remain relatively constant at 6%-7% for the periods of relevance to the tower design. These comparisons have been made on the basis of an assumed constant 5% damping. In reality the Rayleigh damping that is used in the time-history analysis is not constant and so the deviations of the mean input spectrum from the target spectrum will be larger, resulting in additional dispersion of the time-history results. If the 5% horizontal design spectrum is converted to a 2% horizontal design spectrum (which is more representative of the damping governing most tower modes) using the amplification factor of 1.32 as is indicated in the 1992 seismic study by Stretto di Messina (see Section 4.2.1.3 of Specifiche progettuali per l'Opera di Attraversamento), the mean 2% damped spectrum of the time-history inputs is still very consistent with the target spectrum, however, the COV of the time-history inputs in the period range most relevant to the tower design increases to approximately 12% for the case of 2% damping. The 2% design spectrum and mean time-history spectrum are shown in Figure 5-10 with the time-history spectra standard deviation and COV as a function of period.

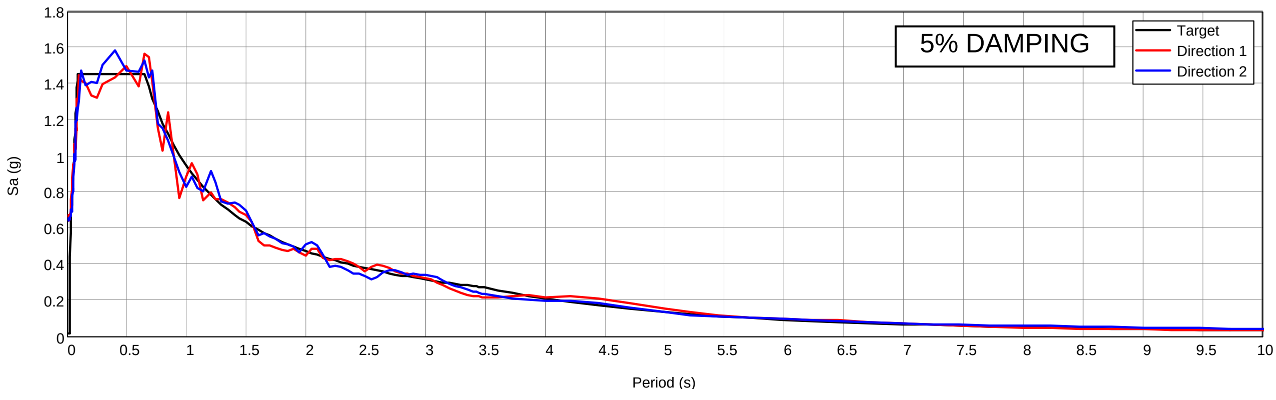

Figure 5-1: Comparison of ULS horizontal design spectrum with the spectrum for time-history input Sicilia 1.

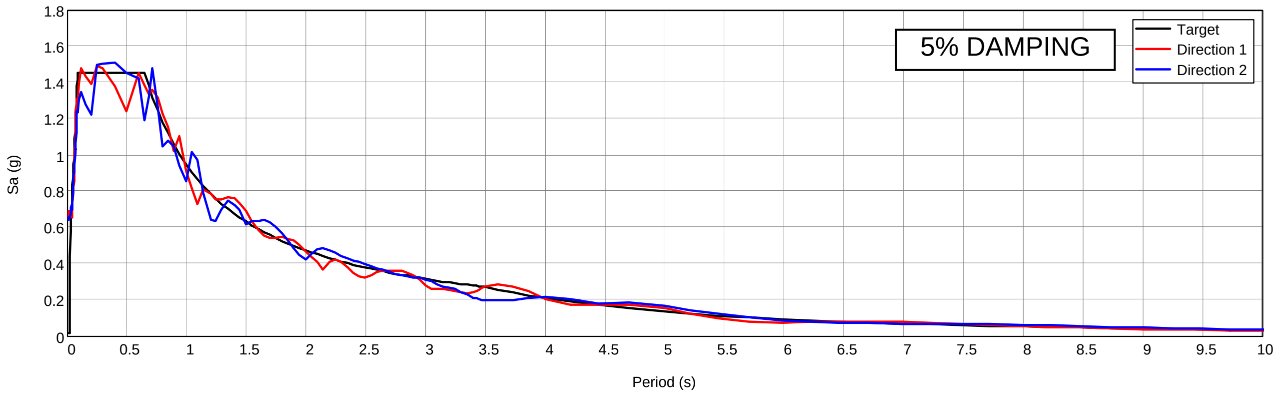

Figure 5-2: Comparison of ULS horizontal design spectrum with the spectrum for time-history input Sicilia 2.

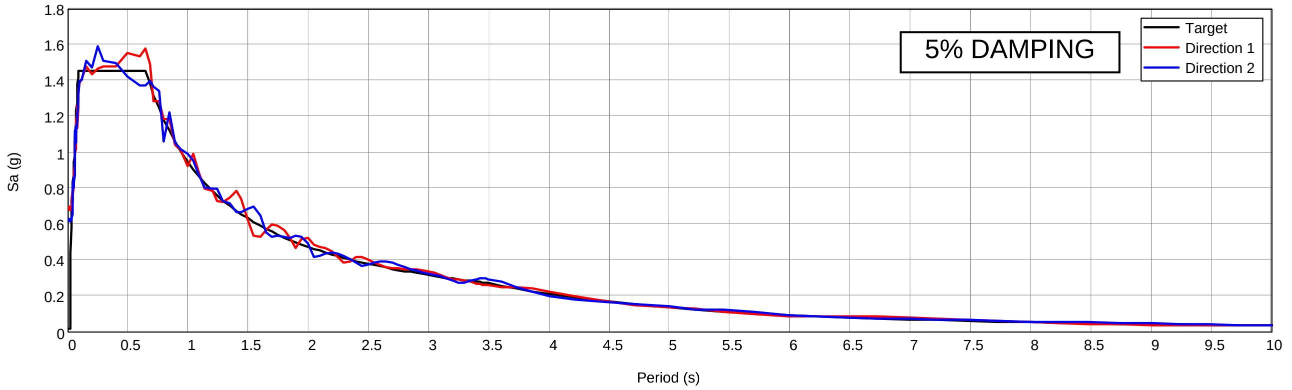

Figure 5-3: Comparison of ULS horizontal design spectrum with the spectrum for time-history input Sicilia 3.

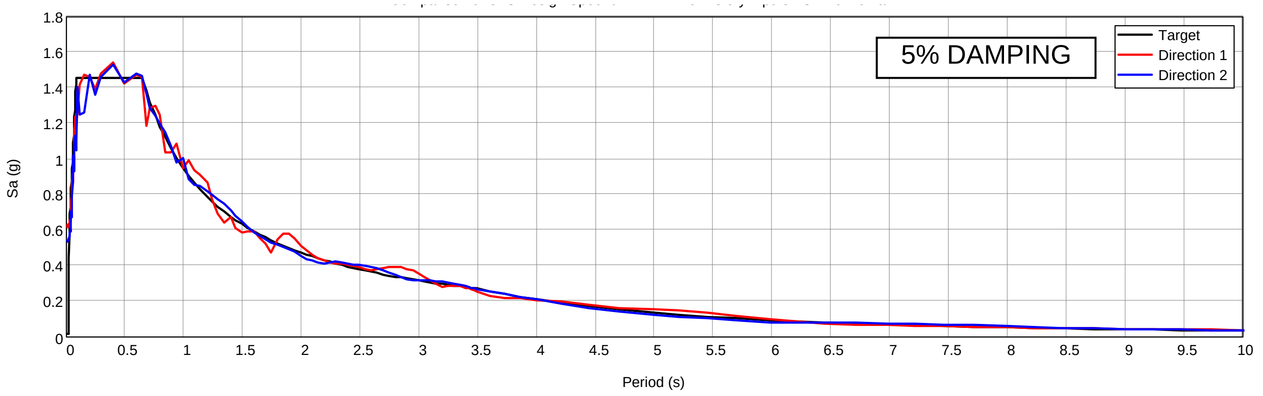

Figure 5-4: Comparison of ULS horizontal design spectrum with the spectrum for time-history input Sicilia 4.

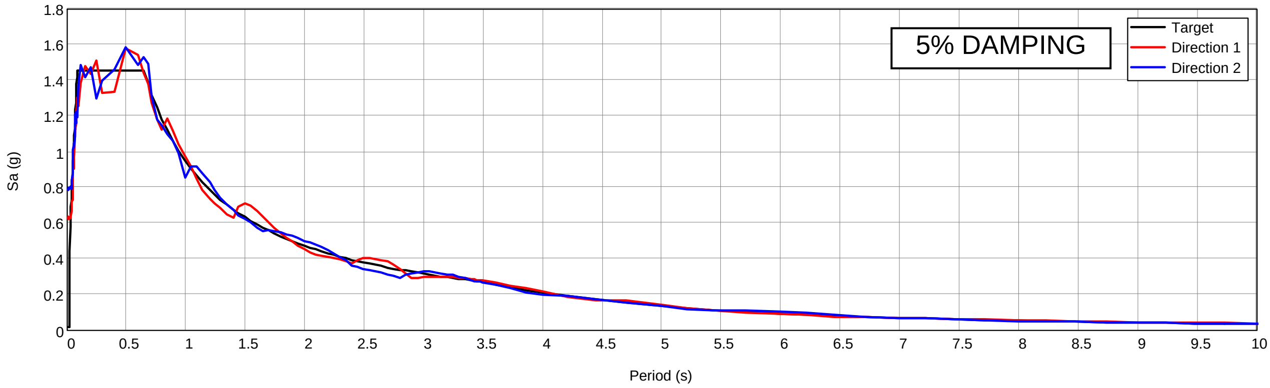

Figure 5-5: Comparison of ULS horizontal design spectrum with the spectrum for time-history input Calabria 1.

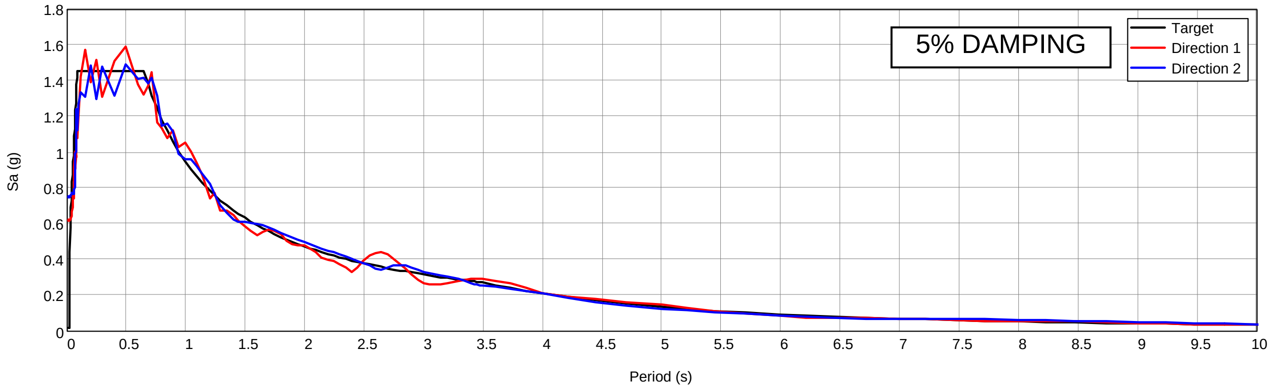

Figure 5-6: Comparison of ULS horizontal design spectrum with the spectrum for time-history input Calabria 2.

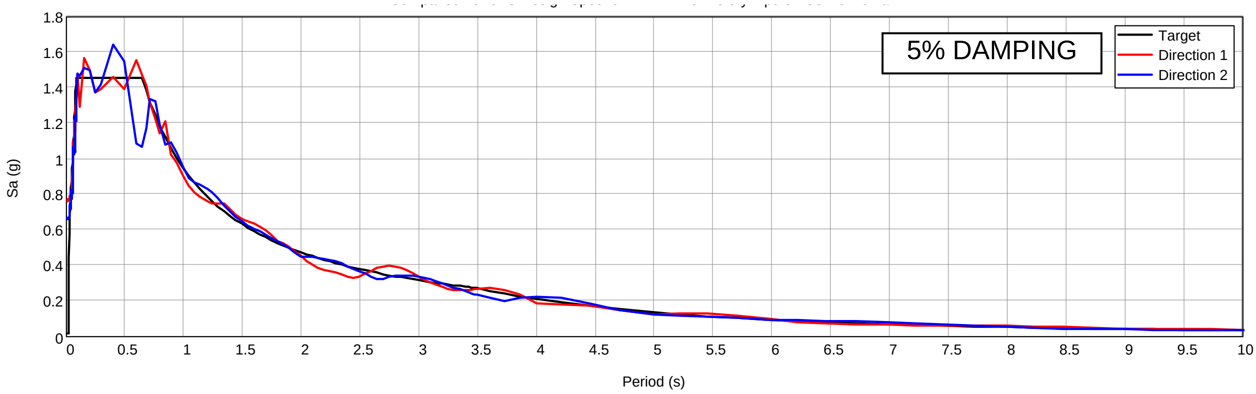

Figure 5-7: Comparison of ULS horizontal design spectrum with the spectrum for time-history input Calabria 3.

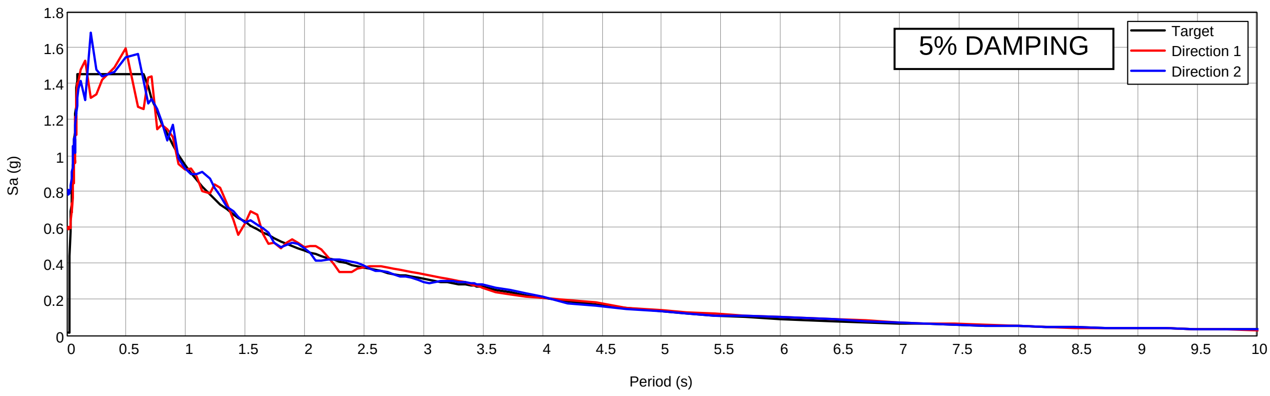

Figure 5-8: Comparison of ULS horizontal design spectrum with the spectrum for time-history input Calabria 4.

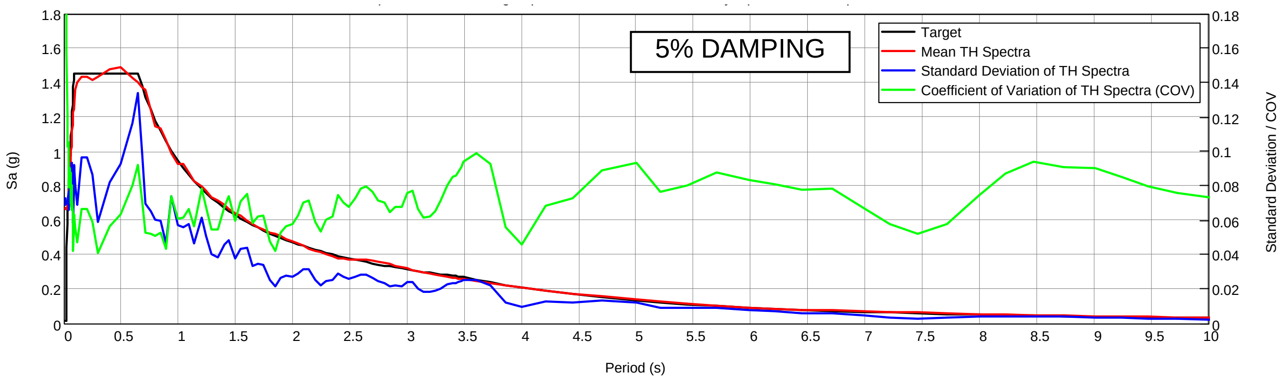

Figure 5-9: Comparison of ULS horizontal design spectrum (5% damping) with the mean 5% damped spectrum of all time-history inputs and the standard deviation and COv in the time-history spectra as a function of period.

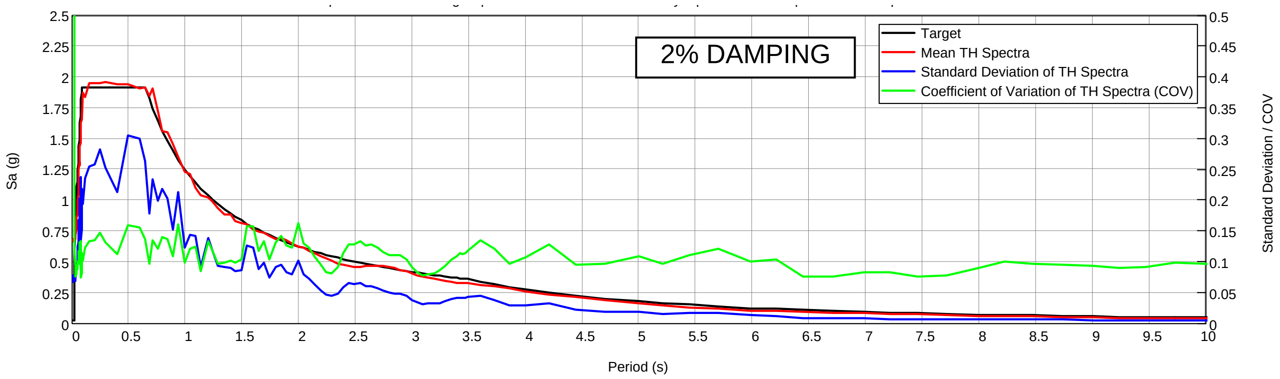

Figure 5-10: Comparison of ULS horizontal design spectrum (2% damping) with the mean 2% damped spectrum of all time-history inputs and the standard deviation and COW in the time-history spectra as a function of period.

Each time-history input comprises a vertical and two horizontal acceleration series. Seismic waves propagate along a certain direction from the rupture point in a source zone to the bridge site, and so the simultaneous use of full strength excitations in all three directions is unnecessarily conservative. Therefore, the Design Basis permits the application of the adjustment factors of 1.0, 0.8 and 0.75 to the two horizontal and one vertical component of the inputs. The following two load cases are considered for each set of input time histories:

<u>Longitudinal Dominant Combination</u>: 1.0·Longitudinal + 0.8·Transverse + 0.75·Vertical

<u>Transverse Dominant Combination</u>: 0.8·Longitudinal + 1.0·Transverse + 0.75·Vertical

Rayleigh damping (mass and stiffness proportional damping) is used to account for viscous damping in the time-history analysis. The mass and stiffness proportional coefficients, $\alpha = 0.07902\ \mathrm{s}^{-1}$ and $\beta = 0.00384\ \mathrm{s}$, respectively, are selected to provide approximately 2% damping for the dominant vibration modes, those contributing most to longitudinal and transverse tower responses (target modes). The Rayleigh damping curve and coefficients are shown in Figure 5-11, in which damping ratio is plotted on the vertical axis and vibration period is plotted on the horizontal axis. The target vibration modes are between 0.75 s and 2.49 s, represented by the black vertical centrelines in the figure. The use of the 2% damping ratio for the dominant tower vibration modes in the time-history analysis is considered to be appropriate for the welded steel towers that are designed to remain essentially elastic at the ultimate limit state.

The use of Rayleigh damping introduces artificial high damping to the low or high vibration modes outside the range of the target modes. The Rayleigh damping tends to damp out the high vibration modes associated with self response of the tower foundations. The effects of this artificial damping are insignificant for tower foundations because the peak response of the steel towers does not occur at the same time as peak self response of the tower foundations and because the tower foundations are being designed using an independent model that captures the self-response. For the same reasons the effects of this artificial damping of the foundations are also insignificant for the towers.

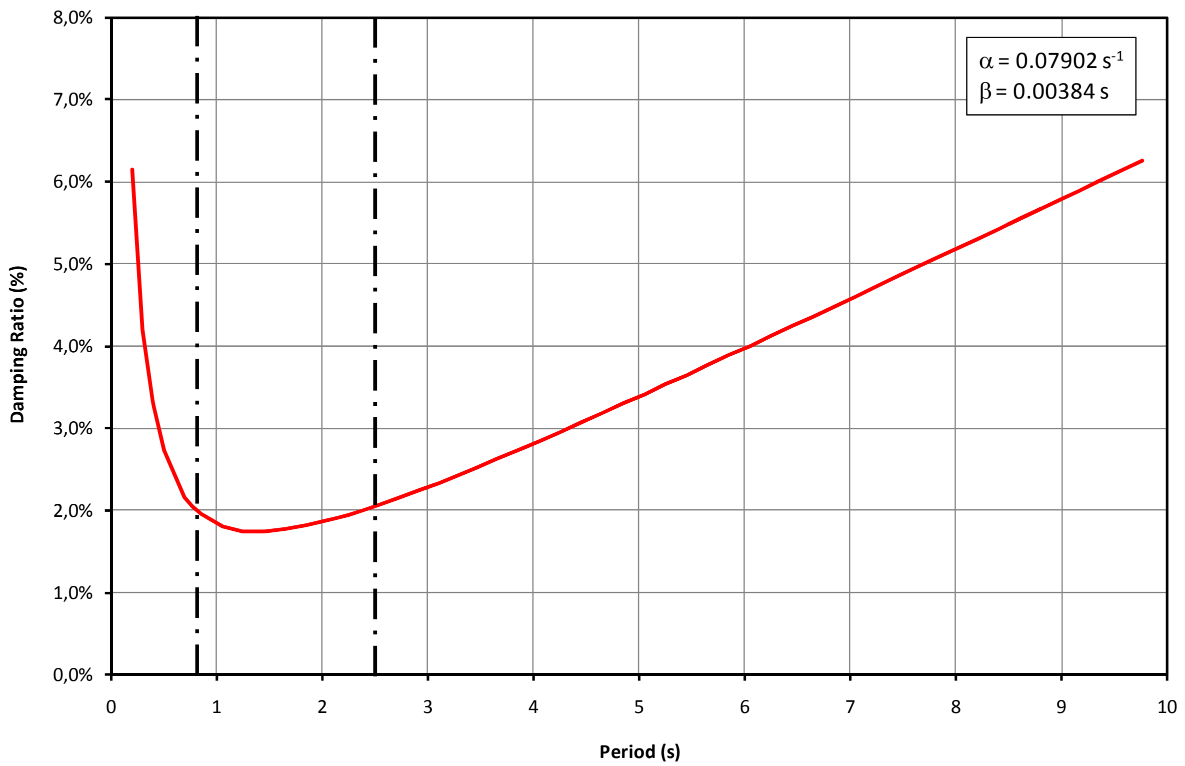

Figure 5-11: Rayleigh damping curve used for time-history analysis.

Because the analysis parameters and the physical properties of the ground on which the structure is founded are uncertain, it is prudent to assess effects of variations in these parameters and properties on the structural response. A series of time-history analyses were run for the longitudinal dominant combination of the first input for the Sicily tower (Acc01_ts92) considering the base case, with the nominal or target values for each parameter and considering the variations of the parameters described below. The sensitivity study was completed using model version 3.3; given the relatively minor changes in the model between versions 3.3 and 3.3f, which is the basis for the tower design, the conclusions of the sensitivity study are still valid.

1 Foundation Stiffness and Foundation Damping

The stiffness and damping values in the matrices for soil-structure interaction provided by Rampello are effective values considering non-linear soil behaviour for a certain level of excitation. The 2004 input time histories were used to develop the stiffness and damping matrices for soil-structure interaction. The 2004 inputs were generated from physical modelling of seismic source zones, rupture mechanism and wave propagation. The response spectra of the 2004 input time histories are significantly lower than the 1992 design spectra within the period range of interest for tower response. The Tender Documents require the use of design spectrum compatible inputs for structural design. Therefore, the input time histories used in structural design are not consistent with those used to develop stiffness and damping matrices. As a result, the stiffness values are overestimated, and the damping values are underestimated, for the input time histories used for structural design. The effects of foundation stiffness and damping are evaluated by running the analysis with the upper and lower bound values of each.

2 Rayleigh Damping

Three sets of mass and stiffness proportional damping coefficients are considered. The first set corresponds to the damping curve shown in Figure 5-11 and is the best match with 2% damping ratio for the target tower modes and is referred to as “Best Fit”. The second set reduces artificial damping for the high modes while maintaining damping ratio reasonably close to 2% for the target modes and is referred to as “High Mode Fit”. The third set reduces artificial damping for the low modes while maintaining damping ratio reasonably close to 2% for the target modes and is referred to as “Low Mode Fit”.

The results of the sensitivity analysis for longitudinal and transverse moments in one leg of the Sicilia tower are shown in Figure 5-12 and Figure 5-13, respectively. In each figure, elevation is plotted on the vertical axis and moment is plotted on the horizontal axis. Longitudinal moments are most affected by the foundation stiffness; however, differences in the structural response from the base case for the lower bound or upper bound stiffnesses are generally small, other than near the inflection point at approximately 125 m. Longitudinal moments are relatively insensitive to variations of the other parameters and so their target or nominal values are used for the final time-history analysis. Similarly, transverse moments are insensitive to variations in any of the input parameters.

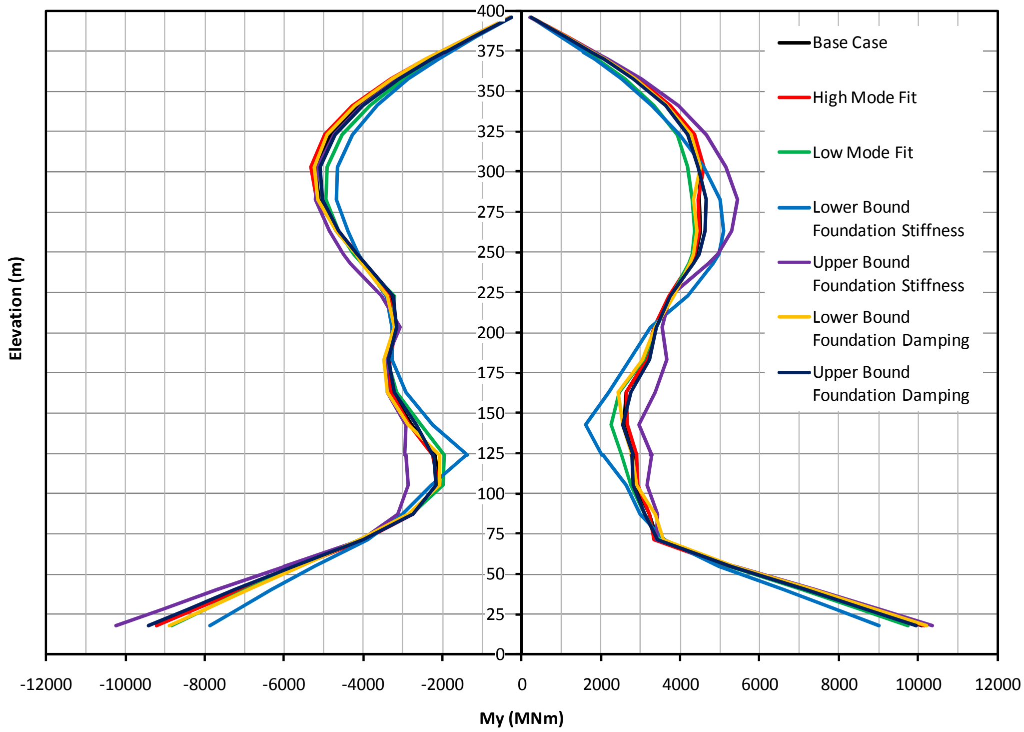

Figure 5-12: Variation of Sicilia tower leg longitudinal moment envelope.

Given the conservative procedures used to develop the foundation stiffnesses, use of the lower bound values would be reasonable. However, it is difficult to assess the actual effect the foundation stiffness has on the design based only on the sensitivity analysis, which was run for only one input motion. Therefore, the full set of eight input motions was run with the nominal foundation stiffnesses and with the lower bound foundation stiffnesses. The mean longitudinal moments in one Sicilia tower leg from these two sets of runs are compared in Figure 5-14. As in the previous figures, elevation is plotted on the vertical axis and moment is plotted on the horizontal axis. In general, the average response of the eight input motions is less than that of the single input considered in the sensitivity analysis. Over most of the tower height the mean moments for the two foundation stiffnesses are quite similar. As noted in the sensitivity analysis, the differences are slightly larger around elevation 125 m.

Given the general lack of sensitivity of the tower leg structural response, and thus design quantities, to variations of the input parameters, the time-history analysis used for the tower design is based on all nominal and target inputs: nominal foundation stiffness, foundation damping and target Rayleigh damping.

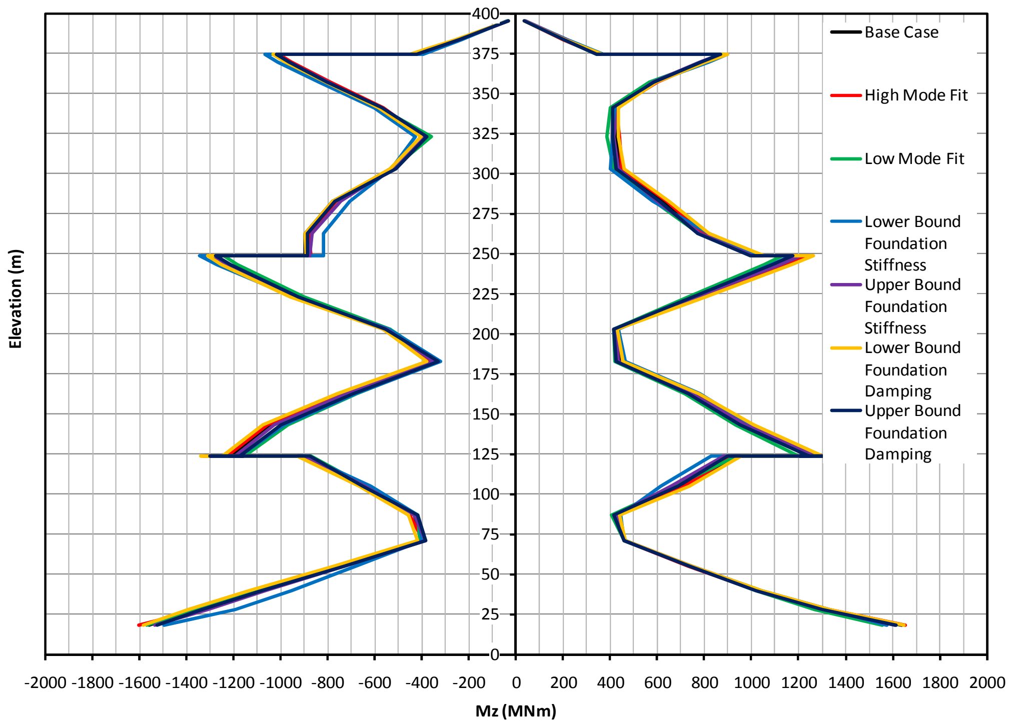

Figure 5-13: Variation of Sicilia tower leg transverse moment envelope.

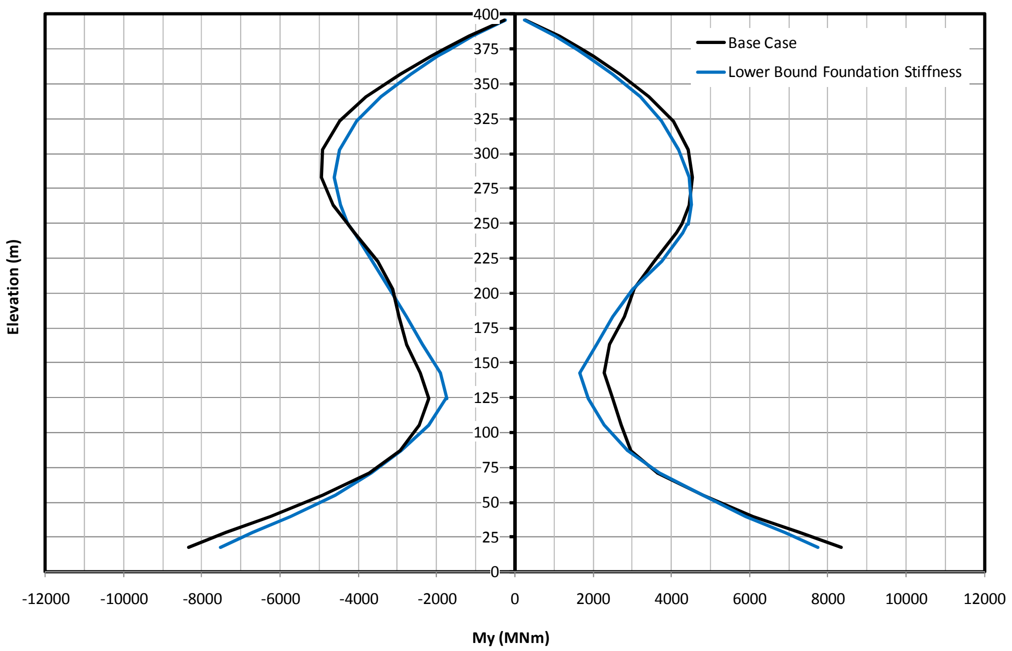

Figure 5-14: Mean longitudinal moments from eight time-history analysis runs.

5.2.5 Accidental Load Scenarios

The design basis GCG.F.04.01 Section 5.4 requires that accidental actions such as fire, explosion and impact be considered at the ULS and SILS for those components whose performance would be affected by these events.

The probabilities of occurrence of these three accidental load scenarios are determined in the Operational Risk Analysis (reference note A09055-NOT-3-024 "Accidental loads resulting from the operational risk assessment"). Scenarios with annual probabilities of occurrence greater than or equal to 0.0001 are considered as design scenarios for ULS and SILS. Scenarios with annual probabilities of occurrence between 0.0001 and 0.00002 are considered as design scenarios for SILS only. Scenarios with annual probabilities of occurrence less than 0.00002, and which are less likely to occur than other SILS scenarios, are considered only as evaluation scenarios.

Design scenarios are addressed by proportioning the structure to resist the imposed effects or by specifying appropriate mitigating or protective measures to reduce the imposed effects to the extent that they can be resisted by the structure as proportioned.

Evaluation scenarios are addressed by assessing the likely consequences of the effects on the structure, including assessments of likely damage, potential force effect redistribution and the potential for collapse. Because of the rare and severe nature of these scenarios, assessments will generally comprise simplified calculations and qualitative descriptions of the expected structural behaviour and potential consequences.

For the tower, the Operational Risk Analysis identified fire as a design scenario and impact and explosion as evaluations scenarios. Assessments of these accidental loads are provided in CG.10.00-P-CL-D-P-SV-T4-00-00-00-00-01 "Design Report - Tower Legs incl. Joints and Splices" and summary of the effects on the tower legs is provide in CG.10.00-P-RX-D-P-SV-00-00-00-00-00-01 "Specialist Technical Design Report, Towers."

5.3 Local Behaviour

The global modelling and design verifications described throughout this report will be supplemented with semi-local and local shell element modelling of the following components:

- Tower leg to cross beam connection;

- Tower leg transverse stiffeners and transverse diaphragm plates; and
- A full tower leg segment.

The bases for these analyses are summarized in the following sections.

5.3.1 Tower Leg to Cross Beam Connection

The global modelling and analysis of the tower legs and cross beams is supplemented with the semi-local modelling of the connection between the cross beams and tower legs. The semi-local modelling is intended to better predict the interaction between the dominant longitudinal stresses in the tower leg components and the introduction of the cross beam web shear forces and the cross beam flange axial forces into the tower leg longitudinal and transverse stiffening system. The semi-local model results are used to verify the adequacy of the preliminary hand calculations used to determine the flow of forces from the cross beam into the tower leg and determine the additional material and stiffening required in the connection region.

The semi-local model is constructed as an integral part of the global IBDAS model so as to properly account for the boundary conditions and have a set of load cases and combinations that are consistent with those used in the global model. Cross beam 2 was selected for the detailed model as it is the most heavily loaded of the three. Isometric and elevation views of the meshed shell element model are shown in Figure 5-15 and Figure 5-16, respectively.

More complete details of the modelling, analysis and results are provided in CG.10.00-P-RG-D-P-SV-00-00-00-00-00-03 “Semi-local IBDAS Model, Towers.” Results of the semi-local analysis are discussed in CG.10.00-P-RX-D-P-SV-00-00-00-00-00-01 “Specialist Technical Design Report, Towers” and calculations related to the tower leg to cross beam connection are presented in CG.10.00-P-CL-D-P-SV-T4-00-00-00-00-01 “Design Report - Tower Legs incl. Joints and Splices.”

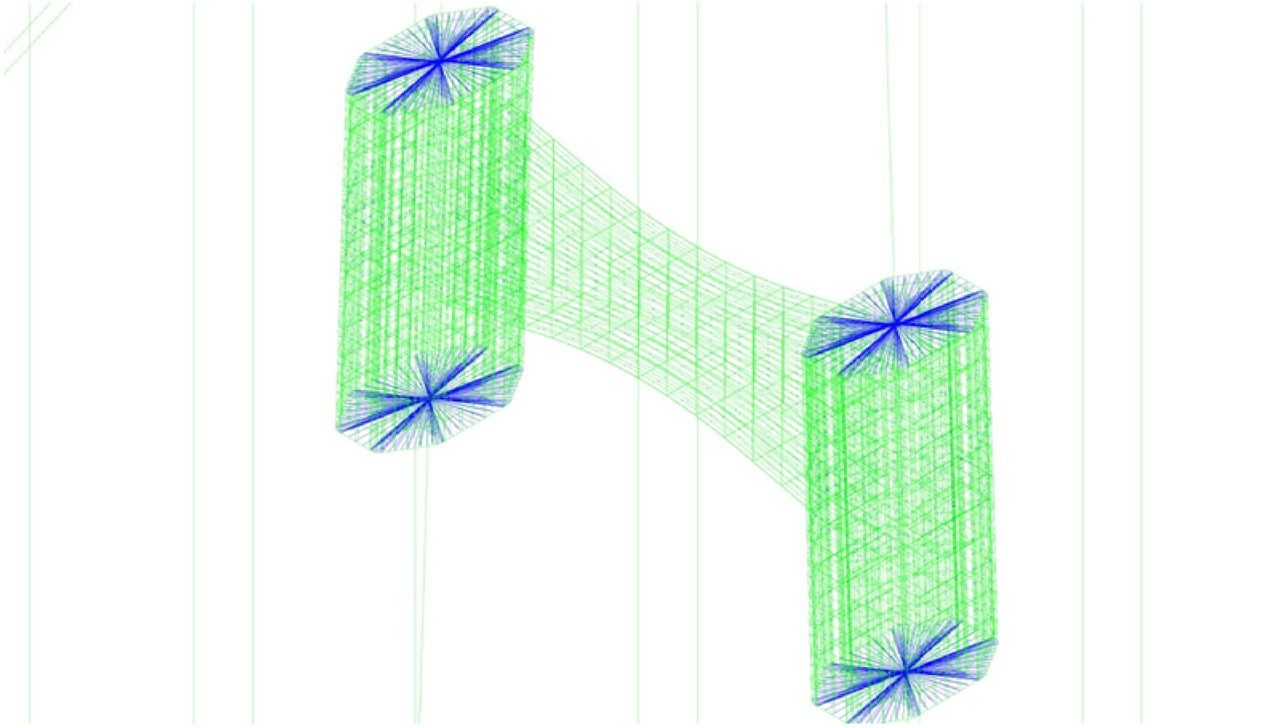

Figure 5-15: Isometric view of cross beam to tower leg connection semi-local model.

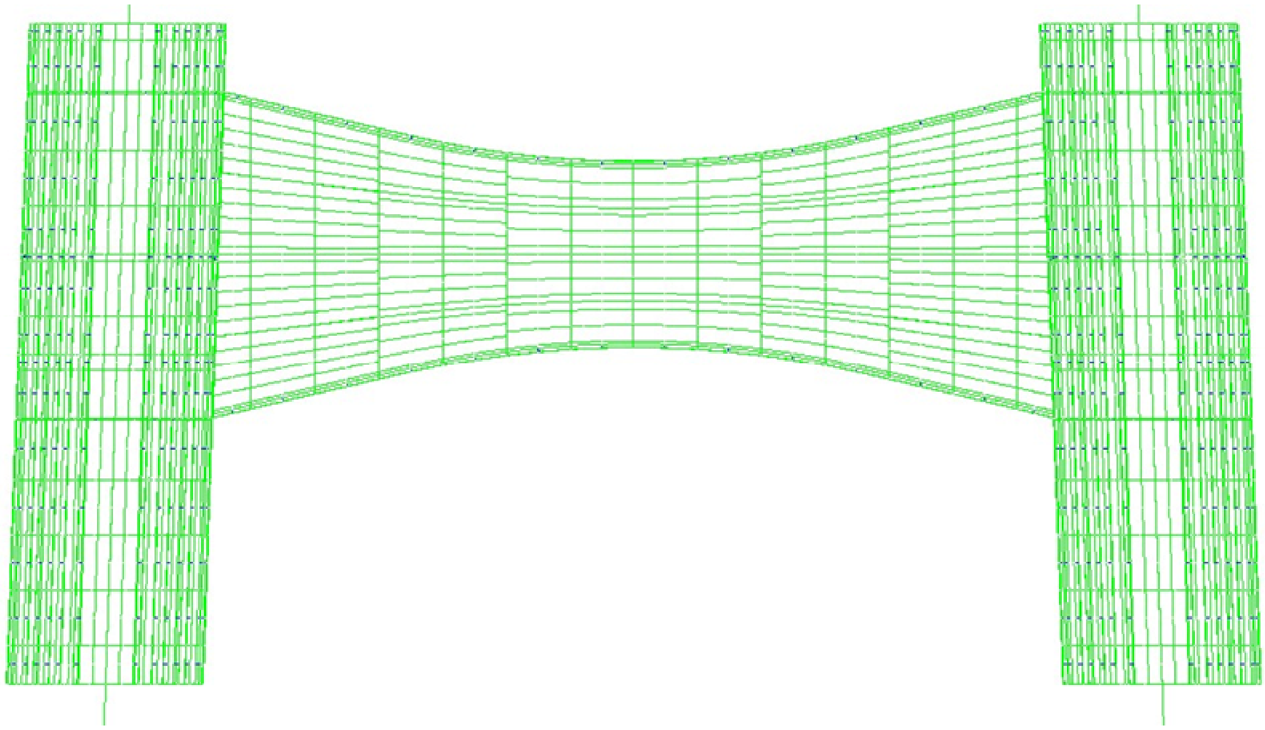

Figure 5-16: Transverse elevation of cross beam to tower leg connection semi-local model.

5.3.2 Tower Leg Transverse Stiffener and Diaphragm Plate Buckling Analysis

In the general concept submission of the tower design the tower leg longitudinal stiffeners were connected to the webs of every transverse stiffener with tab-plates and the transverse stiffener flange was braced to the longitudinal stiffeners at discrete locations to prevent torsional buckling. These flange connections were required to provide the minimum flange weight that satisfied EN 1993-1-5 Section 9.2.1, either by sub-clause (8) or (9).

The removal of both the tab-plates, as described in Section 5.3.3, and the intermediate flange braces was investigated to reduce fabrication costs. Detailed finite element analysis was used to determine the optimum flange size to satisfy the stability requirements of EN 1993-1-5 Section 9.2.1(8) or (9) because traditional hand calculations will tend to underestimate the flange stability.

This investigation was accompanied by a rearrangement of the transverse stiffening elements in the tower legs, that took advantage of the results of the analysis described in Section 5.3.3, and reduces fabrication costs by allowing for a simplified cross-section assembly procedure and reducing the number of transverse stiffening elements through which the longitudinal stiffeners pass. Plate A was thickened so that transverse stiffeners are not required for the stability of the single longitudinal stiffener. The transverse stiffeners to plates B, C, E, F and H were replaced by a triangular diaphragm filling the enclosed cell. Therefore, only plates D and G require transverse stiffeners. The original and revised transverse stiffening arrangements are shown in Figure 5-17. The width of plate G is only 4 metres and so the transverse stiffener does not require intermediate flange bracing. Therefore, the analyses are limited to the plate D stiffeners, which have a clear span between plates H of 8 m.

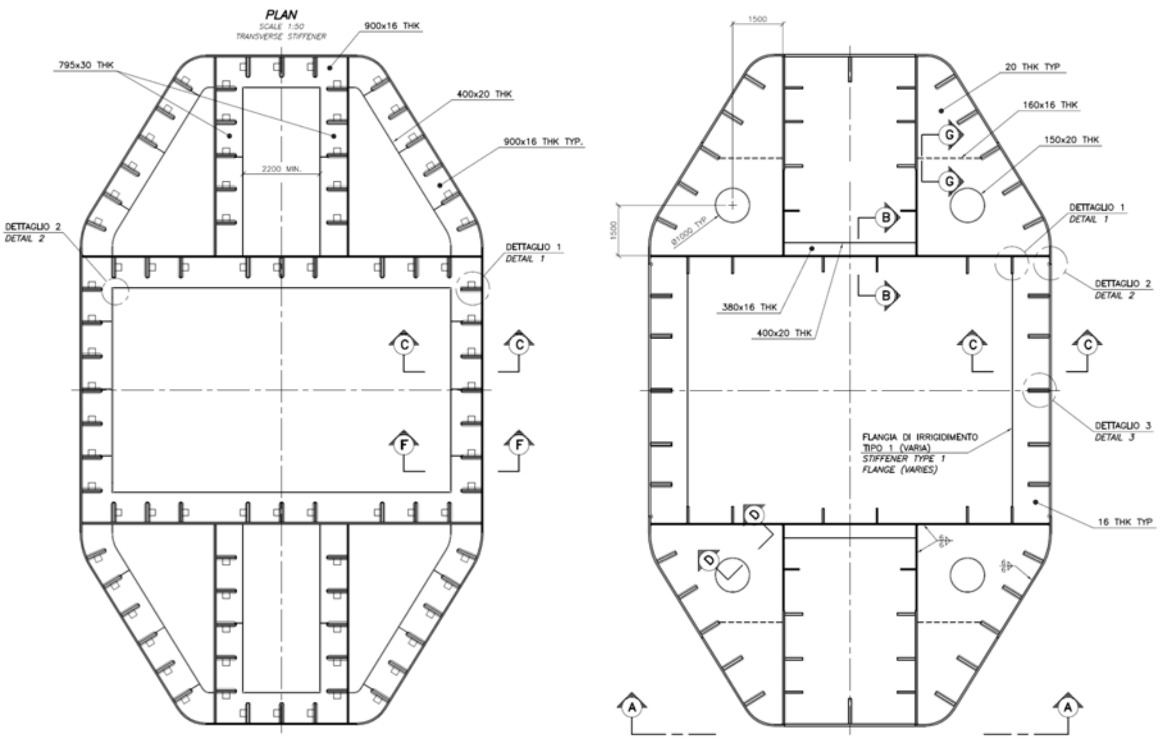

Figure 5-17: General concept and revised transverse stiffening arrangement.

The stability of the transverse stiffener was assessed by determining the elastic critical buckling loads using the finite element analysis software SAP2000. The analysis was used to proportion the transverse stiffeners for low, moderate and high plate D thicknesses, as the out-of-plane load on the transverse stiffener increases with the area of the stiffened plate.

The shell element analysis model comprises:

- a transverse stiffener spanning 8.0 metres between plates H with cut-outs to allow the longitudinal stiffeners to pass;
- the skin-plate extending 3.5 metres above and below the transverse stiffener;
- the longitudinal stiffeners extending 3.5 metres above and below;
- the adjoining plate H extending 3.5 metres above and below (the presence of the longitudinal stiffeners on plate H is ignored because they cannot be relied upon to provide stability as the loading on the leg approaches the ultimate limit state and they are fully stressed from longitudinal loads); and

- a row of elements of extremely low flexural stiffness along the transverse stiffener web at the interface with the skin plate; required to respect the requirement of EN 1993-1-5 Section 9.2.1(9) “not considering rotational restraint from the plate”.

Figure 5-18 shows an isometric view of the typical model used for the analysis. Edge constraints are used to ensure continuity of the displacement field at the interfaces between elements of different sizes.

The model is loaded with the second-order loading calculated in accordance with EN 1993-1-5 Section 9.2.1, applied laterally to the outside face of the skin plate at the transverse stiffener elevation.

Initial finite element analyses with a range of flange cross-sections showed that the requirements of EN 1993-1-5 Section 9.2.1(8) or (9) are impractical for an 8 m clear span, as was suggested by earlier hand calculations. Therefore, the requirements of EN 1993-1-5 Section 9.2.1(8) and (9) were reviewed in the light of traditional design practice, in which the stiffener resistance would be checked as though the flange and half the web were a compression strut. This review showed that the requirements of EN 1993-1-5 Section 9.2.1(8) and (9) are reasonable for “stocky” stiffeners (heavy for their length) but are unreasonable for long stiffeners like that required on plate D. This is demonstrated by the recommended value of $\theta = 6$, which corresponds to a relative slenderness of:

$$\bar{\lambda} = \sqrt{\frac{f_y}{\sigma_{cr}}} = \sqrt{\frac{f_y}{\theta f_y}} = \sqrt{\frac{1}{6}} = 0.41$$

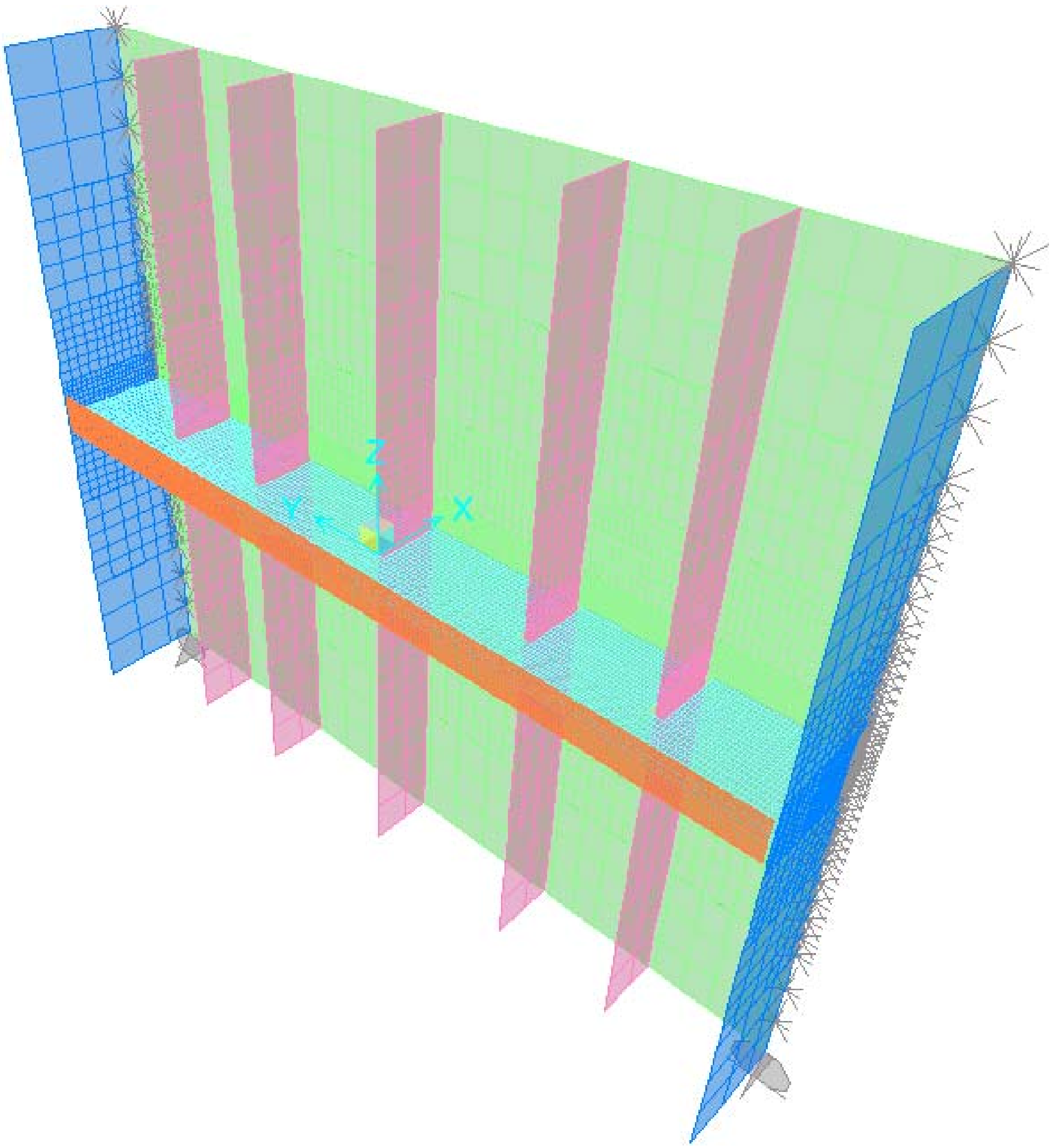

Figure 5-18: Isometric view of transverse stiffener buckling analysis model.

This simplified approach of limiting the slenderness to 0.41 is unnecessarily conservative if the transverse stiffeners are designed with appropriate consideration of loading and behaviour and given that strut slenderness is not similarly restricted. Therefore, the stability verification was revised to use the maximum strut stress, $\chi f_y / \gamma_{M1}$, calculated in accordance with EN 1993-1-1 Section 6.3.1, but using the increased imperfection factor, α_e, from EN 1993-1-5 Section 4.5.3(5), which allows for the greater fabrication tolerance for stiffener flanges than for column flanges.

Flange sizes for a variety of plate D thicknesses were estimated by hand calculations. The estimated flanges were inserted in the finite element model and loaded with the load calculated from EN 1993-1-5 Section 9.2.1, but limited so that the maximum stress would not exceed the resistance derived by the initial calculations. From these loads, the elastic buckling factor is found by the finite element analysis, to give the elastic buckling stress, σ_{cr}, for each flange size. This was then substituted in the calculation of relative slenderness and the maximum stress resistance was calculated. This was used as the limiting stress in EN 1993-1-5 Section 9.2.1 to determine for which plate D thickness each flange size is appropriate.

The finite element analysis accounts for the variation of bending stress along the stiffener, producing greater economy than is convenient with simple hand calculations.

More complete details of the modelling, analysis and results are provided in CG.10.00-P-CL-D-P-SV-T4-00-00-00-00-01 “Design Report - Tower Legs incl. Joints and Splices” and the results of the analysis are summarized in CG.10.00-P-RX-D-P-SV-00-00-00-00-00-01 “Specialist Technical Design Report, Towers.”

STABILITY OF THE TRIANGULAR DIAPHRAGMS

As shown in Figure 5-17, plates B, C, E, F and H are stiffened transversely by triangular plate diaphragms with a circular cut-out to allow for access and inspection. The stability of this diaphragm was checked by EN 1993-1-5 Section 10 and Annex B.1.

The relative plate slenderness is calculated using:

- the buckling factor from a finite element model run for an elastic buckling solution; and
- the ultimate factor, which was found conservatively using the ratio of the maximum von Mises stress divided by the yield stress, where the von Mises stresses are calculated from a linear elastic analysis.

The finite element analysis model comprises:

- a flat plate diaphragm with cut-outs to allow the longitudinal stiffeners to pass through and a circular hole;
- the longitudinal stiffeners extending 3.5 metres above and below; and

• the adjoining plates B, C, E, F and H extending 3.5 metres above and below.

Figure 5-19 shows an isometric view of the typical model used for the analysis.

The loading for both the buckling and ultimate analyses was the second-order in-plane loading calculated from EN 1993-1-5 Section 9.2.1, but assuming no growth of imperfection because of the diaphragm stiffness.

More complete details of the modelling, analysis and results are provided in the CG.10.00-P-CL-D-P-SV-T4-00-00-00-00-01 “Design Report - Tower Legs incl. Joints and Splices” and the results of the analysis are summarized in CG.10.00-P-RX-D-P-SV-00-00-00-00-00-01 “Specialist Technical Design Report, Towers.”

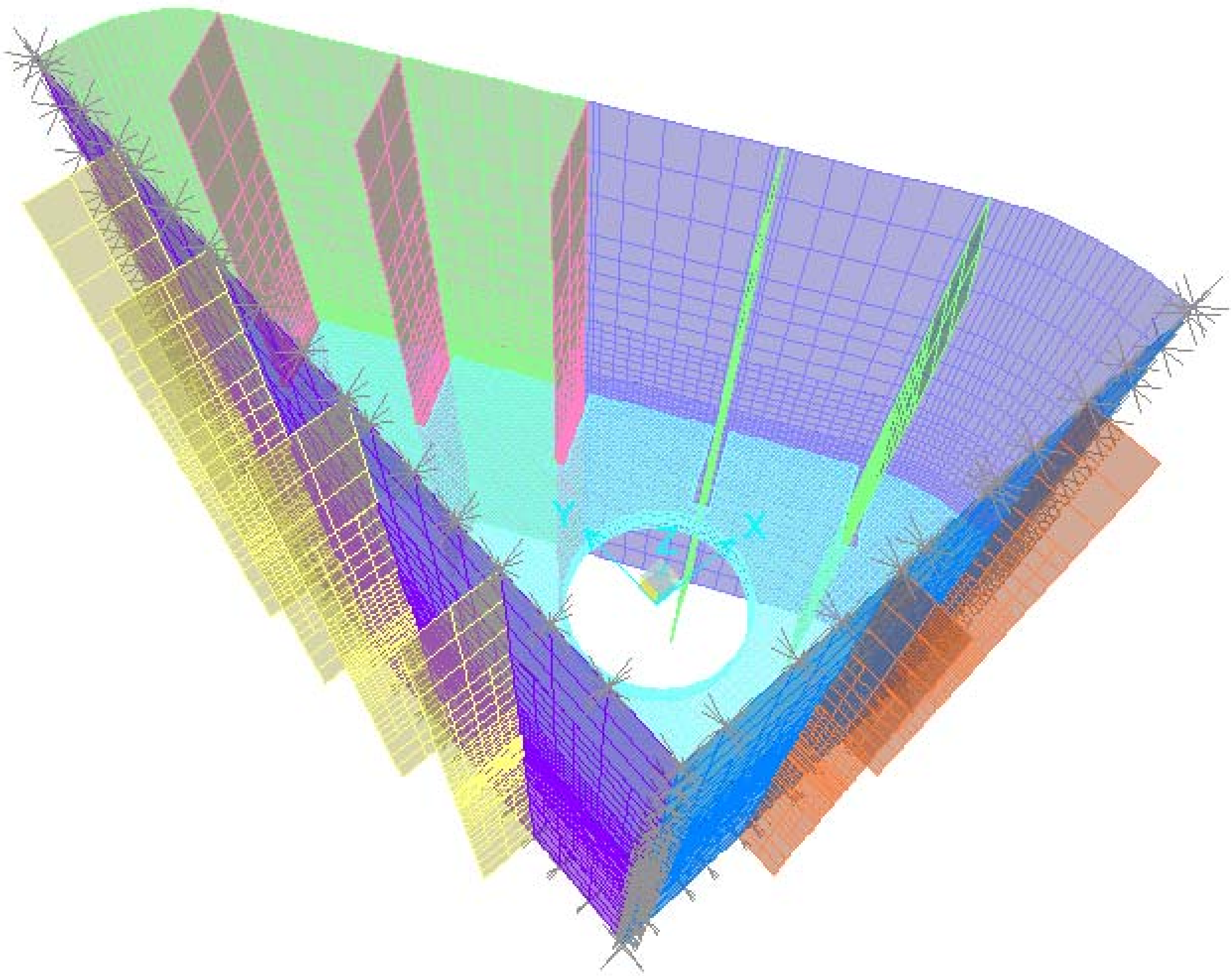

Figure 5-19: Isometric view of triangular diaphragm plate buckling analysis model.

5.3.3 Longitudinal to Transverse Stiffener Connections

In the general concept submission of the tower design the tower leg and cross beam longitudinal stiffeners were connected to the webs of every transverse stiffener with tab-plates. Given the likely fabrication cost benefits of omitting these connections and the successful omission of them on the Akashi Kaikyo Bridge towers, the potential of omitting the tab plates on the Messina Strait Bridge was investigated.

The tab-plates commonly have three functions:

1 To transfer deviation forces (“kick” forces from buckling of the adjacent compressed panels) from the longitudinal stiffener to the transverse stiffener;

2 To improve the stability of the transverse stiffener; and

3 To provide lateral/torsional restraint to the longitudinal stiffener, if required.

The towers use flat plate longitudinal stiffeners that are proportioned to satisfy the maximum width-to-thickness ratios for a Class 3 section in EN 1993-1-1 Table 5.2 and the requirement of EN 1993-1-5 Section 9.2.1(8). Therefore, the longitudinal stiffeners do not require lateral restraint at the transverse stiffeners and so the tab-plates are not required for this function.

As described in Section 5.3.2, detailed finite element analysis was used to size the tower leg transverse stiffeners considering no intermediate restraint along the full 8 m span, and so the tab-plates are not required for this function.

The only remaining function for the tab-plates is to transfer deviation forces from the buckling of the longitudinal stiffener to the transverse stiffener. Without a tab-plate connection, this force must be carried by the welds between the transverse stiffener web and the skin plate and by the welds between the longitudinal stiffener and the skin plate.

Weld demands are found through finite element analysis using the analysis software SAP2000. Three cases were analyzed to assess the effects of panel area on the weld demands:

1 A heavy panel with the largest expected longitudinal stiffeners. This case is considered because it requires the largest restraint forces;

2 A light panel with thin skin plate. This case is considered because the low flexural stiffness of the skin plate might produce higher stress concentrations; and

3 A panel with an intermediate skin-plate thickness. This case is considered to ensure that the weld demands will vary with panel weight as expected.

The model used for the transverse stiffener buckling analysis, shown in Figure 5-18, was also used for investigating the tab plate removal.

The model is loaded with the second-order loading calculated in accordance with EN 1993-1-5 Section 9.2.1, applied laterally to the outside face of the skin plate at the transverse stiffener elevation.

The linear elastic geometry and material analysis gives conservatively high stresses because it does not allow for any yielding of the welds. The welds are verified by summing the forces in an appropriate weld length and comparing the average load/unit length with the fillet weld resistance calculated in accordance with EN 1993-1-8 Section 4.5.3.2. The length used for averaging the force is 2.5 times the skin-plate thickness. The value of 2.5 is derived from EN 1993-1-8 Section 4.10, which uses an equivalent dispersion angle of 1:3.5 on each side of a connection, as shown in Figure 4.8. Because this connection differs from that shown in Figure 4.8, the value of 3.5 was reduced to 2.5 to account for uncertainty.

More complete details of the modelling, analysis and results are provided in the CG.10.00-P-CL-D-P-SV-T4-00-00-00-00-01 “Design Report - Tower Legs incl. Joints and Splices” and the results of the analysis are summarized in CG.10.00-P-RX-D-P-SV-00-00-00-00-00-01 “Specialist Technical Design Report, Towers.”

5.3.4 Tower Leg Segment Detailed Finite Element Modelling

A finite element model was made of a complete tower leg segment to confirm the appropriateness of the resistances calculated using EN 1993-1-5 Section 4, which is the basis for the tower leg design verifications, and to assess the extent of damage that might be caused in the critical tower leg segment by a set of coexisting force effects corresponding to the envelope of all time-history analysis results (rather than the mean values for which the tower components are proportioned). The model considered the effects of non-linear geometry, non-linear material properties, residual stresses and initial imperfections, subtle yet important factors in the tower leg behaviour that are considered only implicitly in the simplified design provisions of EN 1993-1-5 Section 4.

The Sicilia tower leg segment 6 was modelled to confirm the design verification procedures because it has thinner plates relative to the imposed axial load than other segments, and so might show greater sensitivity to buckling effects. Calabria tower leg segment 17 was modelled to assess the effects of the envelope of the time-history analysis results because it was shown to have the highest utilization ratio for the envelope results using the standard design verification methods. Both the plates and the vertical stiffeners are modelled with shell elements. Bar elements are used to model the horizontal stiffeners and to represent the restraint provided by the triangular diaphragms. Bar elements simplify the model and are sufficient. Moments and forces are applied to the top and bottom of the model through a "spider" of rigid elements. Plan and isometric views of the model are shown in Figure 5-20.

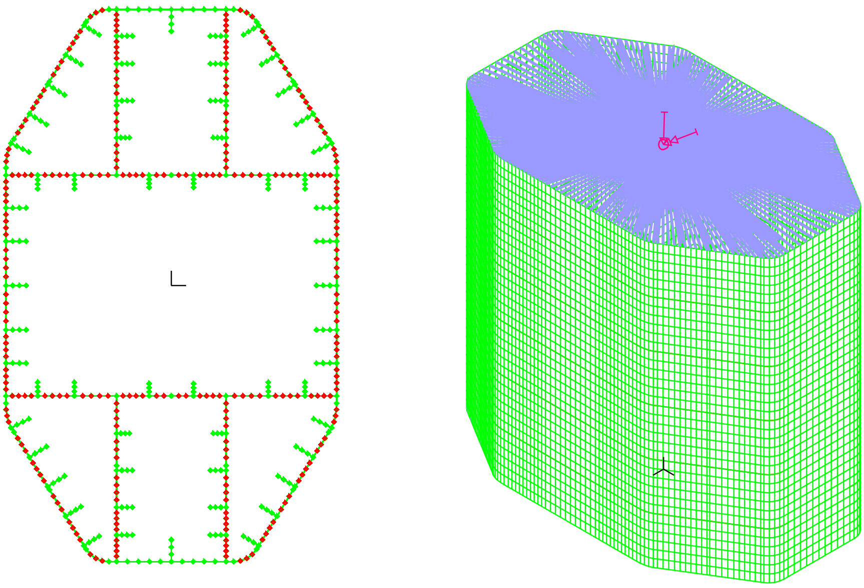

Figure 5-20: Plan and isometric views of tower leg segment finite element model.

It was originally planned to include the effects of imperfections by modelling the plates and stiffeners with the equivalent imperfections specified in EN 1993-1-5 Annex C, using the geometrical form of the elastic buckling modes of the panels as the basis. Several issues were encountered with this approach:

- The 1:400 "equivalent imperfection" specified for longitudinal stiffeners in EN 1993-1-5 Table C.2 is no greater than the manufacturing tolerance allowed in EN 1090-2 Table D.1.6. This means that if the tower leg panels were manufactured to the allowable tolerances, the analysis would have been made with no allowance for residual stresses and therefore might be unconservative;

- The "equivalent imperfections" specified for a plate between stiffeners in Table C.2 will cause a reduction in the resistance of the plate, whereas EN 1993-1-5 Section 4 gives no reduction for the plate slenderness for the width-to-thickness ratios used in the majority of panels in the tower legs;
- It is very difficult to find the most onerous arrangement of "equivalent imperfections" for stiffener twist because there are so many different combinations possible (however, for the width-to-thickness ratios of the stiffeners and plate thicknesses to which they are welded, realistic twist angles are unlikely to significantly affect the capacity); and
- There is no single buckling mode in the panels that gives magnitudes of out-of-plane panel deformations similar to those specified in EN 1993-1-5 Table C.2, so an alternative method of generating suitable initial imperfections was required.

It was concluded that the most realistic resistance assessment would be provided by:

- Using out-of-plane geometric imperfections along the longitudinal stiffeners in the form that occurs when applying equal line loads along each stiffener and accepting the resulting plate between stiffener and stiffener twist imperfections as the appropriate values for those initial imperfections; and
- Account for residual stresses directly (not by equivalent imperfections) using an appropriate stress-strain curve.

The maximum geometric imperfection in each panel was taken as the allowable stiffener fabrication tolerance of 1:400, as specified in EN 1090-2 Table D.1.6. An isometric view and elevation of the model deformed by the initial imperfections is shown in Figure 5-21.

The residual stresses were incorporated by modifying the stress-strain curve from bi-linear elastic/plastic to multi-linear, so as to represent the average stress-strain response of steel with residual stresses, and including the 0.2% proof strain that is expected with higher strength steels such as S460. The assumed residual stress distribution through the material thickness is shown in Figure 5-22, in which residual stresses are plotted on the horizontal axis and relative depth is plotted on the vertical axis. Relative depth values of -1 and 1 correspond to the two plate surfaces. The stress-strain relationships considered in the analysis are shown in Figure 5-23.

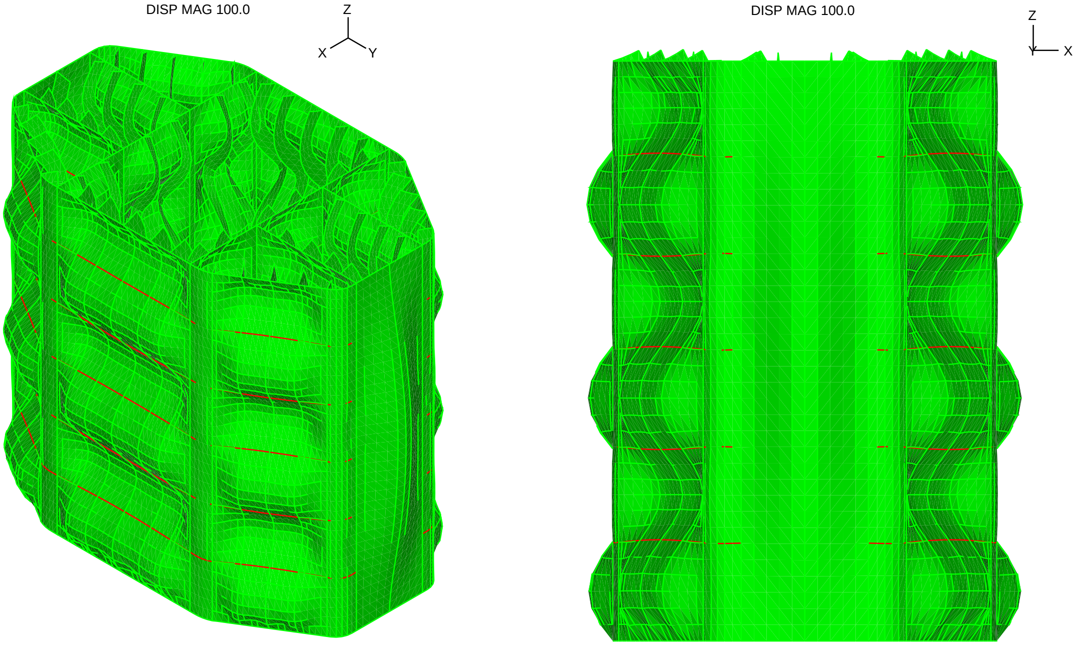

Figure 5-21: Tower leg segment model with initial imperfections.

To assess the magnitude of these effects, the three cases of maximum axial force with coexistent moments, and maximum moments with coexistent axial force and moment were also analyzed using bi-linear elastic/plastic material properties.

The modelling and analysis are described in greater detail in CG.10.00-P-CL-D-P-SV-T4-00-00-00-00-01 “Design Report - Tower Legs incl. Joints and Splices” and the results of the investigation are summarized in CG.10.00-P-RX-D-P-SV-00-00-00-00-00-01 “Specialist Technical Design Report, Towers.”

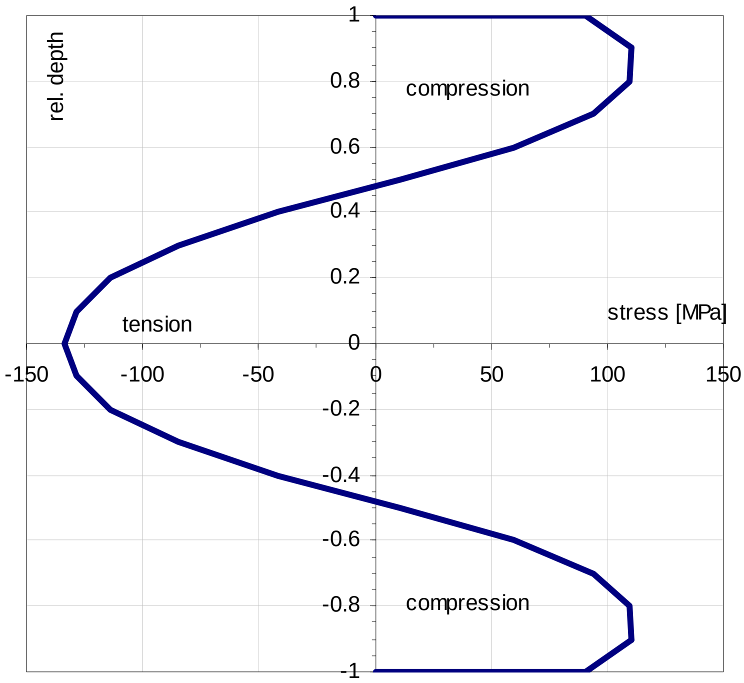

Figure 5-22: Assumed residual stress distribution.

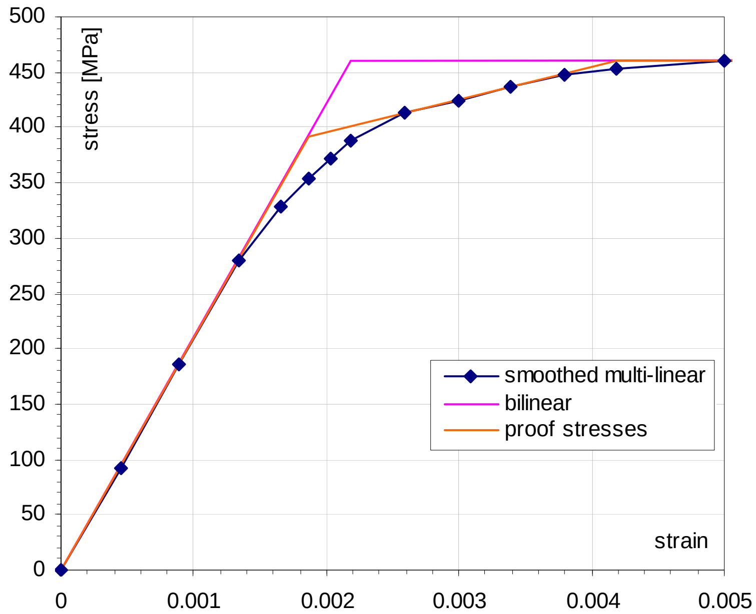

Figure 5-23: Stress-strain relationships considered in tower leg segment analysis.

6 Design Principles

This section describes the methods used to verify the performance of the tower structural components at SLS, ULS, FLS and SILS.

6.1 Serviceability Limit States

This section describes the methods used to verify performance of the tower structural components at SLS. Tower components are divided into four categories: longitudinal elements, transverse elements, joints and splices, and base anchorage components.

6.1.1 Longitudinal Elements

Longitudinal elements are those that are parallel to the tower leg and cross beam axes, such as flanges (skin plates), webs and longitudinal stiffeners.

The tower legs and crossbeams comprise slender longitudinally and transversally stiffened panels. Member capacity is governed by first yield at any cross section point. The section behavior and capacity is the same for all load combinations, with the exception of potential reductions for shear lag under SLS loading. However, shear lag does not affect the tower section properties because of the long lengths over which bending moments develop and therefore ULS and SILS load combinations govern the tower design. Cross section verification for SLS load combinations is not necessary. Verification of the longitudinal elements for ULS and SILS is described in Section 6.2.1.

6.1.2 Transverse Elements

Transverse elements are those that are generally perpendicular to the tower leg and cross beam axes, such as the transverse diaphragms and transverse stiffeners. The transverse diaphragms and stiffeners are used to provide restraint against out-of-plane buckling of the longitudinally stiffened panels and to prevent excess torsional distortions in the members.

Similar to the longitudinal elements, verification of these components for SLS load combinations is not necessary. Verification of the transverse elements for ULS and SILS is described in Section 6.2.2.

6.1.3 Joints and Splices

Individual tower elements are assembled with a combination of welded and bolted connections. The SLS design verification criteria for joints and splices are described in this section. The verification of joints and splices is in accordance with NTC08 Section 4.2.8.

6.1.3.1 Bolted Connections

Bolted connections are used for the construction joint splices of the tower leg longitudinal stiffeners, longitudinal web plates and transverse web plates.

The bolted construction joint splices in the tower leg vertical elements are designed to not slip at ULS so as to provide a similar longitudinal stiffness to the fully welded skin plate splices. Therefore, verification at the SLS is not required. Design verification criteria for these bolted splices are provided in Section 6.2.3.

6.1.3.2 Welded Connections

Welded connections are verified only at the ULS/SILS and FLS as described in Sections 6.2.3 and 6.3, respectively.

6.1.4 Base Anchorage Components

The tower base anchorage comprises the following components:

- Post-tensioned Multi-Strand Anchorage Tendons – transfer tensile stresses in the tower leg plates to the tower foundation;
- Base Plate – distributes the compressive tower base reaction to a sufficient area not to exceed the maximum bearing stress resistance of the concrete foundation; and
- Stiffening Plates – distribute forces between the tower leg plates and the tower base plate or anchorage tendons.

The tower base anchorage is designed not to decompress at ULS and therefore verification for the smaller SLS loads is not required. Design verification criteria for the base anchorage components at ULS are provided in Section 6.2.4.

6.2 Ultimate Limit States / Structural Integrity Limit States

Verification of the tower structural components for the ULS and SILS, in general, follows the same procedures. The only difference in the verifications for the two limit states is that the material partial factors are assumed equal to 1.0 for the SILS verifications.

6.2.1 Longitudinal Elements

The tower leg and cross beam longitudinal elements are verified at each cross-section considering the following:

- Combined axial force and bending moment demands;
- Shear and torsional demands; and
- The interaction of the above effects.

6.2.1.1 Combined Bending and Axial Loads

The tower leg and cross beam stiffened steel panels are designed in accordance with EN 1993-1-1 and EN 1993-1-5. Longitudinally stiffened members are slender Class 4 sections, unless the section satisfies the width-to-thickness ratio requirements of a lower section class when ignoring the longitudinal stiffeners. EN 1993-2 Section 6.5 requires that EN 1993-1-5 Sections 4, 5, 6 and 7 (or Section 10) be used for the plate buckling verification of members like the tower legs and cross beams at the ultimate limit states. The design of the Class 4 sections is based on elastic section properties. Calculation of the elastic section properties includes the effects of:

- Shear lag for bending moment and axial load near the application of concentrated loads;
- Local buckling of subpanels (including stiffeners and plates);
- Overall buckling of stiffened panels between diaphragms; and
- Shifts in the neutral axis between that of gross section and that of the effective section.

As described in Section 5.2.1, the global buckling of the tower legs is considered using equivalent imperfections to determine the additional bending moments due to buckling. As such, no additional reductions for global buckling of the tower legs are required in the cross-section verification. Also, the possibility of additional reductions in moment resistance due to lateral-torsional buckling need not be considered for the closed-hollow sections of the tower legs and cross beams.

The general cross-section verification is performed using the effective width model specified in EN 1993-1-5, Section 4. The effective width model accounts for plate buckling by reducing the area of slender plate elements so that the axial capacity of the reduced section, calculated as the product of the reduced area and the material yield strength, is the same as the actual axial capacity based on the gross area and the critical buckling stresses of the individual slender elements.

The slender plate element areas are reduced by multiplying the gross areas by the following reduction factors:

- ρ_{loc} for local sub-element buckling of plates and stiffeners; and
- ρ_c for buckling of the stiffened panel between diaphragms, including the interaction of:
    - χ_c for column-like buckling of individual stiffeners between diaphragms; and
    - ρ for plate-like buckling of an equivalent orthotropic plate between diaphragms.

The flange area reduction due to shear lag must be considered using EN 1993-1-5 Section 3.3, allowing for the use of elastic-plastic shear lag effects. However, due to the tower height and the resulting bending moment diagram lengths, shear lag does not influence the flange effectiveness. The tower leg design near the cross beam connection will be based on an appropriate load dispersion determined using local analyses. The tower top design accounts for the stress condition present at the underside of the cable saddle.

The optimal tower leg design is achieved by proportioning each panel to carry only the maximum compressive stress to which it is subjected in the governing load combinations. The tower leg design is dominated by a combination of axial and flexural compressive stresses, and thus the optimal design is achieved by proportioning the panels located around the cross section perimeter to be fully effective up to the design yield stress and proportioning the panels closer to the cross section centroid to be more slender and have a lower stress capacity.

LOCAL BUCKLING OF SUB-ELEMENTS

The reduction factor for local buckling of sub-elements is determined in accordance with EN 1993-1-5 Section 4.5.1(4) in conjunction with EN 1993-1-5 Section 4.4. The local stiffener and tributary plate effective area is calculated as follows:

$$A_{c,eff,loc} = A_{sl,eff} + A_{plate,eff}$$

where $A_{sl,eff}$ is the stiffener effective area, calculated as the product of gross stiffener area and the reduction factor for local buckling of the stiffener, $\rho_{loc,stiff}$; and $A_{plate,eff}$ is the plate element effective area between the longitudinal stiffeners, calculated as the product of gross plate area and the reduction factor for local buckling of the plate, $\rho_{loc,plate}$.

The reduction factor, ρ_{loc} , for each sub-element is determined using the method described in EN 1993-1-5, Section 4.4, which deals with buckling of unstiffened plates.

The reduced areas that are considered for the local sub-element buckling are shown in Figure 6-1. Due to the large variety of plate sizes and stiffener spacings, an effective area is calculated for each longitudinal stiffener and panel corner. The reduction factor for panel corners is conservatively taken as the minimum of the factors computed for the individual subpanels framing into the corner.

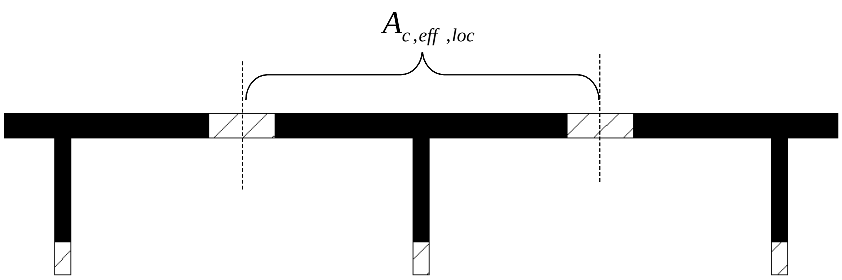

Figure 6-1: Effective area of stiffened panel sub-elements.

As described in Section 5.3.3, fabrication economy is achieved by omitting the connections between the longitudinal and transverse stiffeners. The omission of these connections has no affect on the overall stability of the longitudinal stiffeners. Local and torsional buckling of the longitudinal stiffeners are prevented by appropriate proportioning of the stiffener cross-section. Similar to the case of a flange outstand on a wide-flange column section, the only design check performed on the individual cross-section elements is the verification that the provided element width-to-thickness ratios are sufficiently small to allow the element to yield. In accordance with EN 1993-1-1 Table 5-2, local and torsional buckling of the longitudinal stiffeners is prevented by ensuring that:

$$\frac{c}{t} \leq 14 \cdot \varepsilon = 14 \cdot \sqrt{\frac{235}{f_y}} = 14 \cdot \sqrt{\frac{235}{460}} = 10$$

where c is the stiffener depth and t is the stiffener thickness.

BUCKLING OF STIFFENED PANEL

In addition to the local sub-element buckling area reductions, the entire stiffened panel area is further reduced to account for overall buckling of the stiffened panel between the transverse stiffeners/diaphragms. The reduction factor for the buckling is based on the interaction of the column-like buckling, χ_c (EN 1993-1-5, Section 4.5.3), and plate-like buckling, ρ (EN 1993-1-5 Section 4.5.2). The reduction factor for buckling of the stiffened panel, ρ_c, considering the interaction between the two types of the buckling is determined as follows (Eq. 4.13):

$$\rho_c = (\rho - \chi_c)\xi(2 - \xi) + \chi_c$$

where $\xi = \frac{\sigma_{cr,p}}{\sigma_{cr,c}} - 1$ but $0 \leq \xi \leq 1$; $\sigma_{cr,p}$ is the elastic critical plate buckling stress calculated in accordance with EN 1993-1-5 Annex A.1(2) or Annex A.2.2 for tower leg panel A, which has only a single longitudinal stiffener; and $\sigma_{cr,c}$ is the elastic critical column buckling stress calculated in accordance with EN 1993-1-5 Section 4.5.3(2) and (3).

The interaction equation indicates that the reduction factor for plate buckling is always beneficial to the total reduction factor. Due to the generally large panel widths being considered, relative to the transverse stiffener/diaphragm spacing, the restraining effect along the panel edge is typically minimal and the buckling behavior is dominated by the individual stiffeners buckling as isolated columns. Tower leg panel A, for which intermediate transverse stiffeners are omitted is an exception. For the long narrow panel A, plate-like behavior is dominant and is considered in accordance with Annex A.2.2. For other panels, the benefit of considering plate-like buckling is generally insignificant and therefore is ignored and the reduction factor for buckling of the stiffened panel will be equal to that for column-like buckling:

$\rho_c = \chi_c$

This simplification of the design method does not result in increased conservatism.

The reduction for column-like buckling is calculated in accordance with EN 1993-1-5 Section 4.5.3. The critical elastic stress is calculated from the gross stiffener section and its tributary parts spanning as a column between the transverse stiffeners/diaphragms, with all longitudinal supports removed.

The reduction factor for column-like buckling is calculated using the standard column buckling equations given in the general building code EN 1993-1-1 Section 6.3.1.2. However, due to the less restrictive construction tolerances for stiffeners, the imperfection factor, α, is increased according to EN 1993-1-5 Section 4.5.3(5).

COMBINED LOCAL SUB-ELEMENT AND STIFFENED PANEL BUCKLING

The total buckling effect is considered by combining local sub-element buckling and the overall buckling (column-like and/or plate-like) for each stiffener in the cross-section. The total effective area for a stiffener and its tributary plate width is:

$A_{c,eff} = \rho_c A_{c,eff,loc}$ for tower leg panel A

$A_{c,eff} = \chi_c A_{c,eff,loc}$ for all other panels

CROSS-SECTION VERIFICATION

The cross-section capacity is verified by comparing the stress resistance, σ_{rd}, of each longitudinal cross-section element, comprising a longitudinal stiffener and tributary plate width or the plate elements tributary to panel intersections (corner regions), with the stress demand, σ_{Ed}, calculated on the basis of the gross section properties.

EN 1993-1-5 Section 4.6 permits cross-section verifications to be completed using the partial safety factor, $\gamma_{M0} = 1.05$, in accordance with NTC08 Section 4.2.4.1.1. However, prior to the submission of the final documents, Stretto di Messina requested that the partial factor for cross-section verifications be increased to $\gamma_{M1} = 1.10$. Therefore, the verification equations provided below deviate slightly from those suggested by EN 1993-1-5 and will result in a slightly more conservative design.

The stress resistance of a stiffener and tributary plate, considering local sub-element and overall buckling effects is:

$$\sigma_{rd} = \frac{f_y}{\gamma_{M1}}\left(\frac{\rho_c A_{c,eff,loc}}{A_{gross}}\right)$$ for tower leg panel A

$$\sigma_{rd} = \frac{f_y}{\gamma_{M1}}\left(\frac{\chi_c A_{c,eff,loc}}{A_{gross}}\right)$$ for all other panels

where f_y is the yield strength, A_{gross} is the gross cross-sectional area of the element and γ_{M1} is the material partial factor given in Section 4.1.

The stress resistance of the plate elements tributary to panel intersections, considering only local sub-element buckling effects is:

$$\sigma_{rd} = \frac{f_y}{\gamma_{M1}}\left(\frac{A_{c,eff,loc}}{A_{gross}}\right)$$

The effective area of these intersection regions is not reduced for column-like buckling because the column stability is ensured by the large in-plane stiffnesses of the intersecting panels.

The utilization ratio, η_1, for each cross-section element is calculated as:

$$\eta_1 = \frac{\sigma_{Ed}}{\sigma_{rd}}$$

The adopted verification method differs from that of EN 1993-1-5 Section 4.6 in that the stress demands are based on the gross cross-section properties rather than on the effective section properties. The effect of the required area reductions for local and overall buckling are considered in calculating the stress resistance rather than in calculating the stress demand.

Although this verification method differs slightly from that of EN 1993-1-5 Section 4.6, the intent is consistent with the code intent of ensuring that each cross-section point can carry the required force. The adopted method is also supported by EN 1993-1-5 Section 4.4 (4), which allows for the plate slenderness parameter to be reduced if the actual applied stress is less than yield.

This method more appropriately considers the large variation in stiffener arrangements used in the tower legs and cross beams and allows for more optimal proportioning of the elements near the neutral axis that are never required to reach their yield capacity. Rather than arbitrarily reducing the cross-section properties based on the assumption that all cross-section element areas must be able to yield, the method calculates the actual stress to which the element is subjected and compares that to the stress resistance, considering the required buckling effects. The method also allows for a better understanding of the critical cross-section locations, and therefore, greater optimization of the longitudinal steel.

The verification given in EN 1993-1-5 also states that the effect of any shift in the neutral axis due to loss of effectiveness should be considered in calculating section properties and moments. However, for the tower design, nearly all points on the cross section are generally in compression and any shift in neutral axis will be insignificant.

6.2.1.2 Shear and Torsion

The global shear in the tower legs and cross beams is carried by a combination of panels that are in the plane of the shear being considered and skewed to it. For panels that are skewed to the shear plane, the shear area is reduced to consider only the panel component that is in the shear plane.

For sections subject to shear and torsion, the design shear stresses include the additional stresses due to the torsion. Because the tower legs and cross beams are closed-hollow sections, the effect of torsional warping is neglected and only St. Venant torsional shear stresses are considered.

For any cross-section point the following equation is satisfied:

$$\eta_3 = \frac{\tau_{Ed}}{\tau_{Rd}} \leq 1.0$$

where τ_{Rd} is the maximum allowable panel shear stress and τ_{Ed} is the design shear stress due to combined shear and torsion and is given by $\tau_{Ed} = \tau_{V,Ed} + \tau_{T,Ed}$, where $\tau_{V,Ed}$ is the design shear stress due to shear force and $\tau_{T,Ed}$ is the design shear stress due to St. Venant torsion.

The design shear stresses due to the shear force at a cross-section point are obtained from EN 1993-1-1 Eq. 6.20:

$$\tau_{V,Ed} = \frac{V_{Ed} S}{I \cdot t}$$

where V_{Ed} is the design shear force, S is the first moment of the area outside the point at which the shear stress is being calculated, I is the second moment area of the whole cross section and t is the thickness at the examined point.

The St. Venant torsional shear stresses are conservatively calculated ignoring interior cells as:

$$\tau_{t,Ed} = \frac{T_{Ed}}{2A_o t}$$

where T_{Ed} is the design torsional moment, A_o is the area enclosed by the centre-line of the skin plates and t is the thickness of the plate being considered.

The maximum allowable shear stress is determined based on the plastic shear resistance, making allowance for the presence of shear buckling where required. The stiffened panels are checked for shear buckling by determining the modified slenderness parameter (Eq. 5.6):

$$\bar{\lambda}_w = \frac{h_w}{37.4 t \varepsilon \sqrt{k_t}}$$

where h_w is the panel depth, k_t is the shear buckling coefficient from EN 1991-3-5 Annex A.3 and $\varepsilon = \sqrt{235/f_y}$.

The slenderness parameter is calculated for the entire stiffened panel and for each individual sub-panel between stiffeners, and the maximum value is used. The shear buckling capacity reduction factor, χ_w is obtained from EN 1993-1-5 Table 5.1 and the maximum allowable shear stress, τ_{Rd}, is:

$$\tau_{Rd} = \frac{\chi_w f_{yw}}{\sqrt{3} \cdot \gamma_{M1}}$$

where f_{yw} is the panel yield strength, γ_{M1} is the material partial factor provided in Section 4.1.

The contribution of the flanges to the shear resistance as allowed in EN 1993-1-5 Section 5.4 is ignored. Due the high utilization of the flanges for bending moment and axial load, the additional shear capacity contributed by the flanges is insignificant.

6.2.1.3 Interaction between Bending, Shear and Axial Force

The Class 4 sections of the tower legs and cross beams are verified for the interaction between bending, shear and axial force in accordance with EN 1993-1-5. However, in accordance with Section 7.1(1) the interaction is ignored if the design shear stress is less than half of the allowable shear stress.

For locations where the shear stress exceeds half of the allowable shear stress, the interaction between normal and shear stresses is considered using Von Mises stresses, accounting for the various buckling reductions using EN 1993-1-5 Section 10 (Eq.10.5):

$$\left(\frac{\sigma_{x,Ed}}{\rho_x f_y / \gamma_{M1}}\right)^2 + \left(\frac{\sigma_{z,Ed}}{\rho_z f_y / \gamma_{M1}}\right)^2 - \left(\frac{\sigma_{x,Ed}}{\rho_x f_y / \gamma_{M1}}\right)\left(\frac{\sigma_{z,Ed}}{\rho_z f_y / \gamma_{M1}}\right) + 3 \cdot \left(\frac{\tau_{Ed}}{\chi_w f_y / \gamma_{M1}}\right)^2 \leq 1.0$$

where $\sigma_{x,Ed}$ and $\sigma_{z,Ed}$ are the design normal stresses, ρ_x and ρ_z are the corresponding buckling reduction factors calculated using EN 1993-1-5 Section 4 and τ_{Ed} and χ_w are the design shear stress and corresponding reduction factor for shear buckling, respectively.

6.2.1.4 Flange Induced Buckling

It is assumed in the verification of the stiffened panel (flange) compressive capacity that the intersecting plates (webs) that define the panel width provide a rigid linear support that prevents the flange from buckling out-of-plane along its edges. However, in sections with particularly heavy flanges supported along their edges by slender webs, it is possible for the entire flange to buckle into the web plane as a result of the web buckling.

EN 1993-1-5 Section 8 provides maximum web depth-to-thickness ratios required to resist flange induced buckling. However, the provisions of Section 8 are intended primarily for conventional I-girders and do not account for the presence of longitudinal stiffeners on the supported flange. The behavior of the longitudinally stiffened tower leg panels with transverse diaphragms and stiffeners is typically governed by column-like buckling of the stiffeners spanning between the transverse supports. Therefore, only the panel edges between the web plate and the adjacent longitudinal stiffeners, representing a very small proportion of the panel area, require the web support considered in Section 8. Due to the moderate longitudinal stiffener spacing in all panels, the demands on the supporting web are insignificant. Therefore, the effect of flange induced buckling for tower legs is safely ignored.

The angle change in the cross beam top and bottom flanges results in an additional vertical force on the cross beam webs. However, the resulting deviation forces are primarily concentrated at transverse stiffeners and diaphragm locations. Therefore, the transverse stiffeners are proportioned to resist this additional vertical load, preventing additional web loading that might induce web buckling. Similar to the tower legs, flange induced buckling in the cross beams is safely ignored.

6.2.2 Transverse Elements

Transverse elements are those that are generally perpendicular to the tower leg and cross beam axes, such as the transverse diaphragms and transverse stiffeners. This section describes the verification of the transverse elements for ULS and SILS. The transverse elements are verified considering their resistance to direct stresses and distortional effects.

6.2.2.1 Direct Stresses

The tower leg and crossbeam transverse diaphragms and stiffeners provide out-of-plane restraint to the primary longitudinal plates and stiffeners. They are proportioned to provide sufficient stiffness and strength and are checked for torsional stability. The stiffeners must provide the following:

1 A stiffness not less than the minimum stiffness in EN 1993-1-5 Section 9.3.3; and

2 Stiffness and strength to resist (i) the deviation component of the longitudinal forces in flat panels, which is the typical case in the tower legs, (ii) any deviation force from an intentional angle change in the longitudinally stiffened panels, as for the cross beam flanges, (iii) any axial force arising from an intentional angle change in the longitudinally stiffened panels, as for the transverse stiffeners of the cross beam webs and (iv) axial forces from high shear stresses as described in the Note to EN 1993-1-5 Section 9.3.3. Generally high axial forces do not occur because the shear stresses are relatively low and the shear buckling resistance of the stiffened plate is high.

In the absence of both transverse stiffener axial force and intentional angle changes in the longitudinally stiffened panels, the simplified method for ensuring the transverse stiffener adequacy may be used. The simplified method is provided in EN 1993-1-5 Section 9.2.1(5) and specifies the minimum second area moment for the transverse stiffener (Eq. 9.1):

$$I_{st} = \frac{\sigma_m}{E}\left(\frac{b}{\pi}\right)^4\left(1 + w_0\frac{300}{b}u\right)$$

where

b is the panel width;

w_0 is the initial stiffener bow imperfection that is considered at the panel centreline;

$$u = \frac{\pi \cdot E \cdot e_{\max}}{f_y \cdot 300 \cdot b \big/ \gamma_{M1}} \geq 1.0\,;$$

$e_{\max}$ is the maximum distance from the transverse stiffener extreme fibre to the transverse stiffener centroid, including the adjacent plate parts as shown in EN 1993-1-5 Figure 9.1, and all other variables are as previously defined;

$$\sigma_m = \frac{\sigma_{cr,c}}{\sigma_{cr,p}} \cdot \frac{N_{Ed}}{b} \cdot \left(\frac{1}{a_1} + \frac{1}{a_2}\right);$$

$\sigma_{cr,c}$ and $\sigma_{cr,p}$ are the elastic column buckling and plate buckling stresses, respectively, as defined in EN 1993-1-5 Section 4.5.3 and Annex A. In the wider panels, for which the transverse stiffener demands are highest, the additional buckling capacity of the stiffened panel due to plate-like buckling is so very small that it is ignored. Therefore, the elastic plate buckling stress will be equal to the column buckling stress such that $\sigma_{cr,c} \big/ \sigma_{cr,p} = 1$.

N_{Ed} is the maximum compressive force in either of the stiffened panels being supported by the transverse stiffener (for simplicity, N_{Ed} may taken as the product of the stiffened panel effective area and the yield stress because the longitudinal stresses are very close to yield);

a_1 and a_2 are the panel lengths on either side of the transverse stiffener;

Eq. 9.1 checks both the stiffness and the stresses in the transverse stiffener. The required stiffness is the governing criterion when u is less than or equal to 1.0. Transverse stiffener stress is the governing criterion when u is greater than 1.0, and Eq. 9.1 gives a stiffener size such that the stresses reach yield at the extreme fibre. Stress is generally the governing criterion in the tower, so S460 steel is used for the transverse stiffeners to minimize the steel quantity.

The transverse stiffener torsional stability may be checked using EN 1993-1-5 Section 9.2.1 (8) or (9) taking the value of $\theta = 6$ as recommended in the Note to that section, and considering the beneficial effects of the flange warping stiffness.

For the transverse stiffeners supporting the wide plate D, the above approach does not result in an economical design, as described in Section 5.3.2, and so these stiffeners are proportioned using more detailed finite element buckling analysis to confirm the adequacy of stiffeners with higher slenderness ratios than are implied by the simplified code provisions described above.

The cross beam transverse stiffeners are positioned at panel angle changes and are subjected to considerable axial forces. The cross beam transverse stiffeners are assessed using the procedures developed in Section 6.2.2.2.

6.2.2.2 Specific Requirements for Cross Beam Transverse Stiffening

The loading on and design of the cross beam transverse stiffeners and cross bracing requires additional consideration because of the curved flanges and gantry loads on the top flange. The purpose of this section is to describe the loading on the cross beam transverse stiffeners, describe the structural behaviour and derive design equations.

LOADING ON THE TRANSVERSE STIFFENERS

Transverse stiffener loads come from the following:

1 Inspection gantry;

2 Wind pressure;

3 Change of flange inclination, either from kinks at the transverse stiffeners or from the continuous curvature of the flange loading the longitudinal stiffeners. The change of inclination applies both distributed loads across the flange width and reactions at the stiffener ends giving axial loads on the vertical portions of the transverse stiffeners; and

4 Restraint forces required to stabilize the longitudinally stiffened webs.

STRUCTURAL BEHAVIOUR

The tender design cross beam transverse stiffeners comprised moment resisting frames that are restrained from lateral displacement by the top and bottom flanges and are restrained from vertical displacement by the webs. These restraints are sufficient for overall equilibrium and stability even if the stiffeners are pin-ended, but the height of the webs is so great (up to 22 metres) that the vertical stiffeners would have to be very large to have adequate stiffness. Therefore, the moment resisting frames have been replaced by bracing members, as shown in Figure 6-2, to provide improved stability and economy.

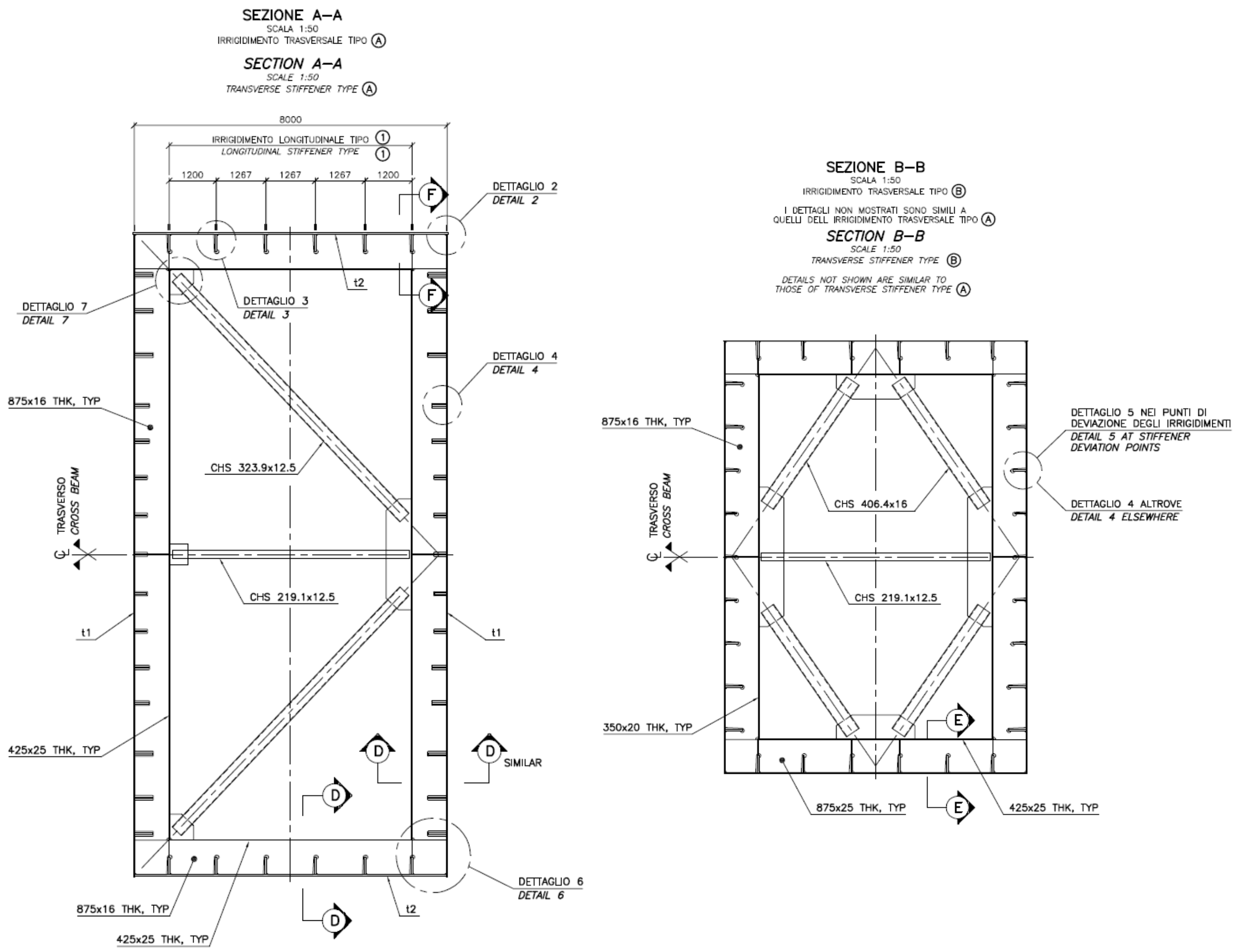

Figure 6-2: Typical cross beam transverse stiffener arrangements.

The structural behaviour of the stiffeners is severely affected by second-order effects arising from the change of flange inclination and restraint forces required to stabilize the longitudinally stiffened webs.

The possible imperfect shapes causing the symmetric and asymmetric loadings are as shown in Figure 6-3 (a) and (b), respectively. The asymmetric (sway) deformations are reduced to an insignificant amount by the cross-bracing. The bracing arrangement shown in Figure 6-2 Section B-B provides the sway resistance, but with the added benefit of supporting the horizontal transverse stiffener element.

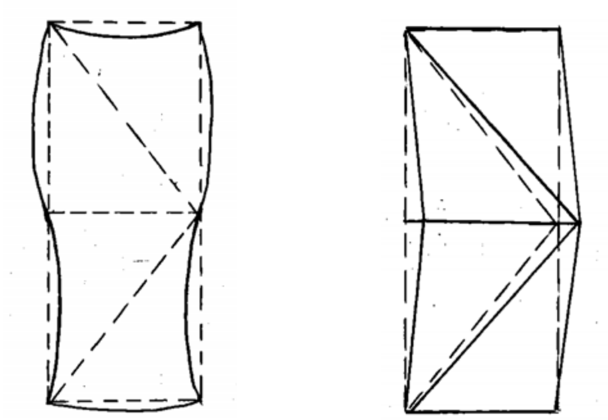
(a) (b)

Figure 6-3: Possible cross beam transverse stiffener imperfect shapes.

Accounting for the Second-Order Effects for Symmetric Loads

Design criteria for transverse stiffeners are given in EN 1993-1-5 Section 9.2.1.

The case of symmetric loads, resulting from the imperfect shape shown in Figure 6-3(a), is simplest to consider because it can be checked as a number of pin-ended stiffeners with an initial sinusoidal imperfection in accordance with EN 1993-1-5 Section 9.2.1(2). A loading diagram for a panel with a pin-ended stiffener subjected to longitudinal axial, transverse axial and out-of-plane loads is shown in Figure 6-4. The stiffener can be designed by extending the method of EN 1993-1-5 Section 9.2.1(5) with the addition of axial compression in the stiffener and a transverse load. This requires consideration of the following initial imperfections and loads:

- w_0, maximum value of initial imperfection with sinusoidal form;

- N_L, longitudinal compression load on panel width, uniform across the panel width, b;
- N_a, axial compression along the transverse stiffener, uniform along the length. In frames, all members potentially have axial compression applied by the reactions from the adjacent members at right-angles.
- F_d, maximum intensity of distributed loading in the plane of the transverse stiffener, sinusoidally distributed. The value of F_d must be calculated so that it gives effects that are equivalent to the loads from change of flange inclination and from the externally applied loads, for example the inspection and maintenance gantry wheel loads and the wind.

Given the above, the resultant elastic deflection, w_1, will also be sinusoidal.

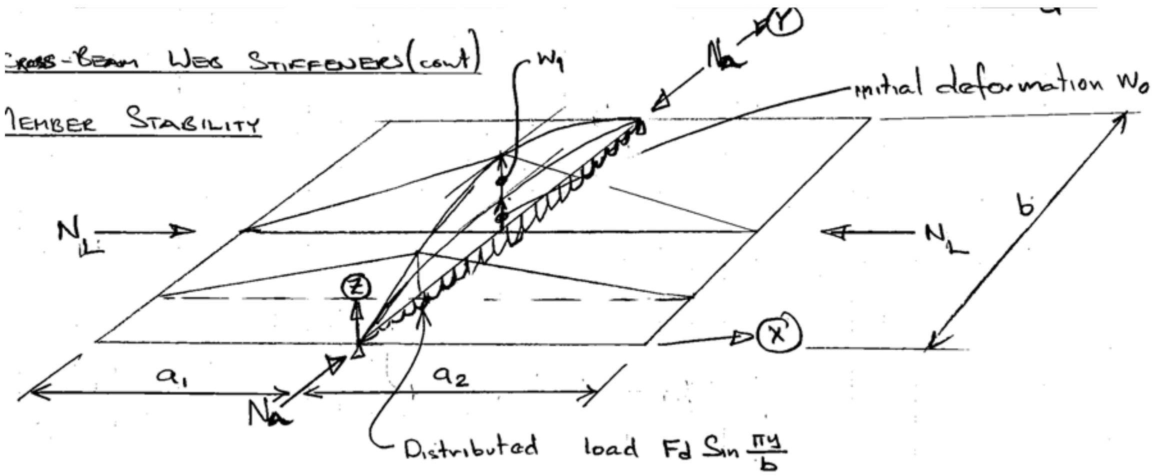

Figure 6-4: Typical cross beam panel subjected to longitudinal axial, transverse axial and out-of-plane loads.

The design procedure for proportioning the transverse stiffeners for strength and stiffness is presented in the following steps:

1. An equilibrium equation is established by equating the sum of the destabilizing forces to the stabilizing reaction;
2. An equation for the minimum inertia, I, is derived in terms of the maximum additional deflection, w_1, that is allowable;
3. A procedure to find values of F_d equivalent to the applied lateral loads is presented; and

4 The allowable values of w_1 are derived to satisfy stiffness and strength

Find an equilibrium equation:

At the equilibrium position, when the displacement is $w_0 + w_1$, the destabilizing loads are:

1 Destabilizing load / unit length from longitudinal compression in the panel:

$$\frac{N_L}{b}\left(\frac{dz}{dx}\right)_1 + \frac{N_L}{b}\left(\frac{dz}{dx}\right)_2 = \frac{N_L}{b}\left(\frac{w_1 + w_0}{a_1}\right)\sin\frac{\pi y}{b} + \frac{N_L}{b}\left(\frac{w_1 + w_0}{a_2}\right)\sin\frac{\pi y}{b}$$

$$= \frac{N_L}{b}(w_1 + w_0)\left(\frac{1}{a_1} + \frac{1}{a_2}\right)\sin\frac{\pi y}{b}$$

2 Destabilizing load / unit length from axial compression in the transverse stiffener:

$$N_a \frac{d^2 z}{dy^2} = N_a \frac{d^2}{dy^2}\left[(w_1 + w_0)\sin\frac{\pi y}{b}\right] = N_a (w_1 + w_0)\left(\frac{\pi}{b}\right)^2 \sin\frac{\pi y}{b}$$

3 Destabilizing out-of-plane transverse load / unit length:

$$F_d \sin\frac{\pi y}{b}$$

Summing these destabilizing loads per unit length gives:

$$= \frac{N_L}{b}(w_1 + w_0)\left(\frac{1}{a_1} + \frac{1}{a_2}\right)\sin\frac{\pi y}{b} + N_a (w_1 + w_0)\left(\frac{\pi}{b}\right)^2 \sin\frac{\pi y}{b} + F_d \sin\frac{\pi y}{b}$$

$$= \left[\frac{N_L}{b}(w_1 + w_0)\left(\frac{1}{a_1} + \frac{1}{a_2}\right) + N_a (w_1 + w_0)\left(\frac{\pi}{b}\right)^2 + F_d\right]\sin\frac{\pi y}{b}$$

The stabilizing reaction per unit length from bending of transverse stiffener is:

$$\frac{d^2 M}{dy^2} = \frac{d^2}{dy^2}\left(EI \frac{d^2 z}{dy^2}\right)$$ where EI is constant,

$$\frac{d^2 M}{dy^2} = EI\left(\frac{d^4 z}{dy^4}\right) = EI\left(\frac{d^4}{dy^4} w_1 \sin\frac{\pi y}{b}\right) = EI\left(\frac{\pi}{b}\right)^4 w_1 \sin\frac{\pi y}{b}$$

Equating the stabilizing reaction and the destabilizing load provides the following equilibrium equation that can be used to determine the required transverse stiffener stiffness.

$$EI\left(\frac{\pi}{b}\right)^4 w_1 \sin\frac{\pi y}{b} = \left[\frac{N_L}{b}(w_1+w_0)\left(\frac{1}{a_1}+\frac{1}{a_2}\right)+N_a(w_1+w_0)\left(\frac{\pi}{b}\right)^2+F_d\right]\sin\frac{\pi y}{b}$$

$$EI\left(\frac{\pi}{b}\right)^4 w_1 = \frac{N_L}{b}(w_1+w_0)\left(\frac{1}{a_1}+\frac{1}{a_2}\right)+N_a(w_1+w_0)\left(\frac{\pi}{b}\right)^2+F_d$$

Find values of F_d equivalent to lateral loads:

The value of F_d must be calculated to be equivalent to lateral loads from change of flange inclination and from the externally applied loads. F_d must give bending moments and deflections that are no smaller than those from the applied loads.

The maximum bending moment from the sinusoidal load is: $\iint F_d \sin\frac{\pi y}{b} = \frac{F_d b^2}{\pi^2}$,

so equivalence of bending moment requires that $\frac{F_d b^2}{\pi^2} \geq M_{load}$, giving $F_d \geq \frac{\pi^2}{b^2} M_{load}$

The maximum deflection from the sinusoidal load is: $\iint \frac{M}{EI} = \frac{F_d b^4}{\pi^4 EI}$

so equivalence of deflection requires that $\frac{F_d b^4}{\pi^4 EI} \geq \delta_{load}$, giving $F_d \geq \frac{\pi^4 EI}{b^4}\delta_{load}$

Values of N_L where the distribution of load is not uniform:

The distribution of longitudinal stresses on the panels will not be uniform in many cases. More often the stress distribution will vary linearly across each panel. In these cases, the force N_L should be taken as the integral of only the compressive forces in the panel. Where a panel is partially in tension, the stabilizing effect of the tensile stresses is ignored.

Values of N_a where the force is not uniform along the stiffener:

For simplicity, the force may be taken as the maximum value, but, if required, it could be reduced to the highest compressive force in the middle third of the stiffener.

Find an equation for the minimum inertia, $I_{\min}$:

Considering stiffness requirements only, the minimum inertia of the transverse stiffener is given by:

$$I_{\min} = \frac{1}{w_1 E}\left(\frac{b}{\pi}\right)^4 \left[\frac{N_L}{b}(w_1 + w_0)\left(\frac{1}{a_1} + \frac{1}{a_2}\right) + N_a(w_1 + w_0)\left(\frac{\pi}{b}\right)^2 + F_d\right]$$

If $F_d = 0$ and $N_a = 0$, this equation may be re-written as:

$$I_{\min} = \frac{1}{E}\left(\frac{b}{\pi}\right)^4 \left(1 + \frac{w_0}{w_1}\right)\left[\frac{N_L}{b}\left(\frac{1}{a_1} + \frac{1}{a_2}\right)\right]$$

which is similar in form to in EN 1993-1-5 Equation 9.1.

Limits on the additional deflection w_1 :

a) For minimum stiffness:

The above gives the minimum stiffness by substituting $w_0 = s/300$, where s is the smallest of $a1$, $a2$ or b as specified in EN 1993-1-5 Section 9.2.1(2), and $w_1 = b/300$, as specified in EN 1993-1-5 Section 9.2.1(4).

b) For minimum strength:

To extend the check to include stresses, w_1 must be limited so that the maximum design stress is not exceeded, which might be the factored yield stress, f_y/γ_{M1} , or whatever stress is required for the stability of the flange.

Using the axes defined in Figure 6-4 and the definition of $e_{\max}$ in EN 1993-1-5 Section 9.2.1(5),

the bending stress, $\sigma_b = Me_{\max}/I$.

From

$$M = EI\frac{d^2 z}{dy^2} = EI\frac{d^2}{dy^2} w_1 \sin\frac{\pi y}{b} = EIw_1\left(\frac{\pi}{b}\right)^2 \sin\frac{\pi y}{b}$$

and the maximum value of $\sin\frac{\pi y}{b} = 1.0$, the maximum bending stress is:

$$\sigma_{b,\max} = \left[EIw_1 \left(\frac{\pi}{b}\right)^2 \right] \frac{e_{\max}}{I} = Ew_1 \left(\frac{\pi}{b}\right)^2 e_{\max}$$

from which $w_1 = \frac{\sigma_{b,\max}}{Ee_{\max}} \left(\frac{b}{\pi}\right)^2$

The maximum bending stress, must be limited so that $\sigma_a + \sigma_{b,\max} \le \sigma_{bR} / \gamma_{M1}$ so $\sigma_{b,\max} \le \sigma_{bR} / \gamma_{M1} - \sigma_a$ where σ_{bR}, is the buckling resistance of the stiffener flange and σ_a is the stress caused by axial loads. In cases where the flange is stable up to yield stress, $\sigma_{bR} = f_y$.

<u>Finding $I_{\min}$ – General case:</u>

For the general case of destabilization by N_L, N_a and F_d, $I_{\min}$ can be found by substituting the smallest of $w_1 = b/300$ or $w_1 = \frac{\sigma_{b\max}}{Ee_{\max}} \left(\frac{b}{\pi}\right)^2$ into the equation for $I_{\min}$ derived above.

Finding $I_{\min}$ – Case of $F_d = 0$ and $N_a = 0$:

In the equation $I_{\min} = \frac{1}{E}\left(\frac{b}{\pi}\right)^4 \left(1 + \frac{w_0}{w_1}\right) \left[\frac{N_L}{b}\left(\frac{1}{a_1} + \frac{1}{a_2}\right)\right]$ derived above, $\frac{1}{w_1}$ may be written as:

$$\frac{1}{w_1} = \frac{1}{\frac{\sigma_{b\max}}{Ee_{\max}}\left(\frac{b}{\pi}\right)^2} = \frac{Ee_{\max}}{\sigma_{b\max}}\left(\frac{\pi}{b}\right)^2 = \frac{\pi^2 Ee_{\max}}{\sigma_{b\max} b^2} = \frac{300}{b} \frac{\pi^2 Ee_{\max}}{\sigma_{b\max} 300b}$$

and substituting into the equation for $I_{\min}$ gives:

$$I_{\min} = \frac{1}{E}\left[\frac{N_L}{b}\left(\frac{1}{a_1} + \frac{1}{a_2}\right)\right]\left(\frac{b}{\pi}\right)^4 \left(1 + w_0 \frac{300}{b}\left(\frac{\pi^2 Ee_{\max}}{\sigma_{b\max} 300b}\right)\right)$$

$\frac{\pi^2 Ee_{\max}}{\sigma_{b\max} 300b}$ is identical to u in EN 1993-1-5 Section 9.2.1(5) if $\sigma_{b\max} = \frac{f_y}{\gamma_{M1}}$

<u>Checking for shear</u>

The shear check in EN 1993-1-5 Section 9.2.4(5) must be treated with caution because it requires the check on the “gross web adjacent to the cut-out,” which could be interpreted either as checking the web near, but not at, the cut-out. This requirement seems to contradict good judgement, and so "adjacent to" is understood to mean "at". Therefore, unless another load path is provided, "gross web adjacent to the cut-out" is interpreted as the web area reduced by the cut-out, but not reduced by other effects such as plate buckling.

The check of Section 9.2.4(5) is correct if the stiffener is sized by strength not stiffness, so the shear increases with increasing inertia. But, for greater economy, the shear can be found from the loads on the stiffener, $q \sin \frac{\pi y}{b}$.

Having found the distributed load, q, (see below), the shear, V, can be found from:

$$V = \int q \sin \frac{\pi y}{b} = q \frac{b}{\pi} \cos \frac{\pi y}{b}$$

The shear check in EN 1993-1-5 Section 9.2.4(5) comes from:

$$V = \frac{d}{dy} M = \frac{d}{dy} M_{\max} \sin \frac{\pi y}{b} = \frac{d}{dy}\left(\frac{\sigma I}{e_{\max}}\right) \sin \frac{\pi y}{b} = \left(\frac{\sigma I}{e_{\max}}\right) \frac{\pi}{b} \cos \frac{\pi y}{b}$$

$$\therefore V_{\max} = \left(\frac{I}{e_{\max}} \frac{f_y}{\gamma_{M0}}\right) \frac{\pi}{b} \cos \frac{\pi y}{b}$$

<u>Loads on the stiffeners</u>

The loads on the stiffeners can be found from the equation for destabilizing loads:

$$q \sin \frac{\pi y}{b} = \left[\frac{N_L}{b}(w_1 + w_0)\left(\frac{1}{a_1} + \frac{1}{a_2}\right) + N_a (w_1 + w_0)\left(\frac{\pi}{b}\right)^2 + F_d\right] \sin \frac{\pi y}{b}$$

by inserting the values of w_0 and w_1, where w_0 is from EN 1993-1-5 Section 9.2.1(2) and w_1 is found from the equilibrium equation:

$$\begin{aligned} EI\left(\frac{\pi}{b}\right)^4 w_1 &= \frac{N_L}{b}(w_1 + w_0)\left(\frac{1}{a_1} + \frac{1}{a_2}\right) + N_a (w_1 + w_0)\left(\frac{\pi}{b}\right)^2 + F_d \\ &= (w_1 + w_0)\left\{\frac{N_L}{b}\left(\frac{1}{a_1} + \frac{1}{a_2}\right) + N_a \left(\frac{\pi}{b}\right)^2\right\} + F_d \\ &= (w_1 + w_0) Q + F_d \end{aligned}$$

where $Q=\left\{\frac{N_L}{b}\left(\frac{1}{a_1}+\frac{1}{a_2}\right)+N_a\left(\frac{\pi}{b}\right)^2\right\}$

$$EI\left(\frac{\pi}{b}\right)^4 w_1 - w_1 Q = w_0 Q + F_d$$

$$w_1 = \frac{w_0 Q + F_d}{EI\left(\frac{\pi}{b}\right)^4 - Q}$$

The distributed loads, shears and moments applied to the transverse stiffeners can be calculated from w_1 as follows:

Moment: $$M = EI\frac{d^2 z}{dy^2} = EI\frac{d^2}{dy^2}w_1 \sin\frac{\pi y}{b} = EIw_1\left(\frac{\pi}{b}\right)^2 \sin\frac{\pi y}{b}$$

Shear: $$V = \frac{d}{dy}M = EIw_1\left(\frac{\pi}{b}\right)^3 \cos\frac{\pi y}{b}$$

Distributed load: $$q = \frac{d}{dy}V = EIw_1\left(\frac{\pi}{b}\right)^4 \sin\frac{\pi y}{b}$$

Internal members in the frames

The buckling resistance and tension resistance of the internal bracing members in the frames must be verified for the reactions from the web stiffeners.

ACCOUNTING FOR THE SECOND-ORDER EFFECTS FOR ASYMMETRIC DEFORMATIONS

EN 1993-1-5 does not cover the design of multi-storey stiffeners. Therefore, the stability will be checked as if the frame were a pin-jointed braced frame, for which the frame stiffness is sufficient to make the second-order effects negligible. The stiffness and strength of the individual frame components are checked for the symmetric loadings as described above. Therefore, the checks on frame action are limited to the effects of the nodal forces acting at members intersections.

The checks on transverse stiffeners in EN 1993-1-5 Section 9 do not consider the interaction of longitudinal compression and shear. It is not clear if this is proven to be unnecessary in all cases, or simply not expected to be necessary in common structures. If such combinations are ignored, the calculations would not contravene the Code, but the structure might not have the required reliability. Given that the cross beam webs are not common, being 20 metres deep, carrying high shear and moment and being heavily stiffened longitudinally, some destabilizing effect of the co-existent shear force in the web panels is considered.

In isotropic plates, shear forces are less destabilizing than axial forces, as shown by the buckling coefficients for infinitely long plates of width b that are hinged along their longitudinal edges. The elastic critical buckling stress for such plates is given by:

$$\sigma_{cr} = \frac{k\pi^2 E}{12(1-\nu^2)}\left(\frac{t}{b}\right)^2$$

with the buckling coefficient, $k = 4$ for longitudinal compression and 5.3 for shear. Therefore, it is slightly conservative to consider that shear forces act in a similar way to longitudinal compression.

Because shear stresses comprise principle stresses of equal compression and tension at 45°, shear buckling can only occur where a buckle can develop at an inclination to the member longitudinal axis. For the cross beam depth and transverse stiffener spacing at least two transverse stiffeners must be involved in a diagonal buckling deflection, as shown in Figure 6-5, compared with only one required for buckling due to longitudinal compression. This reduces the magnitude of the out-of-plane destabilizing forces. For example, on the diagonal line from peak to peak on each stiffener in the buckled position, the out-of-plane force is:

$$\frac{N_{eff}}{b}\left(\frac{dz}{dD}\right)_1 + \frac{N_{eff}}{b}\left(\frac{dz}{dD}\right)_2 = \frac{N_{eff}}{b}\left(\frac{w_{S1}+w_{S0}}{D_1}\right) + \frac{N_{eff}}{b}\left(\frac{0}{D_2}\right) = \frac{N_{eff}}{b}\left(\frac{w_{S1}+w_{S0}}{D_1}\right)$$

which is less than half the effect of axial compression because the diagonal distances, D_1 and D_2, are greater than the stiffeners spacings, a_1 and a_2, and the displacements at the peaks, w_{S0} and w_{S1}, are less than the displacements at the panel mid-heights from longitudinal compression, w_1 and w_2.

To account for all of the potential differences between buckling from shear and buckling from longitudinal compression, longitudinal load N_L, is taken as the longitudinal compression plus 1/3 of the shear force.

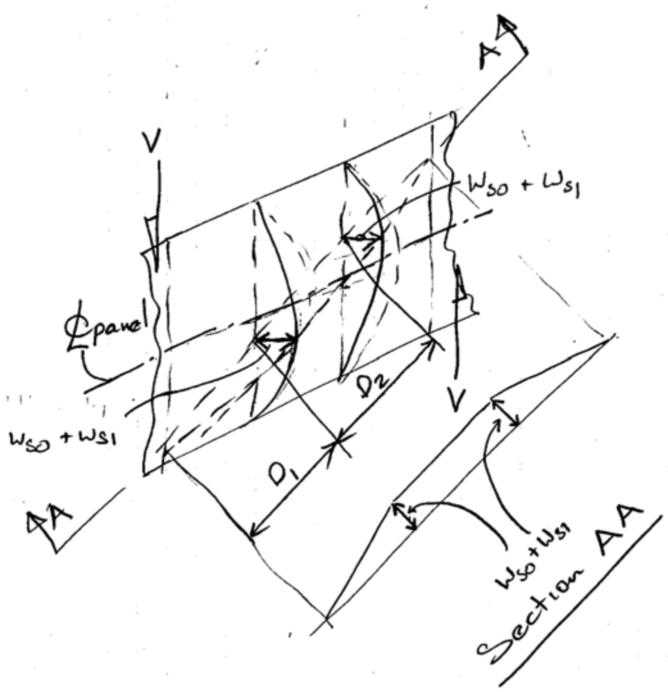

Figure 6-5: Deformations associated with shear buckling of a cross beam web.

<u>Cross-braced frames</u>

Cross-bracing increases the sway stiffness so much that sway deformations are insignificant. The loads on diagonally braced frames without externally applied vertical loads are shown in Figure 6-6. The cross beam bending stress diagram is shown with compression at the top and tension at the bottom. The reactions from the flange stiffeners are shown as acting up or down, either of which is possible if the flange is straight in the adjacent panels.

The reactions from the web stiffeners are:

R_{SSC} the simply supported transverse stiffener reaction in the compression zone;

R_{SST} the reaction from the transverse stiffener in the tension zone, which for simplicity is taken as zero because tensile stresses provide a stabilizing effect (the relatively small externally applied wind loads are ignored to offset the conservatism of ignoring the stabilizing effect of the tension stresses;) and

R_V the destabilizing effect of the shear force. As discussed above, this is taken as 1/3 of the effect of an equal longitudinal compression. Assuming that the cross-bracing reduces the sway deflection to a negligible magnitude, the out-of-plane force is limited to the slope from the initial design imperfection, $s/300$, which in the case of $a = 4000\,\text{mm}$ and $b > 10{,}000\,\text{mm}$ is $a/300$. The resulting slope is $1/300$ on each side of the transverse stiffener, and so the out-of-plane force from the longitudinal load N_L is:

$$N_L \times \frac{2}{300} = \frac{N_L}{150}$$

The tributary shear force is slightly greater than 50% of the shear on the web and may reasonably be taken as 60%. Therefore, the destabilizing reaction from shear on each web is:

$$R_V = \frac{1}{3} \times \frac{0.6 \cdot V_{web}}{150} = \frac{V_{web}}{750}$$

The directions of the forces in the bracing and the resultant reactions in the frame are shown in Figure 6-7.

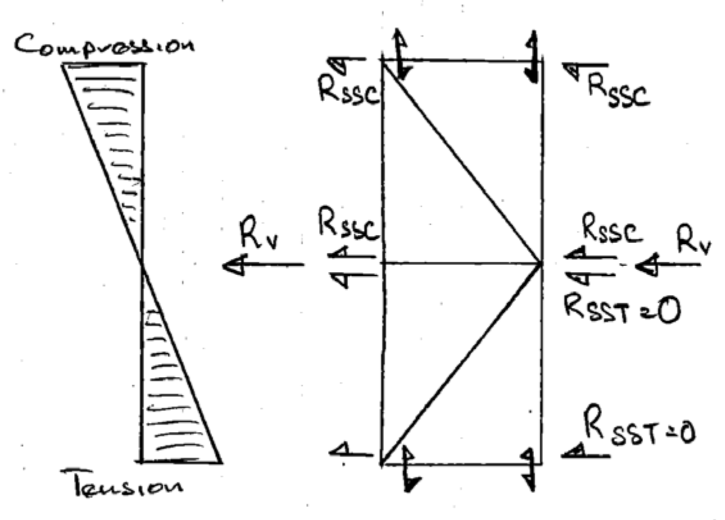

Figure 6-6: Transverse stiffener reactions acting on bracing members.

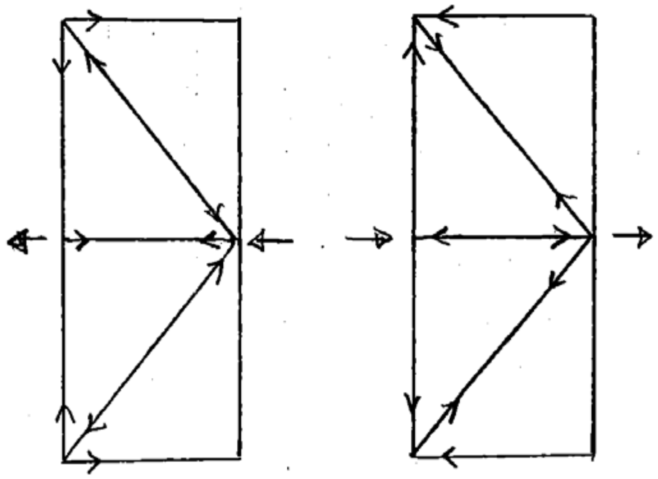

Figure 6-7: Bracing forces and reactions in the transverse stiffeners.

Where there is a change of flange inclination, either as a localized kink or as continuous curvature along the flange length, there are large vertical loads applied to the flange transverse stiffeners and these will apply large axial loads to the web transverse stiffeners. In such cases, the demands on the stiffeners can be reduced by providing K-bracing, as shown in Figure 6-8 with the approximate load distribution.

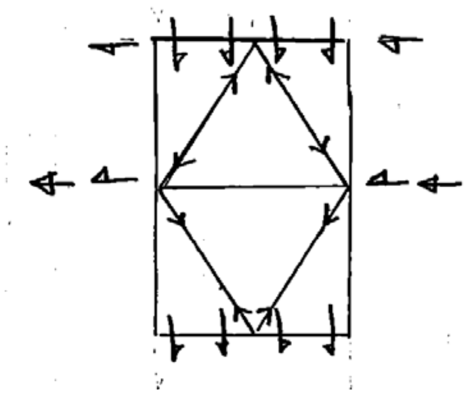

Figure 6-8: K-bracing forces and reactions in the transverse stiffeners.

<u>Minimum stiffness from EN 1993-1-5 Section 9.3.3(3)</u>

These requirements are from old British Standards and were derived from elastic critical buckling theory, but factored up to allow for some modest tension field action. They were intended for webs without the extensive longitudinal stiffening of the cross beams and without cross bracing to prevent sway deformations. The simplest way to demonstrate that the stiffness provided by the methods above is sufficient is to check that the minimum inertia, I_{st}, of EN 1993-1-5 Section 9.3.3(3) is provided for segments between the nodes of the braced frame. In the calculation, h_w is taken as half the cross beam depth at the stiffener location.

In the cross beams, cross-braces provide the distortional restraint.

Where the cross beams connect to the tower legs, the cross beam webs align with tower leg plates G and H and the cross beam web longitudinal stiffeners are continued into the tower leg along plates G and H to transfer their load. The axial forces in the cross beam webs apply considerable transverse compression and tension to the already highly stressed tower leg plates. In the tower leg length between the cross beam top and bottom flanges, the tower leg longitudinal stiffeners on plates G and H must also act as transverse stiffeners and restrain out-of-plane deformations caused by the transverse compression. The design of the stiffening for tower leg plates G and H within the cross beam depth follows very closely the procedures developed for the design of the cross beam transverse stiffeners described above.

6.2.3 Joints and Splices

The Ultimate Limit State design verification criteria for joints and splices are described in this section. The verification of joints and splices is in accordance with NTC08 Section 4.2.8.

6.2.3.1 Bolted Connections

The ULS verification of bolted joints and splices is in accordance with NTC08 Section 4.2.8.1. NTC08 does not reference some criteria typically considered in the ULS verification of bolted connections; as such, its criteria are supplemented with additional criteria from EN 1993-1-8, as required.

Bolted connections are used for the construction joint splices of the tower leg longitudinal stiffeners, longitudinal web plates and transverse web plates.

The bolted construction joint splices in the tower leg vertical elements are designed to be slip-resistant at ULS, so as to provide a similar longitudinal stiffness to the fully welded skin plate splices. EN 1993-1-8 Section 3.9.3 refers to the mixing of bolted and welded components as a hybrid connection and indicates that the bolts and welds may be assumed to share the applied load provided the final tightening of the bolts is completed after the welded splices are completed.

The design of the bolted tower leg splices assumes this sequence is followed. The bolted splices comprise cover-plates on both sides of the webs and stiffeners and pretensioned high-strength bolts.

The tower leg longitudinal and transverse internal webs resist:

- Longitudinal direct stresses from the axial load and the overall bending moments;
- In-plane shear stresses from the overall shear force and overall torsion; and
- Small direct stresses from the strut-action bending moment of the longitudinal stiffeners.

The calculation of the shear stresses takes account of shear flows that arise from the discontinuity of the internal webs.

The splice plates and bolts for the internal webs are proportioned to develop the design axial capacity of the plate acting concurrently with the applied shear stress, and the in-plane moments arising from the web stresses. The forces in each pair of plates are calculated from the stresses in the longitudinal web strip to which the splice plate is bolted. The width of the web strips is taken as the centre-to-centre distance of the longitudinal stiffeners between which the plates are bolted.

The tower leg longitudinal stiffeners resist:

- Longitudinal direct stresses from the axial load and the overall bending moments;
- Direct stresses from the strut-action bending moment of the longitudinal stiffeners; and
- Small shear stresses. These stresses are sufficiently small that they are neglected.

The splice plates and bolts for each stiffener are proportioned to develop the design axial capacity of the stiffener (i.e., splice plate area is always greater than the area of the smaller element being spliced). It is further confirmed that the longitudinal stiffeners provide sufficient capacity to carry the moments caused by the eccentricity resulting from plates of different thicknesses being spliced at a section further than $b_0/2$ or 200 mm from a transverse stiffener, in accordance with EN 1993-1-5 Section 9.2.3.

The following ULS verifications are performed for these bolted connections:

1 Slip resistance, $F_{s,Rd}$.

The slip resistance of a pre-tensioned high-strength bolt is given by Eq. 4.2.66 (NTC08):

$$F_{s,Rd} = \frac{n \cdot \mu \cdot F_{p,C}}{\gamma_{M3}}$$

where $F_{p,C}$ is the design bolt pre-tension, $\gamma_{M3} = 1.25$ is a material partial factor and all other variables are as previously defined. The design slip resistance at the ULS differs from the slip resistance at the SLS only in the application of a material partial factor to the bolt pre-tension force. The design bolt pre-tension force is given by Eq. 4.2.56 (NTC08):

$$F_{p,C} = 0.7 \cdot f_{tb} \cdot A_{res}$$

where f_{tb} is the bolt tensile strength (1000 MPa for Grade 10.9 bolts) and A_{res} is the tensile bolt area (i.e. at a section through the threads).

All construction joint splices use M30 Grade 10.9 bolts.

2 Bearing resistance of the connected plates, $F_{b,Rd}$ (as required by EN 1993-1-8 Table 3.2).

The bearing resistance of the connected plates is given by Eq. 4.2.61 (NTC08):

$$F_{b,Rd} = \frac{k \cdot \alpha \cdot f_{tk} \cdot d \cdot t}{\gamma_{M2}}$$

where d is the bolt diameter, t is the plate thickness, f_{tk} is the plate tensile strength and k and α are factors that depend primarily on the bolt position in the connection and the ratio of the bolt tensile strength to the plate tensile strength. The factors are computed with reference to NTC08 Figure 4.2.3.

3 Plastic net section capacity through the bolt holes, $N_{net,Rd}$ (as required by EN 1993-1-8, Table 3.2).

The plastic net section capacity through the bolt holes is given in EN 1993-1-8, Section 6.2.3 Eq. 6.8:

$$N_{net,Rd} = \frac{A_{net} \cdot f_y}{\gamma_{M0}}$$

where A_{net} is the net section area through the bolt holes, f_y is the plate yield strength and $\gamma_{M0} = 1.05$ is the material partial factor. Bolt holes are assumed to have diameters 3 mm and 2 mm larger than that of the bolt, for bolt diameters greater than and less than 27 mm, respectively. Allowance for shear lag in the connected components is made in accordance with EN 1993-1-1, Section 6.2.2.2.

6.2.3.2 Connection / Splice Plates

In addition to verifying the connector capacity, the resistance of the connected parts to yield of the gross section or fracture of the net tensile section is also verified. The plastic section capacity, $N_{pl,Rd}$, of a connected part is given by Eq. 4.2.7 (NTC08):

$$N_{pl,Rd} = \frac{A \cdot f_{yk}}{\gamma_{M0}}$$

where A is the gross section area, f_{yk} is the characteristic yield strength and $\gamma_{M0} = 1.05$ is the material partial factor.

The net section capacity, $N_{u,Rd}$, of a connected part is given by Eq. 4.2.8:

$$N_{u,Rd} = \frac{0.9 \cdot A_{net} \cdot f_{tk}}{\gamma_{M2}}$$

where A_{net} is the minimum effective net area of the connected part, considering shear lag and failure mechanisms such as block shear (tear-out), f_{tk} is the characteristic tensile strength and $\gamma_{M2} = 1.25$ is the material partial factor.

6.2.3.3 Welded Connections

The ULS design verification of welded joints and splices is in accordance with NTC08 Section 4.2.8.2. Welded connections are made with full or partial penetration butt welds and fillet welds.

The use of appropriate welding electrodes ensures that the theoretical strength of a full penetration weld is greater than or equal to the strength of the connected parts, and thus no further verification is required.

Partial penetration and fillet welds are verified considering the externally applied load induced stress on the effective weld area. The effective weld area is the product of the effective throat "a" and the effective weld length, "L". The weld capacity is verified using Eq. 4.2.75:

$$\left[\sigma_{\perp}^{2} + 3\cdot\left(\tau_{\|}^{2} + \tau_{\perp}^{2}\right)\right]^{0.5} = \frac{f_{tk}}{\beta\cdot\gamma_{M2}}$$

where f_{tk} is the characteristic tensile strength of the weakest of the connected parts, β is a correlation factor dependent on the base metal and γ_{M2} is the material partial factor.

6.2.4 Base Anchorage Components

Tower base anchorage components are verified for ULS/SILS considering the demands imposed during construction and on the completed bridge. ULS verification of the base anchorage components during construction is based on loadings consistent with the SLS2 criteria to reflect the lower return period associated with the temporary construction conditions.

6.2.4.1 Post-tensioned Multi-Strand Anchorage Tendons

The tower base anchorage is designed to not decompress under ULS/SILS loads, so as to maintain a constant base stiffness for all levels of tower response. All anchorage tendons comprise 15.7 mm diameter seven-wire strands, each with an area of 150 mm^2. The number, size and arrangement of the anchorage tendons are based on maximum tensile forces at the tower base under the governing load combinations during construction and in the completed bridge. Tendons are proportioned based on an effective tendon stress after all losses have occurred of $0.65 f_{pk}$ at the anchorage, as specified by the tower foundation designer, divided by an additional safety factor of 1.10. The additional safety factor is considered because although the tendons will not approach their ultimate strength, a margin of safety against the limit state of decompression that is similar to that usually provided for material strength limit states is desired. The tendon anchorage design accounts for both the initial jacking force and the effective tendon force after all losses have occurred.

Anchorage tendons are assumed to resist tensile stresses only. Transverse and longitudinal shear forces at the tower base are resisted by friction between the tower base plate and concrete foundation, as described below.

6.2.4.2 Base Plate

The tower base plate thickness is proportioned to distribute the maximum compressive bearing stresses approximately uniformly to the underlying concrete foundation and to resist bending and shear stresses resulting from the bearing stresses acting on the plate. The base plate bending capacity, $M_{pl,Rd}$, is calculated in accordance with NTC08 Eq. 4.2.13:

$$M_{pl,Rd} = \frac{W_{pl} \cdot f_{yk}}{\gamma_{M0}}$$

where W_{pl} is the plastic section modulus, f_{yk} is the characteristic yield strength and γ_{M0} is as previously defined. The plate shear capacity, $V_{c,Rd}$, is calculated in accordance with NTC08 Eq. 4.2.18:

$$V_{c,Rd} = \frac{A_v \cdot f_{yk}}{\sqrt{3} \cdot \gamma_{M0}}$$

where A_v is the shear area and all other variables are as previously defined.

Because the base plate demands cause a three-dimensional stress state in the base plate, with simultaneous bi-axial and shear stresses, the plate thickness is also verified by summing all stress components using von Mises criterion, in accordance with NTC08 Eq. 4.2.5:

$$\sigma_{x,Ed}^2 + \sigma_{z,Ed}^2 - \sigma_{x,Ed} \cdot \sigma_{z,Ed} + 3 \cdot \tau_{Ed}^2 \leq \left(\frac{f_{yk}}{\gamma_{M0}} \right)^2$$

where $\sigma_{x,Ed}$ and $\sigma_{z,Ed}$ are the two normal stresses, τ_{Ed} is the shear stress and the other variables are as previously defined.

The tower base plate width is proportioned to limit the concrete bearing stresses to approximately 60 MPa and to provide sufficient bearing width to accommodate all tower leg and anchorage components.

The tower base shear capacity is provided by friction between the underside of the base plate and the grout pad. The shear demand, V_{Ed}, is calculated as the vector sum of the co-existing transverse and longitudinal shear forces and the shear capacity, V_{Rd}, is calculated using the provisions of EN 1993-2 Section A.3.3:

$$V_{Rd} = \frac{\mu_k}{\gamma_\mu} \cdot N_{Ed} + V_{pd}$$

where μ_k is the friction coefficient, γ_μ is the partial factor for friction, N_{Ed} is the applied axial force and V_{pd} is the design shear resistance of the tendons(assumed equal to zero). Section A3.3 recommends and partial factor of 1.20 for steel on concrete and Table A1 gives a friction coefficient of 0.6 for steel on concrete. Section A.3.3(3) indicates that friction should not be relied on for rail bridges or bridges subjected to seismic excitation. However, the rail induced vibrations for the Messina Strait Bridge will have a negligible effect of the tower leg axial force, which is dominated by dead loads, and given that the utilization ratio for this check is between 0.3 and 0.4, it is believed that reliance on friction is valid and that sufficient safety against sliding is provided.

6.2.4.3 Base Anchorage Stiffening

The tower base anchorage stiffening comprises short vertical plates welded to steel anchorage pipes to which the post-tensioning tendons are anchored. The stiffening assembly is welded to the main tower leg plates and the tower base plate. The vertical stiffening plates are verified for shear and bending capacity to transfer the tributary compressive base plate bearing pressures and tensile tendon forces to the tower leg plates using NTC08 Eq. 4.2.18, defined in the previous section. The anchorage pipes are verified to have sufficient compressive capacity to carry the tendon pretension force. The compressive capacity, $N_{b,Rd}$, is verified in accordance with NTC08 Eq. 4.2.43 or 4.2..44, depending on the pipe proportions:

$$N_{b,Rd} = \begin{cases} \dfrac{\chi \cdot A \cdot f_{yk}}{\gamma_{M1}} & \text{for Class 1, 2 or 3} \\ \dfrac{\chi \cdot A_{eff} \cdot f_{yk}}{\gamma_{M1}} & \text{for Class 4} \end{cases}$$

where χ is a coefficient that depends on the component slenderness and effect of imperfections, A is the stiffener area and other variables are as previously defined.

Connections between the stiffening plates, the tower legs and base plate are verified as described in 6.2.3.

6.3 Fatigue Limit States

The tower members and details are verified for the stress ranges resulting from the Fatigue Limit State. Details subjected to stress ranges entirely in compression are less critical for fatigue loading, however, fatigue cracking may occur due to residual tensile stresses. As such, details are verified for adequate fatigue life in accordance with NTC08 Section 4.2.4.1.4 supplemented with EN 1993-1-9. The tower fatigue assessment is based on the safe life method with a high consequence of failure. The partial factor for fatigue strength is taken as $\gamma_{mf} = 1.35$, as specified in NTC08 Section 4.2.4.1.4.

The tower legs are subjected to direct stresses from rail and roadway loading and their fatigue design for these loads is described in Sections 6.3.1 and 6.3.2, respectively. Consideration of the vortex shedding induced tower leg vibrations is not required for the fatigue limit state because the wind speeds causing these vibrations will occur only rarely. The tower cross beams are subjected to only small, indirect, compatibility related stresses from rail and roadway loading. The cross beam design is governed by transverse seismic and wind loading. Seismic loads are infrequent and are not considered for fatigue assessment. Wind loads, however, are constantly present and although they are not typically considered in the fatigue design of a road/rail bridge, they do provide the most significant repeated loading for the cross beams. The cross beam fatigue assessment for wind loading is described in Section 6.3.3.

6.3.1 Railway Loading Fatigue Assessment

The tower legs are dominated by dead loads combined with seismic or wind loads and the stress ranges due to live loading are a relatively small component of the total stresses. Therefore, fatigue is not expected to be a governing consideration for the tower legs and the detail fatigue lives are verified using a simplified approach.

EN 1993-2 Section 9A specifies a method for a simplified fatigue assessment that uses the standard design rail loading and allows the modification of the stress range based on the actual traffic loading and design life. However, the damage equivalent factors, λ, are only valid for spans up to 100 m and for a 120-year design life. As such, this method is not suitable for the Messina Strait Bridge and an alternative approach is used to assess the live load tower fatigue. The alternative approach is the same in concept as the simplified assessment specified in 1993-2 Section 9, however, an approximate Miner's summation is used in place of the damage equivalent factors, which are intended to account for Miner's summation.

Considering the influence lines for tower, the stress range due to rail loading will be primarily dependent on the total mass of the train and is not sensitive to the axle configuration of the fatigue train. Therefore, the maximum fatigue stress ranges in the tower legs are determined approximately by comparing the total masses for the design trains with the mass of the actual fatigue loading.

The fatigue loading is based on RFI 44F, which states that the rail traffic should be taken as a "standard" traffic mix as defined in EN 1991-2 Table D.1.

As a simplified and conservative approach, it is assumed that all fatigue trains have the total mass of the heaviest fatigue train. Because the slope of the fatigue curve is less than 1:1, the critical fatigue stresses are caused by simultaneous loading from multiple trains resulting in greater stress ranges and fewer cycles. The design rail loading comprises two trains per track at a minimum spacing of 750 m. For the fatigue assessment it is conservatively assumed that half of all fatigue trains occur in groups of two (i.e., two trains on the bridge simultaneously, one per track) and the other half of the trains occur in groups of four (i.e., four trains on the bridge simultaneously, two per track).

The fatigue life for a given constant amplitude stress range can be determined from the fatigue strength curve EN 1993-1-9 Figure 7.1, shown in Figure 6-9.

From the fatigue strength curves the number of allowable fatigue cycles for a given stress range is given by:

$\Delta\sigma_R^m N_R = \Delta\sigma_c^m 2x10^6$ with $m = 3$ and $N_R \leq 5\times10^6$

$$\Delta\sigma_R^m N_R = \Delta\sigma_D^m 5x10^6 \qquad \text{with } m = 5 \text{ and } 5\times10^6 \le N_R \le 10^8$$

where $\Delta\sigma_R$ is the direct stress range resistance, N_R is the design life time expressed as the number of cycles related to a constant stress range, $\Delta\sigma_c$ is the reference fatigue strength at 2 million cycles and $\Delta\sigma_D$ is $0.737\Delta\sigma_c$,as given in EN 1993-1-9 Tables 8.1-8.10.

The fatigue life of the towers is verified for rail loading using Miner's summation as follows:

$$\frac{\gamma_{Ff} \cdot n_{4traingroup}}{N_{R,4traingroup} / \gamma_{mf}} + \frac{\gamma_{Ff} \cdot n_{2traingroup}}{N_{R,2traingroup} / \gamma_{mf}} \le 1.0$$

where $N_{4traingroup}$ and $N_{2traingroup}$ are the number of fatigue cycles for groups of four trains and groups of two trains, $N_{R,4traingroup}$ and $N_{R,2traingroup}$ are the fatigue life for the stress range resulting from groups of four trains and groups of two trains and γ_{Ff} is the partial safety factor for fatigue loads, taken as 1.0.

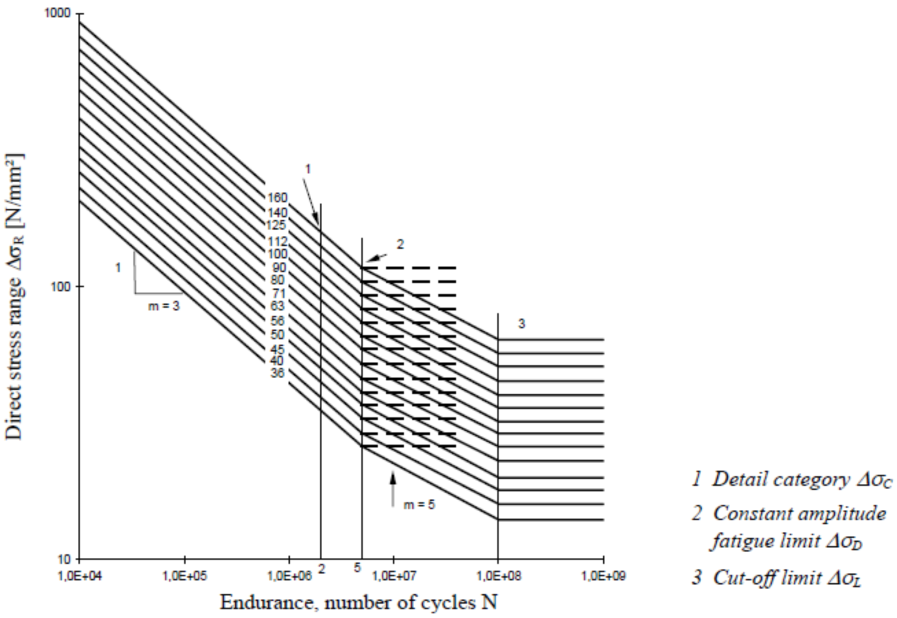

Figure 6-9: Fatigue strength curves.

6.3.2 Roadway Loading Fatigue Assessment

Maximum live load tower demands result from loads placed over long lengths, such as the specified 750 m long trains and the uniformly distributed portion of the roadway loading. Long heavy trains are expected to cross the bridge regularly, and are therefore considered a valid tower fatigue load. The fatigue truck used for the roadway girder fatigue assessment does not produce significant tower leg stresses and will not cause governing tower fatigue stresses. The induced stresses are well below the fatigue curve stress cut-off limit and therefore, roadway loading is not considered in the tower fatigue design.

6.3.3 Wind Loading Fatigue Assessment

The tower cross beams are assessed for fatigue caused by regularly occurring wind loads using a simplified and conservative procedure. The frequency and cumulative frequency distributions of all wind speeds occurring at the bridge site are used to determine the speed below which 95% of all winds blow (i.e, stronger winds only occur 5% of the time). It is conservatively assumed that the wind always blows in the most critical direction and that all of the design stress in the cross beam is caused by wind (no contribution from dead or other load components). The cross beam fatigue stresses caused by this wind speed are determined by scaling the design stresses determined for the critical wind load combinations, and are compared to the fatigue curve cut-off limit stresses in Figure 6-9.

A-1. Effect of Partial Safety Factor on Calculation of Equivalent Imperfection

INCREASED IMPERFECTION TO COMPENSATE FOR GAMMA M0

EN 1993-1-1 # 5.3.2(11) says the mode shape can be used as the imperfection. This method is used to account for the buckling effects in the towers.

EN 1993-1-5 uses γ_{M0} in Chapter 4 for the resistance of stiffened plates.
EN 1993-1-1 uses γ_{M1} in # 6.3.1 for the design of compression members

∴ There is an inconsistency between the two parts of the code

The logical solution is to determine initial imperfections that produce the compression resistance from EN 1993-1-1 # 6.3.1, N_{bRd}, when using EN 1993-1-5 with γ_{M0}

The calculation is based on finding what bending stress, σ_b, must be applied to limit the compression resistance to $N_{b,Rd}$ calculated with γ_{M1}

The compression resistance is taken as the force at which the stress reaches f_y/γ_M. because the initial imperfection includes the effects of residual stresses.

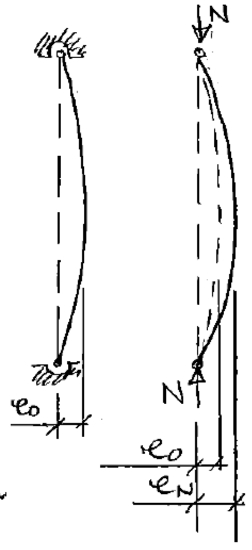

The magnitude of initial imperfection is much greater than the geometrical tolerances because the imperfection also accounts for the effect of residual stresses.

INCREASED IMPERFECTION TO COMPENSATE FOR GAMMA M0

Calculate N_{bRd}

Use pin-ended strut to demonstrate the procedure:-

Assume properties

$$\left.\begin{array}{lll} A = 7.0\times10^{6} & mm^2 \\ I = 300\times10^{12} & mm^4 \\ y = 10.0 & m \end{array}\right\} \text{elastic modulus } W_e = \frac{I}{y} = \frac{300\times10^{12}}{10\times10^{3}} = 30\times10^{9}$$

$L_{cr} = 300$ m

$f_y = 460$ MPa

Calculate N_{bRd} using $\gamma_{M1} = 1.1$ as EN1993-1-1 # 6.3.1

From # 6.3.1.3, $\bar{\lambda} = \sqrt{\frac{Af_y}{N_{cr}}}$

$$N_{cr} = \frac{\pi^2 EI}{L_{cr}^2} = \frac{\pi^2 \times 200\times10^3 \times 300\times10^{6,12}}{(300)^2\times10^{6}} = \boxed{6580 \text{ MN}}$$

$$\therefore \bar{\lambda} = \sqrt{\frac{7.0\times10^{6}\times 460}{6580\times10^{6}}} = 0.700$$

From # 6.3.1.2

Table 6.2 → buckling curve is Welded boxes, generally → buckling curve b

Table 6.2 → Imperfection factor for curve b = 0.34

$$\therefore \phi = 0.5\left[1+\alpha(\bar{\lambda}-0.2)+\bar{\lambda}^2\right] = 0.5\left[1+0.34(0.700-0.2)+0.700^2\right] = 0.830$$

$$\therefore \chi = \frac{1}{\phi+\sqrt{\phi^2-\bar{\lambda}^2}} = \frac{1}{0.830+\sqrt{0.830^2-0.700^2}} = 0.784$$

From # 6.3.1.1

$$N_{bRd} = \frac{\chi A f_y}{\gamma_{M1}} = \frac{0.784\times7.0\times10^{6}\times460}{1.1} = \boxed{2295 \text{ MN}}$$

INCREASED IMPERFECTION TO COMPENSATE FOR GAMMA M0 (cont)

Calculate imperfection used with $\gamma_{M1} = 1.1$

Calculate e_0 for γ_{M1} to demonstrate the increase using γ_{M0}
Using elastic material but non-linear geometry:-

Axial stress, σ_a, + bending stress, σ_b, $= \dfrac{f_y}{\gamma_{M1}}$ at N_{bRd}

$$\therefore \sigma_a + \sigma_b = \frac{f_y}{\gamma_{M1}}$$

$$\therefore \sigma_b = \frac{f_y}{\gamma_{M1}} - \sigma_a = \frac{f_y}{\gamma_{M1}} - \frac{N_{bRd}}{A} = \frac{460}{1.1} - \frac{2295 \times 10^6}{7.0 \times 10^6}$$

$$= 418.2 - 327.9 = 90.3 \text{ MPa}$$

$\therefore$ The internal moment $M_i = \sigma_b W_{ei} = 90.3 \times 30 \times 10^9 = 2709$ MN-m

$\therefore$ The imperfection, e_N, at $N_{bRd} = \dfrac{M_i}{N_{bRd}} = \dfrac{2709}{2295} = 1.180$ metres

$$e_N = e_0 \frac{1}{(1 - N/N_{cr})}$$

$$\therefore e_0 = e_N (1 - N/N_{cr}) = 1.180\left(1 - \frac{2295}{6580}\right) = 0.768 \text{ metres}$$

INCREASED IMPERFECTION TO COMPENSATE FOR GAMMA M0 (cont)

Calculate imperfection used with $\gamma_{M0} = 1{\cdot}05$

Using elastic material but non-linear geometry:-

Axial stress, σ_a, + bending stress, σ_b, $= \frac{f_y}{\gamma_{M0}}$ at N_{bRd}

$$\therefore \sigma_a + \sigma_b = \frac{f_y}{\gamma_{M0}}$$

$$\therefore \sigma_b = \frac{f_y}{\gamma_{M0}} - \sigma_a = \frac{f_y}{\gamma_{M0}} - \frac{N_{bRd}}{A} = \frac{460}{1{\cdot}05} - \frac{2295\times10^6}{7{\cdot}0\times10^6}$$

$$= 438{\cdot}1 - 327{\cdot}9 = 110{\cdot}2 \text{ MPa}$$

$\therefore$ The internal moment $M_i = \sigma_b W_d = 110{\cdot}2 \times 30\times10^9 = 3306$ MN-m

$\therefore$ The imperfection, e_N, at $N_{bRd} = \frac{M_i}{N_{bRd}} = \frac{3306}{2295} = 1{\cdot}441$ metres

$$e_N = e_0 \frac{1}{(1 - N/N_{cr})}$$

$$\therefore e_0 = e_N \frac{1}{(1-N/N_{cr})} = 1{\cdot}441\left(1 - \frac{2295}{6580}\right) = 0{\cdot}938 \text{ metres}$$

Check by calculating stress @ N_{bRd}

$$\sigma_a + \sigma_b = \frac{N_{bRd}}{A} + \frac{N_{bRd}\, e_0}{W_{el}}\left(\frac{1}{1 - N/N_{cr}}\right)$$

$$= \frac{2295\times10^6}{7{\cdot}0\times10^6} + \frac{2295\times10^6 \times 0{\cdot}938\times10^3}{30\times10^9}\left(\frac{1}{1-\frac{2295}{6580}}\right)$$

$$= 327{\cdot}9 + 110{\cdot}2 = 438{\cdot}1 \text{ MPa}$$

$\frac{f_y}{\gamma_{M0}} = \frac{460}{1{\cdot}05} = 438{\cdot}1$ MPa which is the limiting stress.

$\therefore$ Using the initial imperfection, e_0, $= 0{\cdot}938$ together with $\gamma_M = \gamma_{M0} = 1{\cdot}05$ gives the identical value of N_{bRd} as EN 1993-1-1 # 6.3.1

(This compares with $e_0 = 0{\cdot}768$ when using $\gamma_{M1} = 1{\cdot}1$)

INCREASED IMPERFECTION TO COMPENSATE FOR GAMMA MO

Demonstration of formula in General Design Principles document CG1000-P-RG-D-P-SV-T4-00-00-00-01 Rev C page 29

$$e_0 = \left(1 - \frac{N_{bRd}}{N_{vp\,Rd}}\right)\left(1 - \frac{N_{bRd}}{N_{cr}}\right)\left(\frac{M_{vp}}{N_{bRd}}\right)$$

With $\gamma_M = \gamma_{M0} = 1.05$

$$N_{vp\,Rd} = \frac{f_y}{\gamma_{M0}} A = \frac{460}{1.05} \times 7.0 \times 10^6 = 3067 \text{ MN}$$

$$M_{vp} = \frac{f_y}{\gamma_{M0}} W_e = \frac{460}{1.05} \times 30.0 \times 10^9 = 13140 \text{ MN-m}$$

$$\therefore e_0 = \left(1 - \frac{2295}{3067}\right)\left(1 - \frac{2295}{6580}\right)\left(\frac{13140}{2295}\right)$$

$$= (0.2517)(0.6512)(5.725) = 0.938 \text{ metres}$$

This the the same as calculated on page 3214